Evolutionary palaeobiology of deep-water conodonts

Smith, Caroline J.

University of Durham

Evolutionary Palaeobiology of Deep-water Conodonts

By

Caroline J. Smith

A thesis submitted in partial fulfilment of
the requirements for the degree of Doctor of Philosophy

Department of Geological Sciences
University of Durham

October 1999

Declaration

I declare that this thesis, which I submit for the degree of Doctor of Philosophy at the University of Durham, is my own work and not substantially the same as any which has previously been submitted at this or another university.

Caroline J. Smith

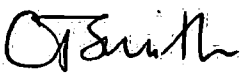

University of Durham

October 1999

Abstract

This study describes the conodont palaeontology of Upper Ordovician sections in Avalonia and Baltica. 24 species from 17 genera are systematically described and are attributed to the North Atlantic Realm. Sections can be correlated using graptolites and conodonts. The taxa are typical of the accepted *Aphelognathus* to *Periodon* shallow to deep-water biofacies. From the late Caradoc in Avalonia and Baltica, the *Amorphognathus* and deeper-water biofacies persisted in shelf settings. The stability of this distribution through the Ashgill, a period when Avalonia and Baltica drifted towards sub-tropical latitudes, suggests ocean cooling associated with glaciation was the dominant control on biofacies.

Microfacies analysis of the phosphatic *Amorphognathus superbus* Biozone limestones from the Nod Glas Formation of the Welsh Borders indicates the presence of the oxygen minimum zone. Biofacies distribution in this section reflects the subtle variations in temperature within this unique habitat. A hypothesis is presented for the evolution of *Amorphognathus ordovicicus* in which range expansion into slope settings enabled parapatric speciation. *Amorphognathus ordovicicus* evolved gradually from a deeper water ancestor by the loss of the lateral process and cusp adjacent denticles on the M element. The initial and subsequent transgressions of the Ashgill brought *Amorphognathus ordovicicus*, and its cool water niche, into shelf areas. Gradual evolution in deep-water is predicted by the Plus ça Change model.

The crown enamel of *Periodon*, *Protopanderodus* and *Drepanodus* records seasonally entrained growth with periods of retractional growth followed by longer functional episodes. *Periodon* exhibits reduced growth and comparatively short growth duration. *Drepanodus* and *Protopanderodus* show continued growth. It is hypothesised that *Periodon* was nektobenthic and adapted to harsh but stable conditions in the deep-sea, an r-strategist. *Drepanodus* and *Protopanderodus* were nektonic and grew to a large size indicating that they were *K*-strategists.

Upper Ordovician North Atlantic Realm nektobenthic conodonts were characterised by a high diversity and abundance of small sized individuals compared with coeval shelf faunas, a situation analogous to the modern oceans.

Acknowledgements

I would like to thank both Howard Armstrong and Alan Owen for their help and encouragement throughout the supervision of this project. I am grateful to NERC (No: GT 4/95/75 E) who funded this PhD.

During this project I have received help and advice from Dr. I.J. Sansom, Dr. P.J. Donoghue, conodont samples from Dr. M.P. Smith and have had the benefit of many useful discussions at meetings of the Palaeontological Association.

Thanks to the postgraduates and staff of the geology departments both here and in Glasgow. Special mentions go to Sarah, Matt, Gordon, Phil, Gail, Jo, Dougal, Fred and Moyra. I will always be grateful to Carol, Karen, Julie, Claire and Christine for providing a welcome diversion from geology during coffee breaks and for their help throughout my time spent in Durham. Thanks should also go to others in the department including the two Daves, Asbery and Schofield, and those who have helped me out during my PhD. Many thanks to Paul and friends from the Engineering Department (University of Durham) for their help with use of the SEM and to my non-geology friends in Durham.

Big love to Tim for getting me back on track throughout the last year of my project and reminding me of what's really important in life. I will always be grateful for his love, support and understanding.

Finally, all my love and special thanks go to Dad and Mum for being wonderful parents, for encouraging me in all the things I do and for supporting the choices I've made over the last few years.

Foreword

Given the content of this thesis it has been convenient to divide it into two parts. The contents for Parts I and II are listed at the beginning of each respective volume. A full reference list is provided at the end of Part II.

University of Durham

Evolutionary Palaeobiology of Deep-water Conodonts

PART I

UPPER ORDOVICIAN CONODONT BIOFACIES

By

Caroline J. Smith

A thesis submitted in partial fulfilment of
the requirements for the degree of Doctor of Philosophy

Department of Geological Sciences
University of Durham
October 1999

PART I CONTENTS

1. INTRODUCTION

2. THE UPPER ORDOVICIAN CONODONT BIOFACIES OF AVALONIA – THE NOD GLAS FORMATION

3. ASHGILL CONODONTS FROM THE LAKE DISTRICT AND THE OSLO GRABEN

4. EVOLUTION AND BIOSTRATIGRAPHICAL UTILITY OF *AMORPHOGNATHUS* ALONG THE SOUTHERN MARGIN OF THE IAPETUS OCEAN

5. CONCLUSIONS

APPENDIX 1A – SYSTEMATIC PALAEONTOLOGY

1B PLATES

1C ABUNDANCE TABLES

Table of Text-Figures PART I

Chapter 1

Chapter 2

Text-Figure 2.4.1. The stratigraphical relationship of the Nod Glas Formation (adapted from Cave, 1965).

Text-Figure 2.8.1. Key for the symbols used in sedimentary logs.
Text-Figure 2.8.2. The schematic sedimentary log of the Nod Glas Formation at Gwern-y-Brain Stream, Welshpool, Welsh Borders. The position of the Gaer Fawr, Nod Glas and Powis Castle Formations are indicated and dashed lines mark unconformities. Lithological aspects are shown within the succession whereas faunal occurrences are indicated on the right hand side of the log.

Text Figure 2.8.3 Photomicrograph of sample 588 in thin section under plane polarised light. Scale bar = 5mm

Text-Figure 2.8.4 Photomicrograph of sample 589 in thin section under plane polarised light. Scale bar = 5mm.

Text-Figure 2.8.5. Photomicrograph of sample 590 in thin section under plane polarised light. Scale bar = 5mm

Text-Figure 2.8.6. Photomicrograph of sample 591 in thin section under plane polarised light. Scale bar = 5mm.

Text Figure 2.8.7. Photomicrograph of sample 587 in thin section under plane polarised light. Scale bar = 5mm.

Text Figure 2.8.8. Photomicrograph of sample 592 in thin section under plane polarised light. Scale bar = 5mm.

Text Figure 2.8.9. Photomicrograph of sample 593 in thin section under plane polarised light. Scale bar = 5mn

Text-Figure 2.8.10. Photomicrograph of sample 586 in thin section under plane polarised light. Scale bar = 5mm.

Text-Figure 2.8.11. Photomicrograph of sample 585 in thin section under plane polarised light. Scale bar = 5mm

Text-Figure 2.8.12. Photomicrograph of sample 584 in thin section under plane polarised light. The darker areas to the right of the picture show the areas of phosphatisation between grains and skeletal fragments. Small phosphatic clasts can be seen in the centre section as elongated dark brown grains. Scale bar = 5mm

Text-Figure 2.9.1. The oceanic conditions required for phosphate formation (adapted from Reading, 1989).

Text-Figure 2.9.2. Proposed development of the Gaer Fawr Formation at Gwern-y-Brain Stream, Guilsfield, Welshpool. A. Shows the development of the packstones of the Gaer Fawr Formation on the shelf. B. Shows subsequent deposition of the greywackes overlying the packestones.

Text-Figure 2.9.3. The deposition of the Nod Glas Formation. Top. Shows the initial development of the OMZ and the position of phosphate deposition. Middle. shows the possible movement of the OMZ as the sea-level rises. Bottom. Shows how the OMZ may impinge upon the continental shelf as the transgression continues. Large grey arrow marks the position of the section at Gwern-y-Brain (GYB), Welshpool. GYB = Gwern-y-Brain, RSL = relative sea-level. OMZ = Oxygen minimum zone

Text-Figure 2.9.4. The development of the Nod Glas Formation. GYB = Gwern-y-Brain, RSL = relative sea-level. OMZ = Oxygen minimum zone

Text-Figure 2.9.5. The proposed ocean state for the Nod Glas Formation, Gwern-y-Brain, Welshpool.

Text-Figure 2.11.1. The conodonts from the upper Gaer Fawr Formation and lower Nod Glas Formation, Gwern-y-Brain Stream, Welshpool extracted during this present study. Thicker bars represent samples of greater abundance as indicated on the diagram.

Text-Figure 2.12.3. The three facies of the Nod Glas Formation and relative species diversity in each.

Text-Figure 2.14.1. The distribution of coniform taxa in the Gaer Fawr and Nod Gas Formations.

Text-figure 2.14.2. The distribution of biofacies in the Nod Glas Formation. OMZ = oxygen minimum zone.

Text-figure 2.16.1. The occurrence of *Plectodina* biofacies in the Nod Gas Formation. A. shows the biofacies occurrences in the OMZ. *Amorphognathus* species dominate the biofacies at the boundaries of the OMZ. B. Represents the temperature gradient within the OMZ. C. Illustrates the warm water band in the centre of the OMZ. Cooler water at the upper and lower boundaries of the Nod Glas Formation is a result of upwelling processes. Anoxic, warm waters lie beneath the OMZ. The warm water layer at the centre of the OMZ is dominated by *Plectodina bullhillensis,* which is postulated to favour a warmer water environment.

Chapter 3

Text figure 3.3.1 The conodont species occurrences from the Ashgill series of northern Britain.

Text-Figure 3.4.1. Field photograph of the northern side of the exposed Dent Group at Greenscoe - the lower part of the unit showing thinly bedded limestones. Scale bar = ~10m

Text-Figure 3.4.2. The relationship between the major units in cross-section. Numbers (25-32 relate to conodont samples D725-D732) along the base of the section show levels from which productive conodont samples were obtained.

Text-Figure 3.4.3. Complete sedimentary log of the Dent Group at Greenscoe (SD 221 756)

Text-Figure 3.7.1. Conodonts from the basal 40 metres of the Dent Group at Greenscoe Road cutting.

Text-Figure 3.9.1 Conodont occurrences in Northern England and corresponding transgressional episodes (adapted from Armstrong *et al.*, 1996). T1= Pusgillian, T2 = Cautleyan 2, T3= Rawtheyan 6.

Text-Figure 3.10.1. The appearance of conodont biofacies from the Pusgillian to the Rawtheyan (from the data of Armstrong *et al.*, 1996). Top – the Pusgillian transgression and biofacies, middle – the Cautleyan (Zone 2) transgression and biofacies, bottom – the Rawtheyan (zone 6) transgression and biofacies. The arrow marks the depositional area of the shelf.

Text-Figure 3.12.1. The Stratigraphy and Formations of the Oslo Graben area showing part of the Ordovician succession from which conodonts are discussed herein. Adapted from Stouge & Rasmussen, 1995 and Owen, 1990 using the revised British Ordovician chronostratigraphy of Fortey *et al.* (1995)

Text-Figure 3.12.2. Map of the Oslo-Asker region (from Owen *et al.*, 1990).

Text-Figure 3.18.1. Schematic log of the formations at north Raudskjer, Oslo-Asker. The numbers indicate the approximate positions of conodont samples.

Text-Figure 3.19.1. Key for abundance charts used for the Oslo conodont samples.

Text-Figure 3.19.2. Conodont range chart for sample set 16881-1. The interpreted sea-level curve is shown to the right of the sedimentary log.
Text-Figure 3.20.1. The position of conodont biofacies in North Rauskjer (sample set 16881-1)

Text Figure 3.21.1. The successions at Ringerike, Frognøya (adapted from information in Owen, 1979; Owen *et al.*, 1990).

Text Figure 3.21.2. Simplified geological map of the Ringerike District showing the position of Frognøya Island (from Owen, 1979)

Text-figure 3.25.1. Correlation of the formations on North Raudskjer and Frognøya. The sequence stratigraphy on Frognøya correlates to the transition from the Solvang to Venstøp Formation in North Raudskjer. The phosphate layer is therefore equivalent to the Høgberg Member.

Text-figure 3.25.2. Abundance chart of conodonts from sample 7881-1

Text-Figure 3.26.1. Conodont Biofacies (Frognøya).

Text-figure 3.28.1. Abundance of conodonts from sample set 1338-1

Chapter 4

Text-figure 4.2.1. The occurrence of *Amorphognathus superbus* and *ordovicicus* in Britain (see text for explanation). Chronostratigraphy and graptolite zones based on Fortey *et al.*, (1995).

Text-Figure 4.4.1. The M element from the Nod Glas Formation sample 593 (*Amorphognathus* cf. A. *superbus*, x200)

Text-Figure 4.4.2. The *Amorphognathus* M element from the Nod Gas Formation sample number 584 (*Amorphognathus* cf. *A. ordovicicus x* 180).

Text-Figure 4.4.3. Example of the *A. ordovicicus* M element from the Oslo Graben (Frognøya, lower Sorbakken Formation - Pusgillian x180).

Text-Figure 4.6.1. The occurrence of *Amorphognathus*. Figures of *A. tvaerensis* and *A. superbus* are adapted from Bergström & Orchard (1985). Other element specimens were collected and photographed by the author. Sea-level curve adapted from Ross & Ross (1992) and chronostratigraphy and biozones based on Fortey *et al.*, 1995 and data herein. Transgressions are marked by crosses next to the sea-level curve.

Text-figure 4.7.1. Conceptual model for the range expansion of *A. superbus* during the Cheneyan regressive episode. Note: the area of the slope ecozone is restricted due to greenhouse ocean bottom anoxia.

Text-Figure 4.7.2. The gradual evolution of *Amorphognathus*. Figures of *A. tvaerensis* and *A. superbus* are adapted from Bergström & Orchard (1985). Other element specimens were collected and photographed by the author.

Text-Figure 4.9.1. The conceptual model linking evolution and appearance of faunas due to sea-level fluctuations.

List of Tables Part I

Chapter 2

Chapter 3

Part I – Chapter 1

1. Introduction

1.1 Introduction

Part I of this thesis concerns the identification and discussion of late Caradoc and Ashgill conodont biofacies from the palaeocontinents of Avalonia and Baltica. During the Ordovician, conodonts were markedly provincial and ecologically diverse, ranging from shallow shelf to abyssal(?) depths (e.g. Sweet & Bergström, 1984, Sweet, 1988, Bergström, 1990). British conodonts are typically placed in the North Atlantic Realm characterised by deep, cold water (Sweet & Bergström, 1984).

The largely siliciclastic nature of sedimentary rocks from localities in the North of England, Wales and the Welsh Borders has resulted in the limited study of their Upper Ordovician conodont faunas. Caradoc and Ashgill conodont faunas in Wales and the Welsh borders have been documented by Rhodes (1953) and Savage & Bassett (1985). Other studies included those of Lindström (1959), Bergström (1964, 1971) and Orchard (1980).

Conodonts were primitive agnathan marine vertebrates ranging from the Cambrian to the latest Triassic. Evidence from examples with preserved soft tissues led to the general acceptance that most were active swimming predators with a nektobenthic or pelagic mode of life (e.g. Briggs *et al.*, 1983). Conodonts from the Ordovician have been divided into a number of depth related biofacies (Sweet & Bergström, 1984). The factors controlling conodont distribution have been the subject of much debate resulting in a wide range of alternative models. The key papers include those of Seddon & Sweet (1971), Druce (1973), Barnes & Fåhraeus (1975), Aldridge (1976) and Klapper & Johnson (1980). Factors that could potentially explain the distribution of conodonts in the geological record include variables such as depth (vertical stratification), salinity, distance from the shore (lateral segregation) and larval stage distribution dependent on configuration of the palaeo-continents. Although depth is widely postulated to be a major controlling factor (Sweet & Bergström, 1984), it may not be the primary control as light intensity, turbidity, salinity, oxygenation and water density can all vary with water depth.

During the late Ordovician several further factors have affected the conodont biofacies associated with both Avalonia and Baltica. The first is the position or latitude of the particular palaeocontinent in question. Evidence suggests that, during the late Ordovician, Avalonia drifted northwards towards Laurentia during closure of the Iapetus Ocean (Cocks *et al.*, 1997). Baltica collided with Avalonia in the late Ordovician (Cocks *et al.*, 1997) and with Laurentia in the middle to late Silurian (Cocks & Fortey, 1998). Secondly, it is inferred that processes of global cooling were operating at this time leading up to the end-Ordovician glaciation. Both of these processes may have had an influence on the appearance, composition and stability of conodont biofacies by affecting the palaeo-oceanographic conditions. Moreover, the late Ordovician is characterised by a number of global transgressions or highstands (Ross & Ross, 1992, Goldman & Bergström, 1997).

The present chapter considers the main aspects of Ordovician palaeogeography and palaeo-oceanography and outlines the models against which the data will be tested.

1.2 Aims

The aims of Part I of this thesis are therefore as follows:

1. The description of Upper Ordovician conodont faunas from Avalonia (Wales and the Lake District) and Baltica (Oslo Graben) attributed to the *A. naerensis* to *A. ordovicicus* biozones. The largely siliciclastic nature of rocks from these areas has meant limited research and generally poor yields.
2. To document the temporal and spatial changes in conodont faunas and biofacies through this interval.
3. To test the phylogenetic emergence and submergence model.

1.3 Palaeoecological controls on conodonts

Various models have been used to explain conodont distribution through time. Seddon & Sweet (1971) produced an ecologic model for conodont distribution based on early inferences of conodont ecology (e.g. Müller, 1960). The model predicted a free-swimming but pelagic organism that exhibited depth stratification. Seddon & Sweet proposed that at different times in the life of a conodont animal, it could inhabit different levels in the water column in a similar way to that observed in modern chaetognaths. This distribution was postulated to correlate with corresponding changes in temperature, light and nutrient supply as water depth increased. Furthermore, the model could explain the observation that not all conodont species could be found in all lithofacies and that some species would be concentrated in the lithofacies that directly corresponded with the position of the species within the water column. For example, on death, certain taxa would be restricted to deep-water facies while surface dwellers would be found in both shallow and deep facies. In a study of *Plectodina* and *Phragmodus* from the Upper Ordovician, Seddon & Sweet (1971) speculated how the boundary between these two genera could be a biological filter and this would prevent the deeper genus *Phragmodus* from occurring alongside the shallow water genus *Plectodina*.

In contrast to the depth stratification model of Seddon & Sweet (1971), Barnes & Fåhraeus (1975) proposed a lateral segregation model to explain conodont distribution. Moreover, they postulated that conodonts were dominantly benthic or nektobenthic in habit with only a few pelagic species. This was in contrast to Seddon & Sweet (1971) who proposed that vertical stratification was dominated mainly by pelagic conodonts. The alternative model was based largely on the observations of Druce (1973), and Barnes & Fåhraeus (1975) suggested that lateral segregation was controlled by environmental factors and that several distinct conodont communities could be recognised. They demonstrated how faunas from both the North Atlantic and Midcontinent Provinces could be arranged into a lateral sequence ranging from near-shore to progressively deeper-water environments. The main controlling factors for the conodont faunas from both provinces were a result of water temperature, salinity, water depth, oxygen content and substrate.

1.4 Conodont biofacies and provincialism during the Upper Ordovician

1.4.1 Provincialism

There have been numerous papers on Early Palaeozoic conodont provincialism since it was first discussed by Sweet *et al.* (1959) such as those by Bergström, (1971; 1973), Barnes *et al.*, 1973, Sweet & Bergström (1974; 1984), Lindström (1976) and Dzik (1983). Sweet *et al.* (1959) documented the presence of a North American Midcontinent Province and an Anglo-Scandinavian-Appalachian Province amongst late Ordovician conodonts. The latter was later re-named as the North Atlantic Province (Bergström, 1971). In general, this division of two conodont realms around the Iapetus Ocean throughout the Ordovician is widely accepted. However, there has often been confusion about the terminology used to describe the observed associations of conodont faunas. Early work characterised the principal biogeographic unit as a 'province'. However, more recently Bergström (1990) characterised this principal biogeographic unit as a 'faunal region' and divided it into sub-units called 'provinces'. However, as noted by Rasmussen (1998), Pohler and Barnes (1990) used the term 'realm' as the major unit, which was sub-divided into 'provinces'. According to Scotese & McKerrow (1990) provinces are regions separated by barriers whereas realms are climate controlled.

The North Atlantic Province included Baltoscandia and the easternmost part of Laurentia whilst the Midcontinent Province characterised Laurentia and Siberia. As described by Sweet & Bergström (1974) conodont faunas from the Midcontinent Province were believed to represent deposition in warm water conditions. These authors presented sedimentary information that inferred deposition in waters above 15° C within a latitudinal belt no more than 25-30° from the equator. Conversely, the North Atlantic Province was postulated by Sweet & Bergström (1974; 1984) to be dominated by cold water environments. Sweet and Bergström (1974) observed that conodont faunas from these two provinces remained generally discrete throughout the Ordovician.

Bergström (1990) provided an excellent review of conodont provincialism in the Late Ordovician. The Midcontinent Faunal Region *sensu* Bergström (1990) was further subdivided into the North American Interior Province and the Siberian

Province. He noted the Red River Province and Ohio Province in Laurentia and Australia and the Siberian Province in Siberia (see also Text-figure 1.4.1.).

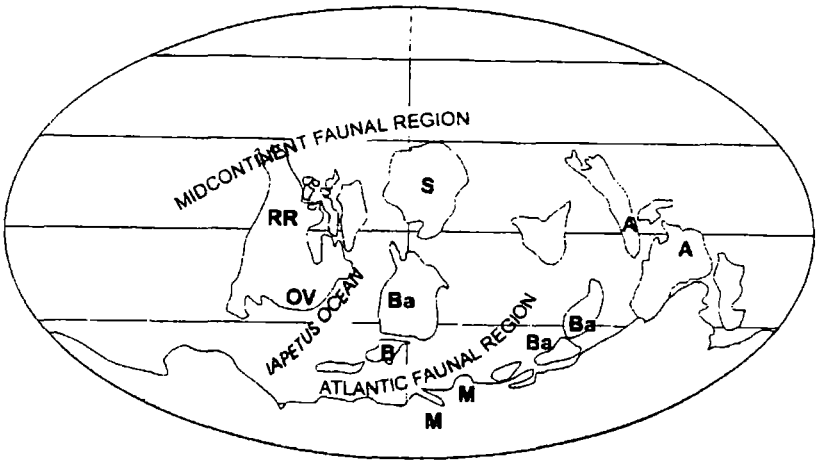

Text-Figure 1.4.1. The Conodont faunal regions and provinces for the Late Ordovician from Nowlan *et al.*, 1997. The Midcontinent Faunal Region includes the RR-Red River, OV-Ohio Valley, S-Siberian and A-Australasian. The Atlantic Faunal Region includes the Baltic –Ba, the British – B and the Mediterranean – M provinces.

In addition, Bergström (1990) separated the Atlantic Faunal Region into the Baltic and Mediterranean provinces including both the Baltoscandian and North American localities in the former. He recognised a similarity between the Baltic and British Provinces but noted that a distinctive high-latitude conodont fauna dominated the high latitude Mediterranean Province.

More recent reviews have been provided by Nowlan *et al.*, (1997) and Rasmussen (1998). Nowlan *et al.* (1997, p.533) proposed a new province on the basis of examinations of conodont faunas from the Late Ordovician of eastern Australia, the Australasian province (Nowlan *et al.*, 1997, p. 533) (see Text-figure 1.4.1.). Faunal Provinces are therefore largely latitudinally controlled which suggests that climate and temperature are the major controlling factors.

1.4.2 Biofacies

Biofacies is a term used to describe different faunal groups within specific lithofacies of a depositional unit i.e. an objective term to define groups of conodont taxa derived from certain lithologies (Pohler & Barnes, 1990). One of the most comprehensive studies of conodont biofacies is that of Sweet & Bergström (1984). Sweet & Bergström (1984) conducted a statistical cluster analysis on the occurrence and distribution of Late Ordovician conodonts from the warm water North American Red River and Ohio Valley provinces. They recognised six intergradational biofacies each named after its most distinctive conodont occurrence and believed to represent near shore, shallow water environments to offshore, deeper-water environments. Species characterising the two environments were shown by Sweet & Bergström (1984) to be mainly endemic in the shallow waters but cosmopolitan in deeper environments. Further analyses of conodont faunas from other provinces (British, Baltoscandian and Mediterranean) revealed only three distinct biofacies (defined at generic level) in what was believed by the authors to be a dominantly cold-water environment. Furthermore, Sweet & Bergström (1984) stated that only a third of the taxa in the Late Ordovician cold water region were also represented in warm water areas where they characterised deeper water biofacies or had a distribution indicative of eurythermal cosmopolites.

Palaeo-environment	Lower Ashgill Biofacies	Upper Ashgill Biofacies	Modern Ocean
Continental shelf	*Aphelognathus* – *Oulodus* *Plectodina*	*Plectodina* *Pseudobelodina*	Shelf
Continental slope	*Amorphognathus* *Phragmodus*	*Ozarkodina* *Oulodus*	Bathyal
Continental rise – abyssal	*Dapsilodus* *Periodon*	*Distomodus* *Dapsilodus*	Abyssal

Text -Figure 1.4.2. Ashgill Biofacies as described in the text (information derived from Sweet & Bergström, 1984, drawn from Armstrong, 1996).

Sweet & Bergström (1984) identified a shelf edge *Amorphognathus superbus – Amorphognathus ordovicicus* Biofacies. Within this Biofacies, elements of *Amorphognathus* comprised 16-63% of the fauna. Other elements within this Biofacies could also reach high abundance (e.g. *Plectodina* and *Phragmodus* 27% and 19% respectively, and *Panderodus* 30%). Sweet & Bergström (1984) also included the coniform genera *Drepanoistodus*, *Dapsilodus* and *Protopanderodus* in the *Amorphognathus* Biofacies. The deep-water *Dapsilodus mutatus – Periodon grandis* Biofacies was identified close to the Carbonate Compensation Depth. *Dapsilodus mutatus* and *Periodon grandis*, with percentage abundance values of 38% and 18% respectively, dominated the fauna comprising this Biofacies (Sweet & Bergström, 1984). Other taxa assigned to this Biofacies included *Phragmodus undatus* (<1%), *Icriodella superba* (<1%) and the coniform taxa of the *Amorphognathus* Biofacies as listed above.

Sweet & Bergström (1984) postulated that water depth may not have been the fundamental controlling factor on the occurrence of the Midcontinent biofacies suggesting that temperature, salinity, turbidity and other depth related environmental factors played an important role. The characteristics of each biofacies are fully discussed in Sweet & Bergström (1984) and the pertinent information is summarised in Text-figure 1.4.2.

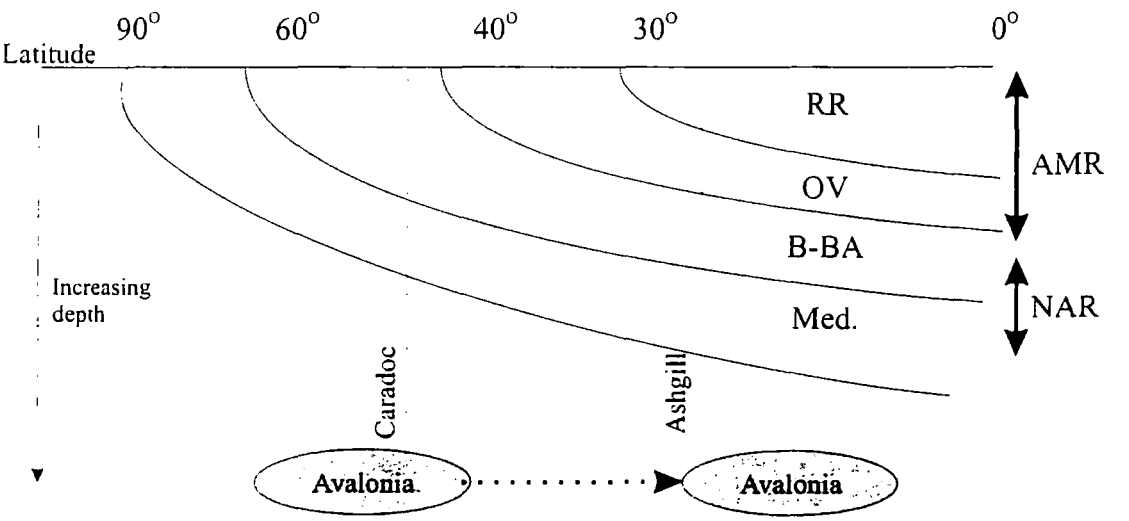

Text-Figure 1.4.3. The link between Provincialism and Biofacies. AMR = American Midcontinent Realm, NAR = North Atlantic Realm, RR= Red River Province, OV = Ohio Valley Province, B-Ba = British-Baltic Provinces, Med = Mediterranean Province.

At the present day organisms adapted to high latitude conditions occur at increasing depth towards lower latitudes. In the context of the Upper Ordovician a conceptual link between conodont provincialism and biofacies is that higher latitude province faunas will be found at depth in lower latitudes (Text-figure 1.4.3). Therefore, the progressive drift of Avalonia throughout the Caradoc and Ashgill should track such changes and record the appearance of lower latitude conodont faunas of the Ohio Valley and Red River.

1.5 Palaeogeographical context

A number of independent continental plates existed during early Palaeozoic times. These included Laurentia, Baltica, Siberia and North China, in addition to the Gondwana plate which was fully assembled by the late Precambrian (Torsvik, 1998). North America, Greenland and the components of Scotland and northern Ireland which lay on the margin of the Laurentian plate, collided with Baltica and probably Avalonia during Silurian times (Torsvik, 1998, figs 1-5, pp. 110-114) although the latter may have docked earlier (Pickering *et al.*, 1985).

Ordovician palaeogeography has been reconstructed using palaeomagnetic data and includes a variety of controversial and conflicting interpretations. For example, palaeomagnetic data have been used to record the progressive drift of southern Britain across the Iapetus Ocean during Ordovician times. The destruction of this ocean has been suggested on both geological and palaeomagnetic data to have occurred either in the late Ordovician (e.g. Pickering *et al.*, 1988), the Silurian (Soper *et al.*, 1992) or the Early Devonian (Woodcock *et al.*, 1988).

Palaeomagnetic evidence suggests (e.g. McKerrow, 1988; Scotese & McKerrow, 1990) that in Early Ordovician times Avalonia rifted from Gondwana. This has been further constrained from volcanic evidence to have occurred in the Late Tremadoc (Kokelaar *et al.*, 1984). Some palaeomagnetic data (e.g. Johnson *et al.*, 1990) place Avalonia at temperate latitudes during the Ordovician. Plots of poles from England suggest that Avalonia was situated in sub-tropical latitudes by late Ordovician times (Torsvik, 1998).

During the early Ordovician, Laurentia, Siberia and the North China block occupied equatorial latitudes (Text-figure 1.5.1.). Faunal evidence from the early Ordovician (e.g. Cocks & Fortey, 1990) indicates that in general there was a separation of palaeocontinents into three distinct areas depending on their latitude. Laurentia, Siberia and North China were all in low-latitudes whereas Baltica was situated in intermediate latitudes. High latitude areas included areas of northwest Gondwana, Avalonia and Armorica (Torsvik, 1998).

In lower Ordovician times (Arenig) Avalonia moved from the margins of Gondwana and the northwards drift of this palaeocontinent through the mid- and late Ordovician opened the Rheic Ocean (see Text Figure 1.5.2.). Detrital limestones were common in Baltica until the late Ordovician when carbonate build-ups developed (Bruton *et al.*, 1985), this suggesting a slow northward movement into lower latitudes through time. This indicates that the climate was warm in Baltica during the mid Ordovician and became equatorial (like Laurentia) by the end of the Ordovician. During the Ordovician Baltica rotated counter clockwise as it moved northwards (Text Figure 1.5.1).

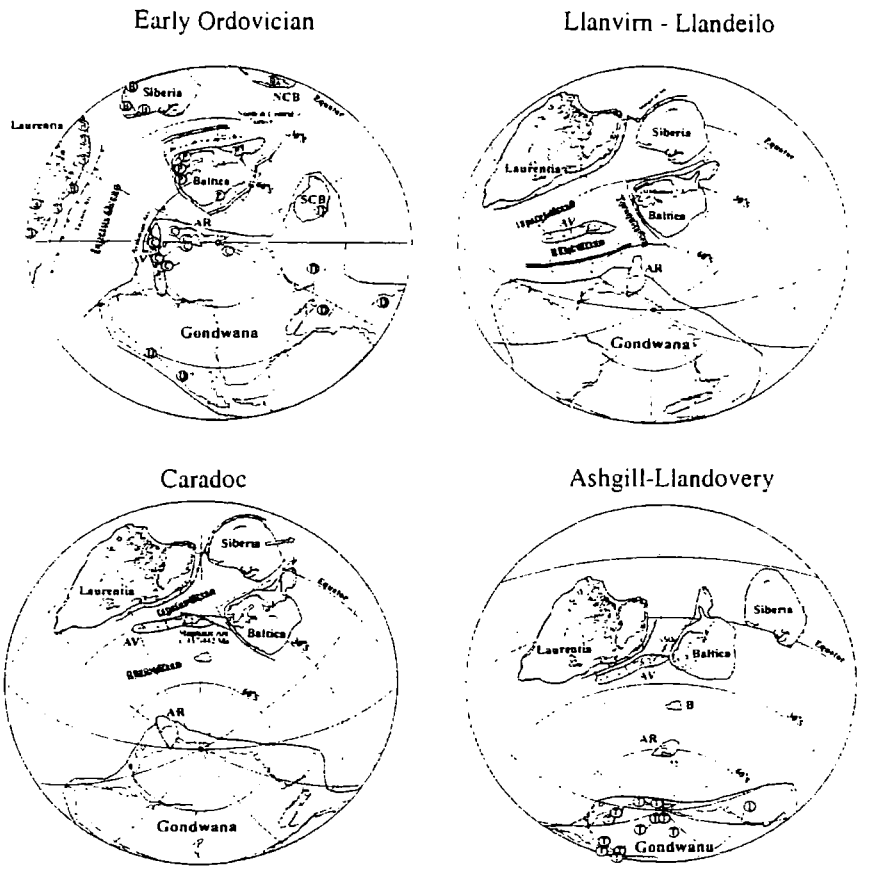

Text Figure 1.5.1. Plate reconstructions through the Ordovician showing the changing positions of the palaeocontinents. Late Tremodoc – early Arenig (top left) c. 480-490Ma, Llanvirn to early Caradoc (Llandeilian) (top right) c. 464 Ma, Caradoc (btm left) c. 450 Ma and Ashgill to Llandovery (btm right) c. 443 Ma. NCB = North China Block, SCB = South China Block, AV = Avalonia, AR = European Massifs. Adapted from Torsvik (1998).

Text-figure 1.5.1 shows the inferred relationships between Laurentia, Avalonia, Baltica and Gondwana and their palaeolatitudinal positions through time. From their results of palaeomagnetic reconstruction from Wenlock strata Trench & Torsvik (1991) stated there was no oceanic separation between Britain and Laurentia/Baltica and the Iapetus Ocean was closed prior to the Arcadian Orogeny. From Text-figure 1.5.1 it can be seen that the latitudinal position of Eastern Avalonia during the Caradoc and Ashgill was approximately 30 - 35° S and by early Wenlock times (c. 430 Ma) this landmass had moved to a position of 13 ± 5° S (Trench & Torsvik, 1990). Trench & Torsvik (1995) also documented data for the latitudinal

positions of Eastern Avalonia and Baltica from Ordovician to mid-Silurian times concluding that this favoured their amalgamation prior to the collision of Avalonia with Laurentia. More precisely, it has been documented (McKerrow, 1988; Scotese & McKerrow, 1990) that the collision of Avalonia and Baltica started early in the Ashgill.

Part I of this thesis will focus on the conodont faunas from the oceans bordering both Avalonia and Baltica during the late Ordovician (Caradoc and Ashgill). Text-figure 1.5.2 shows the inferred positions of Avalonia, Baltica and Laurentia at this time with Avalonia at ~40° S, Baltica at ~30° S and Laurentia straddling the equator.

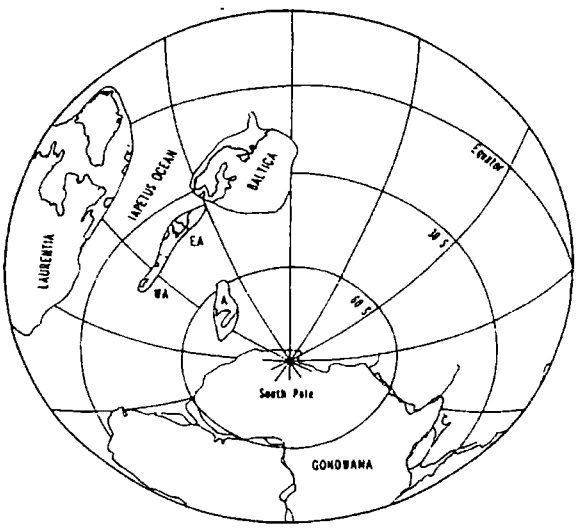

Text-Figure 1.5.2. The reconstruction from palaeomagnetic data (Trench & Torsvik, 1995, p. 868) of the Iapetus bordering continents in the Late Ordovician (Caradoc and Ashgill *c.* 450Ma).

The latitudinal position of a continent affects its climate. The northwards drift of both Avalonia and Baltica to positions nearer the equator should be reflected in climate changes. Moreoever, the global and regional climate regime will also affect the ocean-state. These aspects are therefore important when considering the occurrence of conodont biofacies in the late Ordovician oceans.

The Ordovician was a time of marked faunal provinciality within groups such as the conodonts, trilobites and graptolites (e.g. Cocks & Fortey, 1990). Palaeogeography and the positions of continents therefore also affect the distribution of faunas in respect to availability of migration routes.

1.6 Palaeoclimate and palaeo-oceanographic context

After the late Precambrian glaciation the Earth entered a warm phase lasting over 100 million years (Frakes *et al.*, 1992). The onset of glaciation and the development of ice sheets over North Africa in the mid- to late Ordovician terminated this warm phase.

Global oceanography responds to variations in climate. Lower Palaeozoic ocean conditions have been broadly divided into two end-members; P-state and S-state (Jeppsson, 1990). P-State oceans are characterised by thermohaline circulation and thermal stratification (Text-figure 1.6.1). In contrast, S-state oceans are salinity stratified. As a result, ocean bottom circulation is not active and oceans are poorly ventilated (Text-figure 1.6.1). Jeppsson (1990) developed this model by linking climate changes, biotic changes and changes in ocean state.

Conditions opposite of the greenhouse climate in the Cambrian are indicated by oxygenation of the deep-ocean floor. The sedimentary record of the Palaeozoic shows the world's oceans were oxic during the Late-Cambrian, mid-Ordovician, Ashgill and mid-Wenlock (Leggett *et al.*, 1988; Frakes *et al.*, 1992).

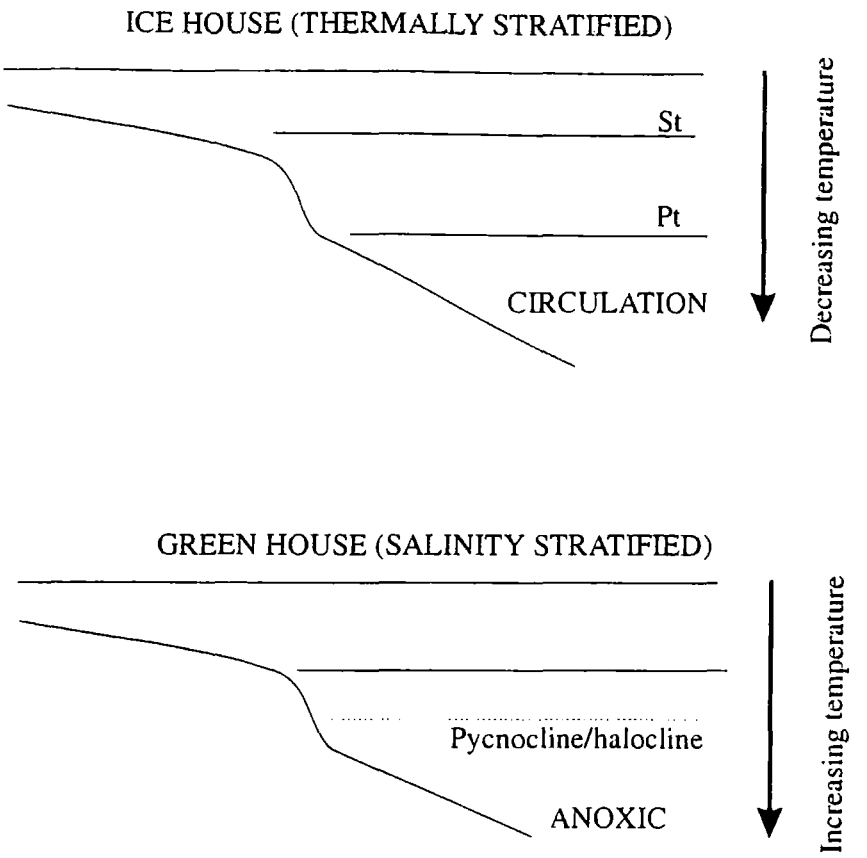

Text-Figure 1.6.1. Thermally and salinity stratified oceans. Pt = permanent thermocline. St = seasonal thermocline.

Modern oceanographic studies show how oceans are divisible into distinct zones (Gage & Tyler, 1991). These zones are effectively divided by the position of thermoclines within the oceans. Text -figure 1.6.2 (middle) shows the structure of an ocean at mid-latitudes. The seasonal thermocline (ST) (varies throughout the year) is positioned at the shelf break and marks the upper limit of the bathyal ecozone. The permanent thermocline (PT) is found at deeper levels within the ocean and marks the upper limit of the lower or abyssal ecozone and normally coincides with the upper slope rise. At high latitudes ocean structure is notably different. In this case the seasonal thermocline is absent and the PT occupies higher levels in the water column intersecting with the surface at approximately 60° north and south. This reduces the space of the bathyal ecozone but increases that of the abyssal zone. During a marine transgression, the permanent thermocline rises up the water column to higher levels therefore moving the position of the corresponding ecozone (see Armstrong, 1996

for full review). The depth of these fundamental boundaries within the early Ordovician is likely to have been markedly different at times to those of the Recent.

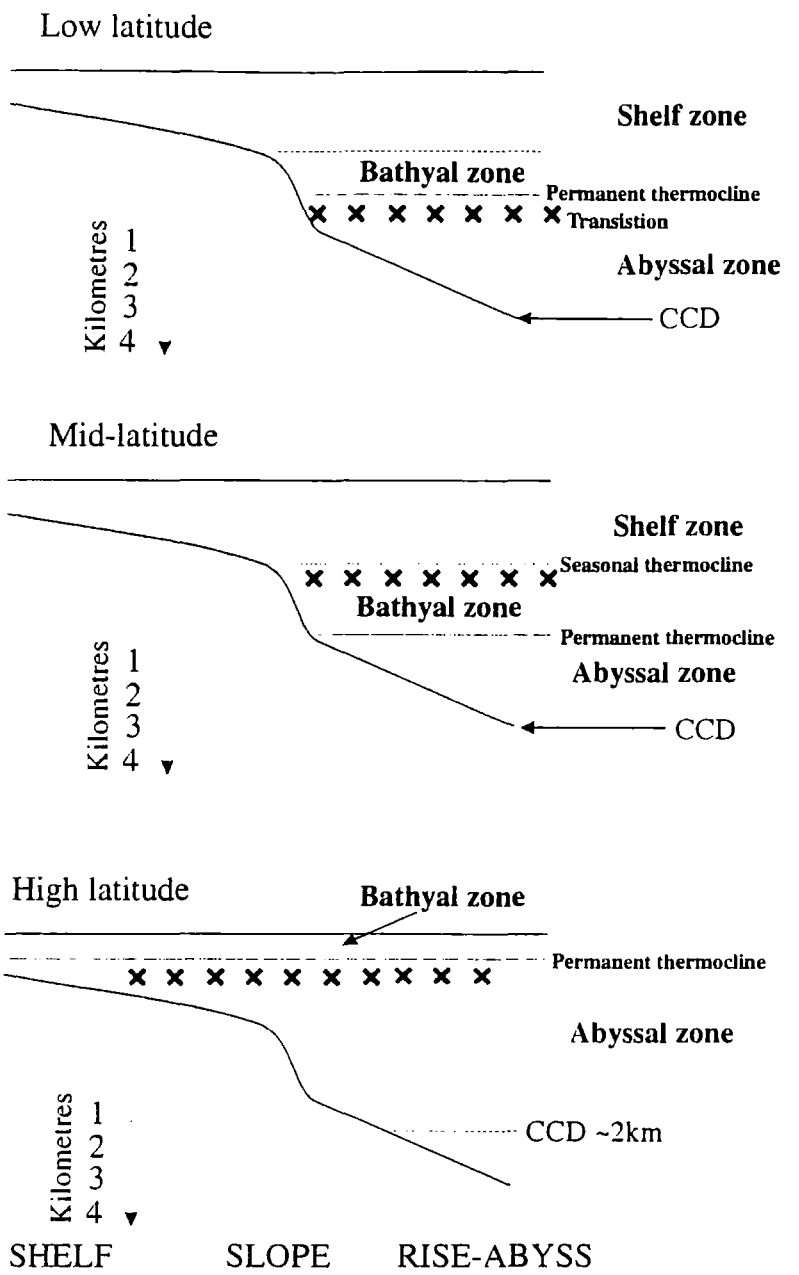

Text-Figure 1.6.2. Ocean states and ecozones in low latitude (top), mid-latitude (middle) and high latitudes (btm) oceans. Adapted from Armstrong (1996).

Armstrong & Coe (1997) described the sedimentological changes associated with the end Ordovician glaciation. Their evidence suggested that global cooling began with the initiation of ocean bottom circulation in the Pusgillian. This was followed by a period of increasingly intense thermohaline circulation by the late Rawtheyan and a rapid de-glaciation in the mid-upper Hirnantian.

This change in ocean-state i.e. the resumption of thermohaline circulation and its effect on the faunal component of the ecozones was proposed by Armstrong (1996) and is outlined in Text-figure 1.6.3. This model predicted that during an extended greenhouse period, low latitude oceans would be salinity stratified and lack of deep-ocean circulation would cause extinction of abyssal species unable to move into the bathyal ecozone. Armstrong (1996) further described a transitional stage from an S to a P-state ocean spanning the period of pre-glacial global cooling. This stage would be reflected in the development of a seasonal thermocline leading to isolation of both the bathyal and shelf ecozones, although the former would expand down the slope. Armstrong (1996) postulated this expansion would cause a decrease in population densities, isolation and restricted gene flow resulting in cladogenesis and increased zonation in the bathyal ecozone. In a P-state ocean, Armstrong (1996) predicted that, during the regression, shelf species would migrate towards the shelf break, and potentially, the shelf ecozone could expand down the slope. In higher latitudes or with ocean cooling, the upward movement of the permanent thermocline would restrict the bathyal ecozone and reduce downwards migration of shelf species. Armstrong (1996) further postulated that as surface waters cooled, habitats on the shelf would become vacant as warmer water taxa became extinct. As the permanent thermocline moved up through the water column, bathyal taxa could migrate and occupy these habitats. On the return to S-state ocean conditions, resumption of deep-sea anoxia would isolate eurytopic bathyal species and leave them restricted to shallower waters.

During subsequent transgression, this fauna would expand onto the shelf and deeper bathyal species would migrate in deeper waters on the shelf.

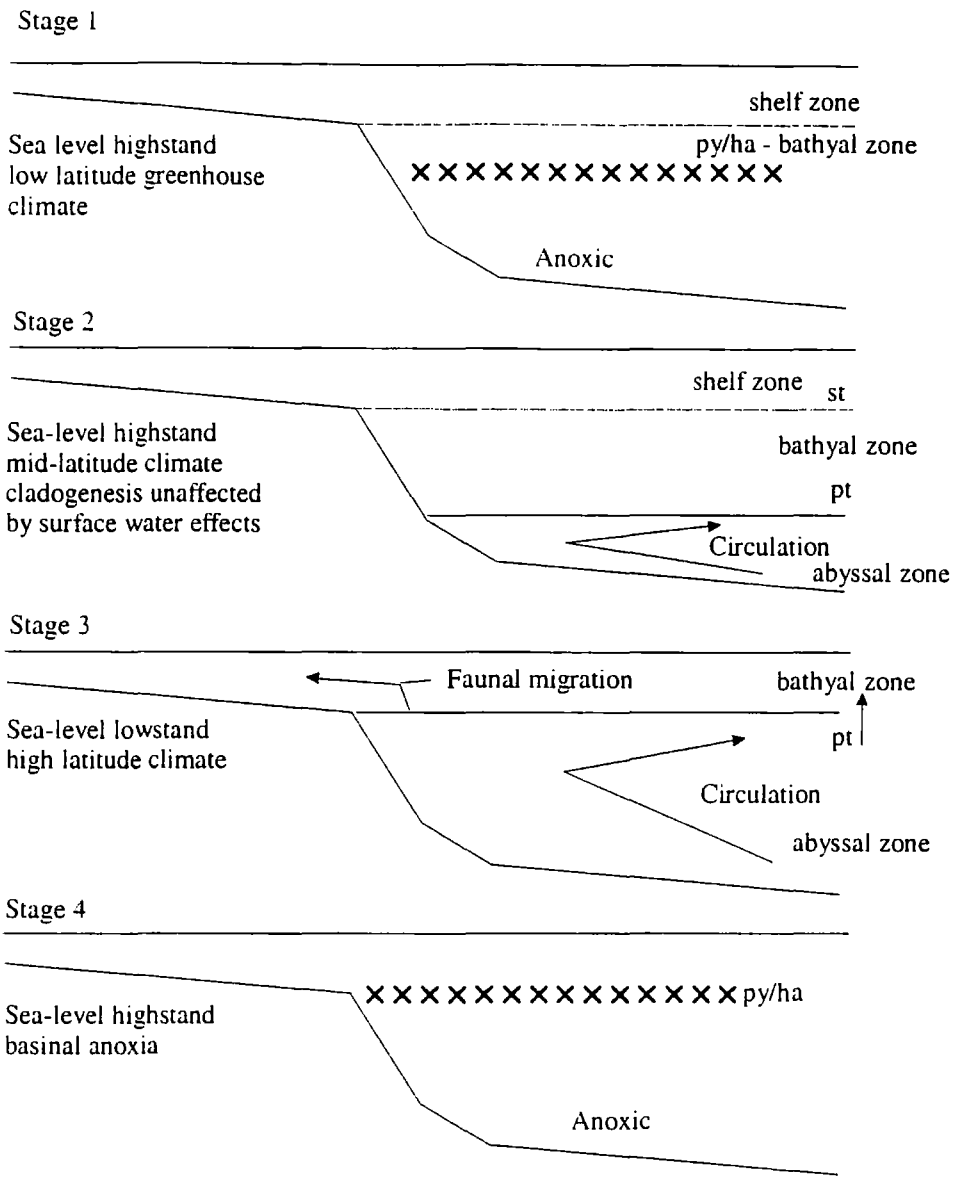

Text-Figure 1.6.3. The proposed changes in ocean state from s-state to P-state. Pt = permanent thermocline, py = pycnocline, ha = halocline (after Armstrong, 1996).

This model (Armstrong, 1996) therefore predicts faunal movement in response to both changing ocean states and sea level. During cooling and regression faunas will move offshore and during transgression or warming, faunas move inshore.

The Caradoc and Ashgill conodont faunas of Avalonia and Baltica were subject to two fundamental and competing processes affecting environmental change. Firstly the global and ocean cooling which should have led to the emergence

of deeper, cooler biofacies and secondly, the northwards drift of these micro-continents into warmer latitudes. Sedimentological evidence indicates ocean states altered in Pusgillian times.

Cooper (1999) proposed an ecostratigraphic model for early Ordovician graptolites assessing the distribution of graptolites in terms of depth, facies, palaeolatitude and time. This work showed the pattern and distribution of Tremadoc graptolite species from the shore to ocean profile and how fluctuations in this pattern could be related to eustatic changes.

Cooper *et al.* (1991) reviewed the distribution of early Ordovician graptolites across a range of depth facies. This resulted in the division of graptolites into three groups representing those restricted to shallow water sediments (didymograptid biofacies), deep-water sediments (isograptid biofacies) and a third group common to both shallow and deep environments and therefore not facies dependent.

In terms of the oceanic ecozones occupied by each group, Cooper *et al.* (1991) stated that graptolites restricted to the isograptid biofacies inhabited deep water meso-bathypelagic depths whereas those common to deep and shallow were likely to have inhabited the epipelagic (shallow) depth zone. Didymograptid biofacies were also postulated to inhabit shallow, but inshore waters of the epipelagic zone.

Application of this model to early Tremadoc graptolites indicated that most inhabited the deep-water biotope, particularly the continental slope. Cooper (1999) attributed this to the oceanographic conditions within this environment. He postulated that because the continental slope is subject to upwelling and the influx of high nutrient waters/plankton productivity (e.g. Berry *et al.*, 1987) this would result in a favourable habitat for graptolites. Such oceanic conditions in the continental slope region may therefore result in a complex association of forms comprising a mixture of biofacies.

Graptolites occupying the epipelagic biotope found in both biofacies, were noted to only encroach on the inner shelf at times of sea-level high stand, and in general the inner shelf is an area of low diversity. In contrast, during sea level low stands, forms normally confined to the inner shelf zone reached outer shelf areas and sometimes encroached onto areas of the upper slope (Text-Figure 1.6.4).

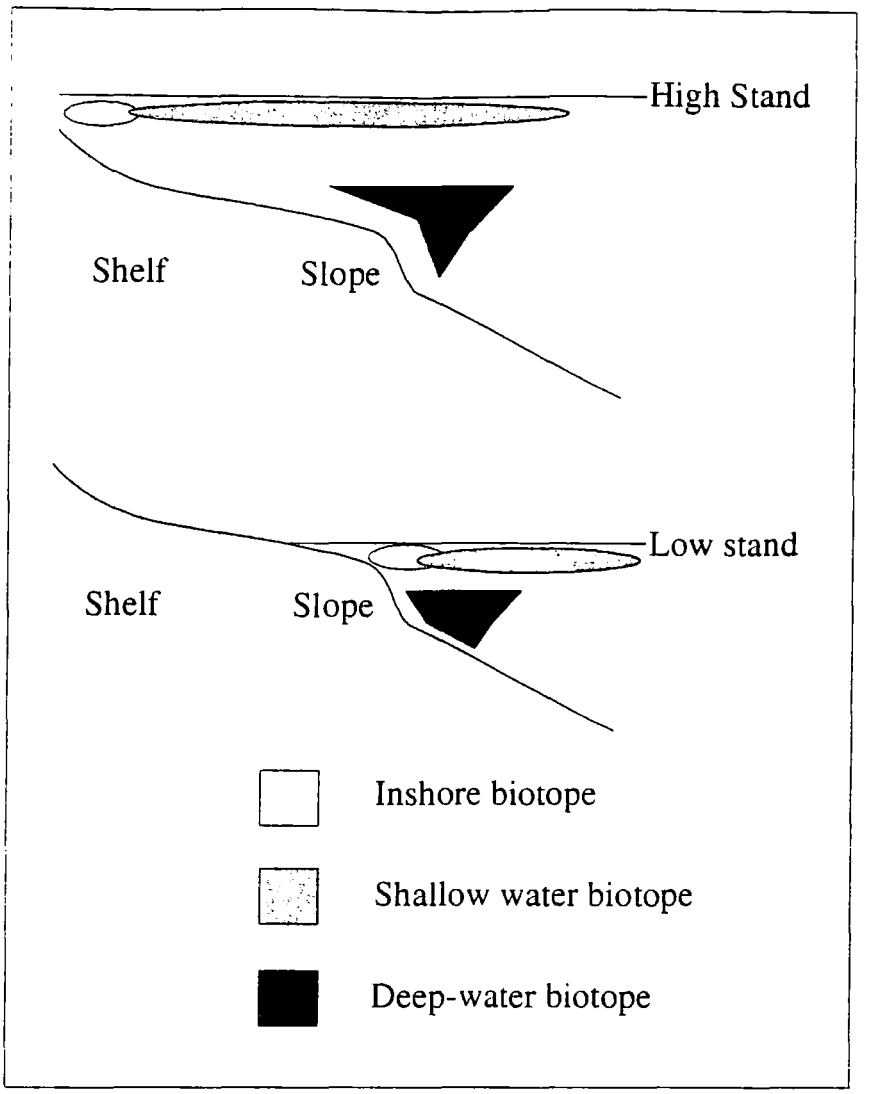

Text-Figure 1.6.4. The shore-ocean profiles showing the distribution of graptolite biotopes at times of high stand and low stand (drawn from Cooper, 1999).

The upper slope area can therefore occupy deep-water biofacies at times of highstand, inshore biotopes at times of lowstand coupled with the background 'rain' of pandemic forms of the epipelagic zone (Cooper, 1999). This model predicts that faunal emergence accompanies highstands and submergence accompanies lowstands.

Cooper (1999) also concluded that the oceans at this time had a well-developed oxygen minimum zone between the surface waters and the anoxic bottom waters (Text-figure 1.6.5.).

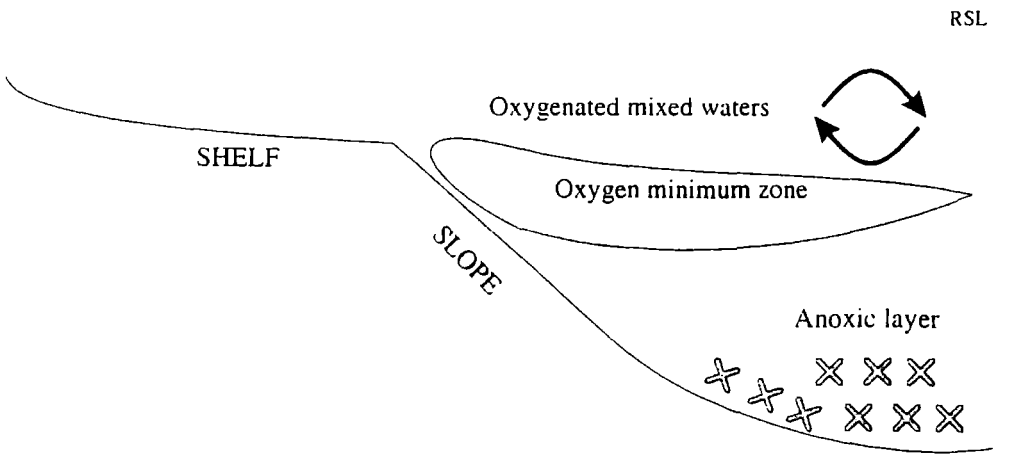

Text-Figure 1.6.5 Simplified vertical profile of the proposed oceanic conditions operating in the early Ordovician (see Cooper, 1999 and references therein).

The oxygen minimum zone (OMZ) is characterised by a richness of nutrient minerals and bacteria, which was postulated to provide a preferred habitat for graptolites belonging to the deep-water biotope (Finney & Berry, 1997). The habitat would however be restricted by regressive episodes caused by ice cap growth as cold water, density driven, bottom currents would ventilate the ocean and minimise the development of the sulphidic layer (Cooper, 1999). Cooper *et al.* (1990, figure 5, p. 9) showed how this could explain the restricted distribution of graptolites at times of major regression. The opposite is true during episodes of marine transgression when the preferred habitat of graptolites would be extensively developed promoting diversification of faunas (Cooper, 1999).

The implications of this model (Cooper, 1999) are as follows:

1. Major transgressions are accompanied by a rapid increase in abundance and diversity of graptolites.

2. Graptolites are most abundant and diverse along the continental margin
3. During times of regression graptolites are rare or absent from oceanic facies.

1.7 Phylogenetic emergence and submergence in the evolution of conodont clades

The phylogenetic emergence hypothesis predicts that during a marine transgression (highstand) there should be progressive appearance of deeper water conodont biofacies at higher levels in the marine profile. The impingement of slope conodont biofacies on the continental shelf and deep biofacies on the continental slope should therefore be seen in a section representing a continuous transgressive episode/highstand. The phylogenetic emergence of deeper water conodont biofacies of Avalonia and Baltica is potentially complicated by the northward drift of these microcontinents during the Upper Ordovician. Nektobenthic conodonts from slope biofacies potentially occupied the OMZ. If they were adapted to oxygen depleted and nutrient rich waters then they should parallel the graptolites in temporal and spatial variations whilst sea-level changes.

The critical test of this hypothesis is to demonstrate that deep-water conodont biofacies emerge on successive transgressions.

1.8 Ordovician sea-level fluctuations as a test of phylogenetic emergence

The Upper Ordovician (Caradoc and Ashgill) is characterised by a series of transgressions or highstands (Ross & Ross, 1992). These occurred repeatedly during a relatively short duration especially during the Ashgill. The Ashgill has been estimated to be only between 4 and 8 million years in duration (Barnes, 1992) or, more precisely, 5 million years duration (Tucker *et al.*, 1996). Text-figure 1.8.1 illustrates how the sections studied in this thesis relate to the global, eustatic sea level curve.

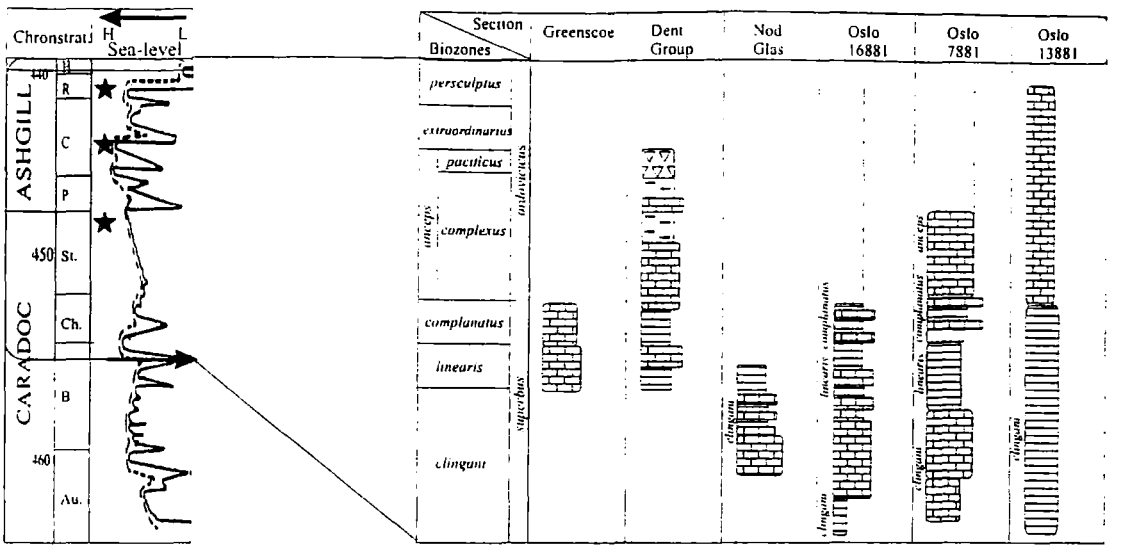

Text-Figure 1.8.1. The proposed sea-level curve for the Caradoc and Ashgill (adapted from Ross & Ross, 1992) and the chronostratigraphy and biozones (graptolite & conodont) based on Fortey *et al.*, 1995. Additionally, each of the sections described in Part I are placed in their stratigraphical positions and major transgressive episodes described are marked by star symbols.

Brenchley *et al.* (1994, p. 295) noted sea-level rose from the early Caradoc (the *gracilis* transgression) whereas the Ashgill curve shows a short-term fall in sea-level close to the end of the series. The latter is correlated with the glacial episode (Hirnantian) and calculations (Brenchley & Newall, 1983; Crowley & Baum, 1991) have indicated a sea-level fall of either 60 or 45 metres. Armstrong & Coe (1997) further divided the Rawtheyan and Hirnantian (glacial maximum) into a series of distinct cycles believed to represent the changing oceanographic and climatic conditions. The sections analysed as Part I of this thesis relate to transgressive episodes of the Onnian (end Caradoc), Cautleyan (Zone 2) and the Rawtheyan (see Text-figure 1.8.1).

1.9 Summary

Palaeo-oceanographic models predict an S-state or greenhouse ocean during most of the Ordovician. A consequence of this is a three-layered ocean with an anoxic bottom layer, a well-developed OMZ, particularly in areas of coastal upwelling (e.g. the edges of basins) and an upper oxygenated well-mixed layer. The temporal occurrence of conodont biofacies in any stratigraphic succession may be a result of these fundamental oceanic conditions and associated fluctuations in temperature, sea-level, oxygenation and ocean state. The late Ordovician was a time when many glacially induced transgressive/regressive episodes occurred and such conditions are ideal for studying the relative movement and stability of deep-water biofacies. If the model of Sweet & Bergström (1984) is to be sustained then characteristically deep-water conodont genera (e.g. *Amorphognathus*, *Phragmodus* and *Periodon*) will be present in shallow water sediments during a relative sea-level rise or global/ocean cooling.

Two competing processes were operating on the Iapetus Ocean and hence conodont facies distribution.

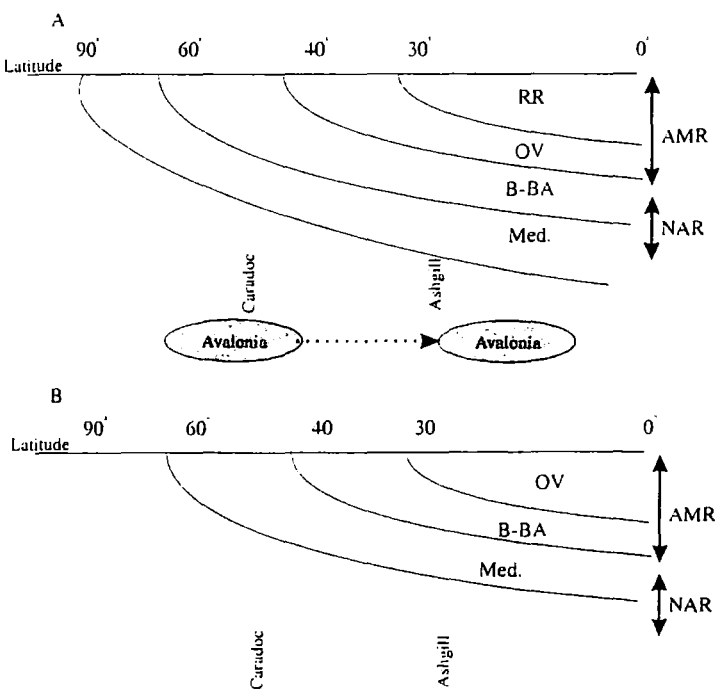

Text-Figure 1.9.1. A. The effect on conodont biofacies with northward drift. B. The effect on biofacies with global cooling. Biofacies move towards the equator.

1. Northwards drift of Avalonia and Baltica into subtropical latitudes (Text-figure 1.9.1A)
2. Global cooling associated with the onset of Glaciation (Text-figure 1.9.1B) leading to the equator-ward movement of biofacies boundaries.

The temporal changes in conodont biofacies distribution provides an independent test of the response of the tropics to global cooling during the late Ordovician.

Having documented the temporal distribution of conodonts in the critical sections. Part I of this thesis aims to test Sweet & Bergström's (1984) model of depth related conodont biofacies and to test models of phylogenetic emergence of deep-water conodont biofacies during transgressive episodes. Moreover, it will assess the stability of the deep-ocean conodont community and outline the aspects of palaeo-oceanic variables (oxygenation, salinity, temperature etc.) versus sea level on distribution of deep-water conodont biofacies. In particular, the section at Gwern-y-Brain is characterised by abundant primary phosphate indicative of deposition in the oxygen minimum zone (OMZ). Chapter 2 provides a detailed analysis of the sedimentology and conodont species distribution in this unusual environment.

Because conodonts are difficult to extract from clastic deep-sea sediments, transgressive episodes may provide a window for the study of deep-water conodont biofacies.

1.10 Localities, materials and methods

Text-figure 1.10.1. shows the chronostratigraphy of the Ordovician system as produced by Fortey *et al.* (1995) and includes both the graptolite and conodont zonation. Within this part of the thesis the emphasis will be on conodonts ranging through the Streffordian (Caradoc), Pusgillian, Cautleyan and Rawtheyan stages of the Ashgill.

All of the analysed sections are of primary importance in the discussion of the placement of the *Amorphognathus superbus* - *Amorphognathus ordovicicus* biozone boundary and this subject will therefore be approached throughout Part I of this thesis. In addition to samples collected by the author, Drs. M.P. Smith (University of

Birmingham) and H.A. Armstrong (University of Durham) provided other conodont collections.

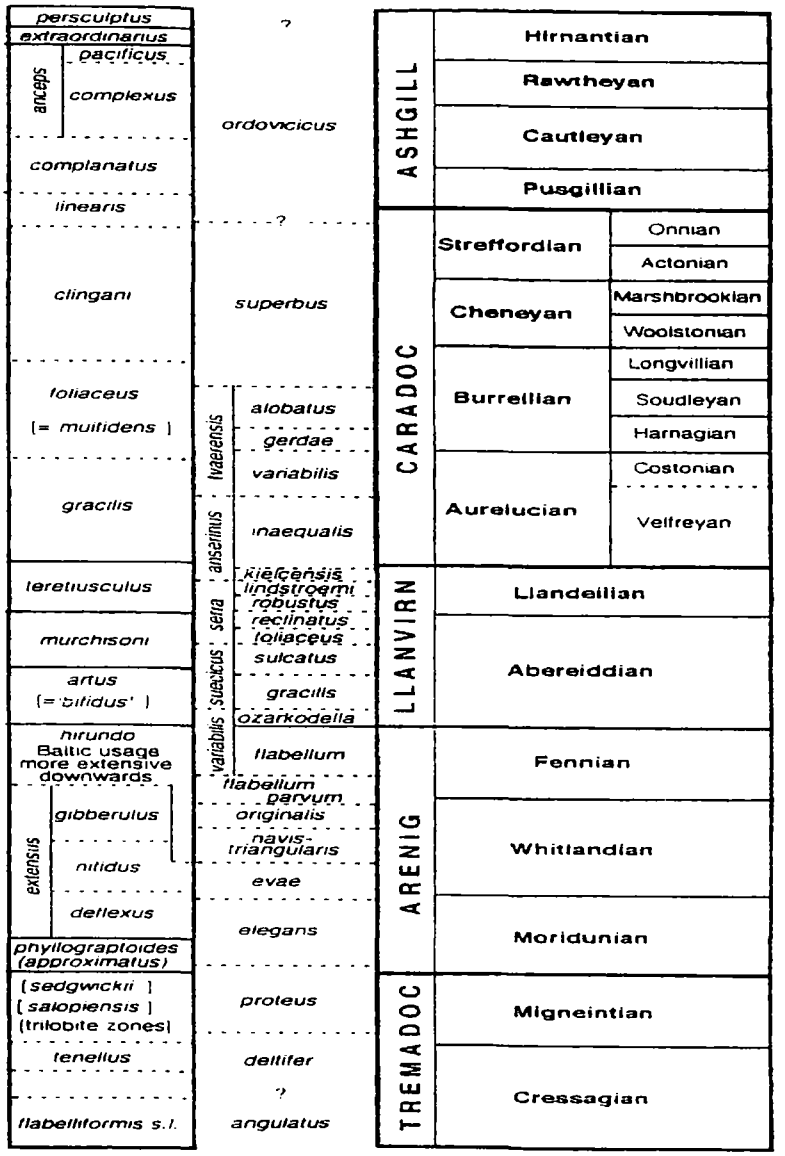

Text-Figure 1.10.1. Ordovician chronostratigraphy. Left hand column = British Graptolite zonation, Middle column = Baltoscandian conodont zonation, Right hand column = Chronostratigraphy (drawn from Fortey *et al.*, 1995).

1.11 Conodont Sample Preparation

Conodont samples collected by the author were typically between 1 and 2 kilograms in weight and were processed for conodonts using unbuffered acetic acid and a 63µm sieve. Large residues were often magnetically separated prior to heavy liquid separation in bromoform. Most specimens were easily studied by the use of a light-reflecting microscope and photomicrographs were taken by use of SEM (after gold coatings applied) facilities both at the Universities of Glasgow (Cambridge 360) and Durham (Camscan Series 2).

Part I - Chapter 2

2. The upper Ordovician conodont biofacies of Avalonia – The Nod Glas Formation

2.1 Introduction

This analysis of the Nod Glas Formation of the Welsh Borders represents a detailed case study of conodont faunas and biofacies during the latest Caradoc. The widespread Nod Glas Formation represents a late Caradoc deepening of the Welsh Basin. Sedimentological analysis of the phosphatic limestones from this unit suggests that initial deepening occurred during deposition of the lower part of the formation. Further deepening is reflected by the transition to black shales with graptolitic horizons occurring in the upper part. Although conodont samples have only been obtained from the basal few metres, distinctive faunal assemblages there reflect the changing environmental conditions and have wider implications for both deep-water conodont palaeobiology and basin evolution. The presence of phosphate within sediments from the lower section of the Nod Glas also has considerable implications for interpretation of the palaeo-oceanographic conditions at this time.

Conodont faunas within the Nod Glas Formation are also important in terms of biofacies analysis and the resolution of the biozonal boundaries for the base of the Ashgill, particularly with respect to the position of the *Amorphognathus superbus* - *Amorphognathus ordovicicus* biozone boundary. Aspects of this discussion will be fully addressed in Part I Chapter 4.

2.2 Aims

1. To document and the sedimentology and conodont occurrences within the Nod Glas Formation based on detailed field studies.
2. To analyse the sedimentology of the Nod Glas Formation in order to make more detailed palaeo-oceanographic interpretations.
3. To interpret the occurrences of conodonts in terms of the placement of the biofacies.

2.3 The Welsh Basin

The Welsh Basin is regarded as belonging to Eastern Avalonia, a continental fragment with Gondwanan affinities, rifting during Cambrian or early Ordovician times (Woodcock, 1990; Cocks *et al.*, 1997) and moving northwards impinging on both Baltica and Laurentia in the late Ordovician (Woodcock, 1990). Authors such as Hutton (1987), Pickering (1987), Soper (1988) and Cocks *et al.* (1997) have debated the timing of this collision.

Through the early Palaeozoic the Welsh Basin was an area of rapid sedimentation lying between the Midland Platform to the south-east and the Irish Sea Platform to the north-west (Jones, 1938; Woodcock, 1990). The three areas were believed to be discrete arc terranes assembled in Late Precambrian or early Cambrian time with the Midland Platform and Welsh Basin subject to strike-slip displacement in the late Ordovician (Gibbons, 1987; Woodcock & Gibbons, 1988).

The fill of the Welsh Basin includes sediments ranging from fine grained clastics to hemipelagic sediments with intermittent turbidites and volcanics deposited between the early Cambrian and early Devonian (Woodcock, 1990). The Ordovician volcanic activity is believed to be connected with arc processes in the late Tremadoc and inter-arc or back-arc extension from the Arenig to the Caradoc (e.g. Kokelaar, 1988).

Woodcock (1990) conducted a sequence stratigraphical analysis of the Welsh Basin succession identifying four basin-wide unconformities and less extensive unconformities bounding 18 component sequences. Woodcock postulated that the majority of these sequence boundaries reflected a component of tectonic (or volcanotectonic) influence rather than just eustatic sea-level change. He further attributed major sequence boundaries such as those in the early Cambrian, Tremadoc, late Caradoc and early Devonian to events such as rifting, onset of subduction, end of subduction and collisional deformation respectively. These events were also correlated across other basinal sections along the margin of Avalonia (Woodcock, 1990, figure, 7, p. 545) such as those in the Lake District (northern England) and Leinster (SE Ireland).

The Nod Glas Formation forms part of the Gwynedd Supergroup, a lithostratigraphic unit corresponding to megasequence II of Woodcock (1990). Woodcock proposed that of the six sequence boundaries within this megasequence only three (in the Arenig, upper Llanvirn, middle-Caradoc) could be attributed to purely eustatic control and stated that the rest could have had a volcanotectonic component. Given that the Nod Glas Formation is late Caradoc in age it seems tenable that the latter hypothesis is applicable to this formation.

2.4 Caradoc Outcrops

Caradoc outcrops extend over much of the Welshpool area. The majority of Caradoc rocks in this area are sandstones and mudstones indicative of shallow marine deposition in a mainly oxic environment (Cave & Price, 1978) but later in the Caradoc, conditions changed and increasingly anoxic conditions prevailed. The lower Caradoc includes grey friable mudstones (Trelydan Shale Formation, Harnagian), coarsening in the Soudleyan and Longvillian into the silty calcareous sandstones of the Woolstonian Gaer Fawr Formation. The Gaer Fawr Formation is shelly and bioturbated in its upper part indicating deposition on the outer edge of shelf areas (Cave & Price, 1978). Marshbrookian and Actonian sediments have not been recorded in the Welshpool area over the rest of North Wales (Cave & Dixon, 1993).

In the Welshpool area, the black shales and mudstones that constitute the Nod Glas Formation conformably overlie Longvillian rocks (Text-figure 2.4.1). The Nod Glas Formation crops out at Gwern-y-Brain Stream, Guilsfield near Welshpool (SJ 2180 1265 - SJ 2180 1285). It also crops out over parts of Northern and central Wales but Gwern-y-Brain is the only section in the formation to contain graptolites, conodonts and shelly fossils. The Nod Glas Formation at this locality therefore provides a rare association between the shelly and graptolitic zonal schemes in the Welsh Basin. Moreover, the composition of the conodont fauna is critical in the argument concerning the conflation of graptolite and conodont biozonal schemes at the base of the Ashgill series. The outcrop at Welshpool is close to the southern most extent of the formation. Cave (1965), and subsequently Cave & Price (1978) provided detailed maps and descriptions of this locality, and although Cave (1965;

fig. 2) presented a schematic sedimentary log of the Nod Glas Formation, it is not easy to relate this to the actual exposure at Gwern-y-Brain Stream. He subdivided the formation at Welshpool into two main divisions, the Pen-y-garnedd Phosphorite Member succeeded by the Pen-y-garnedd Shale Member. The basal Pen-y-garnedd Phosphorite was further subdivided by Cave into a basal limestone and above it a nodular bed. This division holds true for much of the southern Berwyns area (Cave & Dixon 1993).

Cave (1965) postulated that the Nod Glas Formation marked a significant change in depositional environments within the Welsh Basin such that after the cessation of Longvillian volcanicity, marine conditions became more anoxic and clastic input decreased. This change in the marine environment is reflected in the rocks of the Nod Glas at Gwern-y-Brain. Cave (1965) stated that the black mud deposits seemed to have formed under stagnant conditions but the fauna was neither sparse not dwarfed and had a high proportion of benthonic forms. Cave & Dixon (1993) suggested that the basal phosphatic limestones were formed under conditions that may represent the condensed Marshbrookian and Actonian stages, although Cave (1965) first speculated that these stages may be absent and an episode of non-deposition took place between the deposition of the limestone and the underlying Gaer Fawr Formation.

The reason for the change in sedimentary cycle from the Gaer Fawr to the Nod Glas Formation is unknown, but Cave & Price (1978) noted that it was probably a result of oceanic water influx from the west displacing the existing shelf regime.

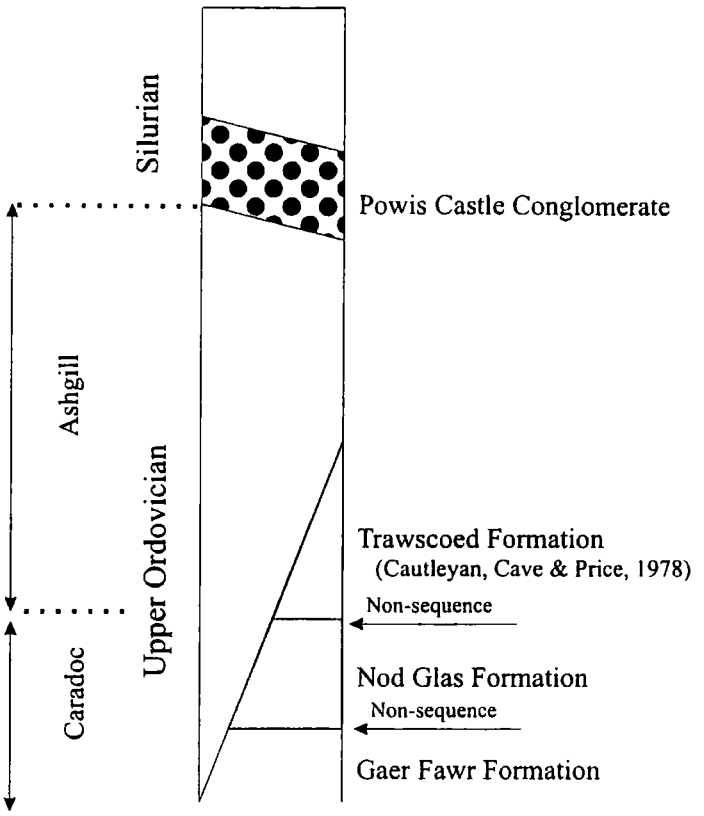

Text-Figure 2.4.1. The stratigraphical relationship of the Nod Glas Formation (adapted from Cave, 1965).

2.5 Age Constraints on the Nod Glas Formation

Constraining the age of the Nod Glas Formation near Guilsfield has proved to be problematical even though it is the only section in the formation to yield graptolite, trilobite, ostracode and conodont faunas.

The beds beneath the Nod Glas Formation in the Bala area contain a diagnostic fauna of *Estoniops alifrons* (M'Coy), *Platystrophia* cf. *sublimis* (Opik) and *Nicolella actoniae obesa* (Williams) (Cave, 1965). This fauna is indicative of a Woolstonian age and at Welshpool occurs in the Gaer Fawr Formation above beds containing *Dalmanella indica* (Whittington). The graptolites from the upper Penygarnedd Shale Member belong to the *Dicranograptus clingani* Zone (Cave, 1965). The boundary between the *clingani* and *linearis* biozones lies within the uppermost Caradoc (Fortey *et al.*, 1995). The trilobite *Onnia gracilis* was also found at this locality in the upper shale member of the Nod Glas Formation (Cave, 1965). Although *Onnia* is generally thought indicative of Onnian strata the earliest

occurrence of *O.gracilis* as a rare component in the Actonian fauna of the type Caradoc, Shropshire was noted by Owen & Ingham (1988).

Jones (1986) recorded an ostracode assemblage similar to that of the *O.gracilis* Acme Zone in the middle of the type Onnian although it is not clear whether samples were taken from the lower or upper member. A similar ostracode fauna was recovered from the lower phosphorites during this present study. The presence of the conodonts *Plectodina bullhillensis* and *Amorphgnathus* aff. *A. tvarensis* within the basal 50cm of the phosphorite led Savage & Bassett (1985) to suggest a Woolstonian age for this part of the Nod Glas Formation. This was based on the occurrence of *Plectodina* in other sections from Shropshire although they noted the fact that none of these sections are continuous.

2.6 Previous Conodont work

Conodonts from the Nod Glas Formation in the Gwern-y-Brain Steam have previously been described by Savage & Bassett (1985) who documented the occurrence of two distinctive faunas within the basal 80cm of the lower member. *Plectodina bullhillensis* and *Amorphognathus* aff. *A. tvaerensis* were found in a sample from the basal 50cm (Sample 77 of Savage & Bassett) whereas the upper 30cm of the phosphorites yielded abundant specimens which they ascribed to *Amorphognathus ordovicicus.* This led Savage & Bassett to speculate that the *Amorphognathus superbus-Amorphognathus ordovicicus* biozone boundary could be found within the basal Nod Glas phosphorites. They noted that *Plectodina bullhillensis* occurs in Shropshire only in strata from the Costonian to the Woolstonian and that the occurrence of *A.* aff. *A. tvaerensis* may support an even earlier (pre-mid Soudleyan) age for the Nod Glas Formation. Savage & Bassett's (1985) faunal list is shown in Table 2.6.

Table 2.6

Sample 77 (basal 50cm of phosphorite Member)	Sample 78 (upper 30cm of phosphorite member)
Amorphognathus aff A. tvaerensis	*Amorphognathus ordovicicus*
Icriodella superba	*Drepanoistodus*
Plectodina bullhillensis	*Panderodus*
Rhodesognathus elgans	*Phragmodus*
	Rhodesognathus
	Protopanderodus

Table 2.6. The Nod Glas Phosphorites conodont faunal list of Savage and Bassett (1985).

Additional work by Bergström & Orchard (1985) revealed the presence of two *Amorphognathus* - *Rhodesognathus* bearing faunules from low and high in the Nod Glas Phosphorites. They further stated that the lower fauna also included *Icriodella superba* and *Plectodina* whilst the higher one was found to contain both *Phragmodus* and *Protopanderodus*. Bergström & Orchard (1985) also document the presence of *Amorphognathus* cf. *A. complicatus* in the higher faunule of the Nod Glas Formation.

Although these previous studies have revealed the presence of a diverse conodont fauna, this information has not yet led to the definite location of the *Amorphognathus superbus* - *Amorphognathus ordovicicus* biozone boundary as the discovery of *A. superbus* from the section has not yet been documented. The identification of *Amorphognathus ordovicicus* from the Nod Glas formation (Savage & Bassett, 1985) also remains controversial (e.g. Bergström & Massa, 1992, Ferretti & Barnes, 1997).

2.7 Description

Both the lower phosphorite and upper shale members of the Nod Glas Formation are well exposed in the bed and banks of Gwern-y-Brain Stream. The section in the Gwern-y-Brain was re-logged as part of the present study (Text-figure 2.8.2) and shows variations from the log of Cave (1965). The most notable difference is in the position of several of the discrete phosphate and nodular bands within the section. Several of these were not found to be at the same horizon assigned by Cave (1965) and the complete section was found to be of greater vertical thickness. The contact between the Nod Glas Formation and the underlying formation cannot be seen clearly but the basal phosphorite member of the Nod Glas Formation forms a series of small steps or waterfalls. The upper Penygarnedd Shale Member crops out above the phosphorites although these outcrops in the banks of the stream are difficult of access. From the upper Gaer Fawr Formation Sample 591 is a pale grey slightly bioclastic greywacke showing few signs of phosphatisation. 592 is however, considerably darker in colour and contains small black fragments.

The basal five metres of the Penygarnedd Phosphorites is dominantly composed of dark grey crystalline limestones where slight changes in lithology can be seen in hand specimen. Within the initial few metres of the Penygarnedd Phosphorites several gaps in exposure are apparent and may represent intermittent bands of softer, more easily weathered mudstones. The first outcrop of mudstone is seen at approximately 2 metres from the contact with the lower Gaer Fawr Formation and yields a sparse shelly fauna of brachiopods preserved as small moulds. Above this horizon, harder intermittent phosphatic limestones are prominent within fissile mudstone beds. Although locally obscured, the higher limestone beds again appear to contain phosphatic nodules at discrete horizons (samples 586, 585 & 584).

The mudstones between these harder bands are thinly bedded, extremely fissile and heavily iron stained on weathered surfaces. The beds dip to the northwest at approximately 25°. A three metre gap follows, above which more intermittent phosphatic limestone bands are apparent. The phosphates at this position up section form small steps within the stream. The mudstone bed, 18 metres into this section above the harder bands appears to contain nodules, particularly at its base. These are black in colour and appear to be flattened and elongate. Up section from this point

there is a change to a dominantly mudstone/shale lithology and at around 25-30 metres a small adit is visible on the stream banks. The shales here are black and extremely fissile and highly weathered. A poorly preserved fauna of both graptolites and brachiopods was noted here. In addition to the faunas mentioned above, Cave (1965) reported the presence of hexactinellid sponges and bryozoa within the phosphatic nodules.

The uppermost few metres of the shale are not exposed; however, upstream of the adit a coarse quartz and feldspar dominated conglomerate forms a small waterfall in Gwern-y-Brain Stream (SJ2180 1285). This marks the position of the overlying formation, the Powis Castle Conglomerate (Llandovery), although the boundary between this and the Nod Glas does not crop out.

2.8 Sedimentology

The Nod Glas Formation cropping out at Gwern y Brain, shows distinct lithological variation thought to represent a late Caradoc transgressive episode (Cave, 1965). Thin sections provide evidence for the microfacies interpretation of the lower part of the measured section.

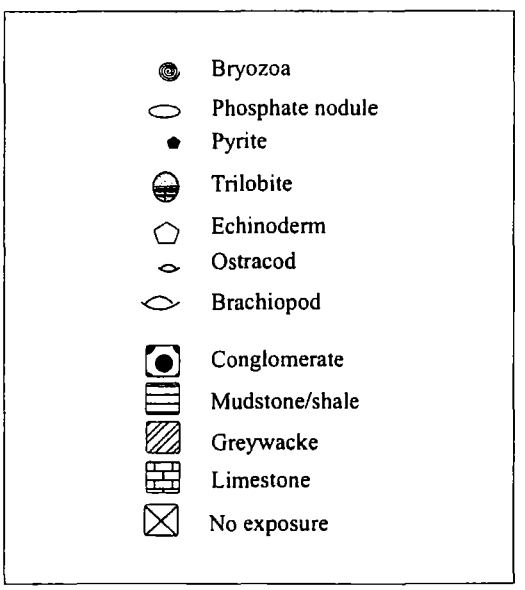

Text-Figure 2.8.1. Key for the symbols used in sedimentary logs.

Standard size (2″x3″) thin sections were made from the ten samples collected from the Nod Glas Formation and the underlying unit (Gaer Fawr Formation). The positions of the samples are shown on Text-figure 2.8.2 and a key to the symbols used is provided (Text-figure 2.8.1.)

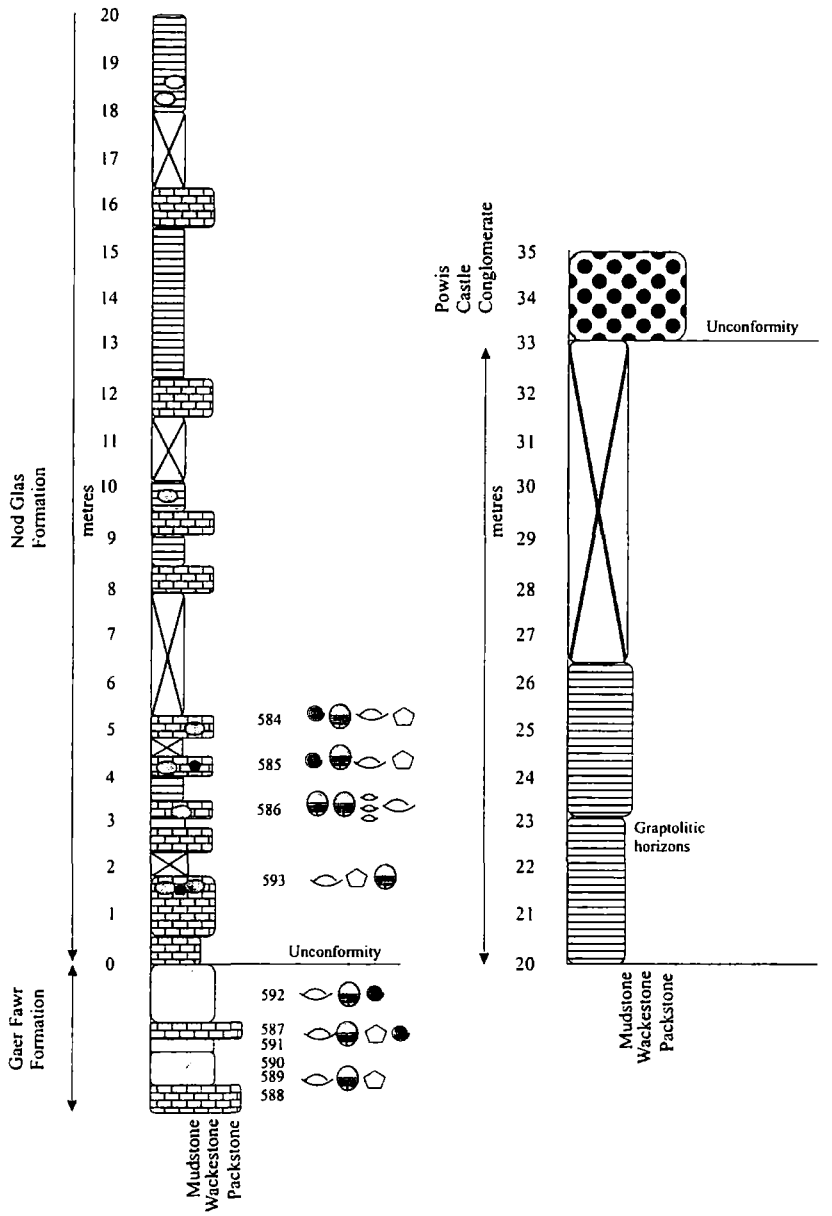

Text-Figure 2.8.2. The schematic sedimentary log of the Nod Glas Formation at Gwern-y-Brain Stream, Welshpool, Welsh Borders. The position of the Gaer Fawr, Nod Glas and Powis Castle Formations are indicated and dashed lines mark unconformities. Lithological aspects are shown within the succession whereas faunal occurrences are indicated on the right hand side of the log.

Samples 587 - 591 all came from the underlying Gaer Fawr Formation. Sample 587 represents the top of that formation directly underlying the lower Nod Glas Formation phosphorites. Samples 588-591 are all from a quarry downstream of the boundary between the Nod Glas and the Gaer Fawr Formation. Sample 592 represents the upper horizon of the Gaer Fawr Formation and samples 593, 584 and 585 are all from the basal 5 metres of the Nod Glas Formation.

The thin sections are described in terms of their composition and, where appropriate, classified using the textural scheme of Dunham (1962).

2.8.1 Sample 588

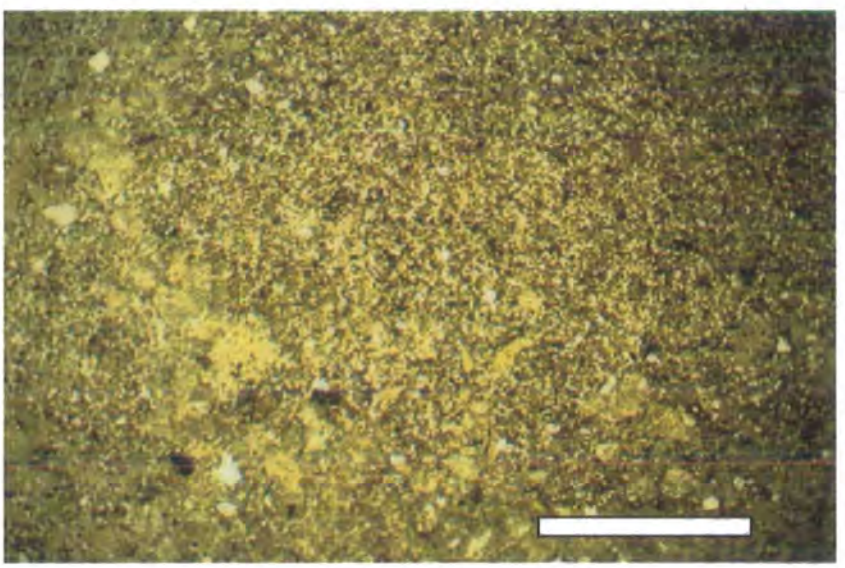

Text Figure 2.8.3 Photomicrograph of sample 588 in thin section under plane polarised light. Scale bar = 5mm

Formation

Gaer Fawr (lowest sample) sample number 588 (see Text-figures 2.8.2 & 2.8.3)

Grains

The grains within this sample are well-preserved bioclasts including brachiopod and trilobite fragments. These skeletal fragments are commonly altered along their external margins suggesting the sample has been subject to alteration and recrystallisation. The external margins of some of the bioclasts are pitted, indicative of boring activity. Evidence of bioturbation within this sample is seen as small (~2-3 mm diameter), branching micrite infilled burrows.

Matrix

The matrix of sample 588 is fine-grained and shows some degree of recrystallisation. Compaction features within the matrix include stylolites with a concentration of pyrite. This indicates both post-depositional compaction and opening of fluid pathways. The presence of patches of brown material within the matrix suggests there has been some phosphatisation of the sample. Additionally, the matrix contains rare (<5%) glauconite crystals. Pyrite is also rare in the sample but does occur as small (< 1mm) cubic crystals. There are also rare grains of quartz in the matrix (<5%)

Texture

The bioclasts within this rock show no alignment but are common (>40%) and support the main fabric of the rock.

Classification

Given the bioclastic grain-supported nature of this rock it is classified as a packstone.

Environmental Interpretation

The grains in this sample are reasonably well preserved, although many are broken. There is a variety in types of bioclast and this indicates that the environment of deposition was of moderate energy. It is suggested that this sample was deposited on a continental shelf environment, a conclusion also supported by the types of fossils present, by the bioturbation and the presence of glauconite within the matrix.

2.8.2 Sample 589

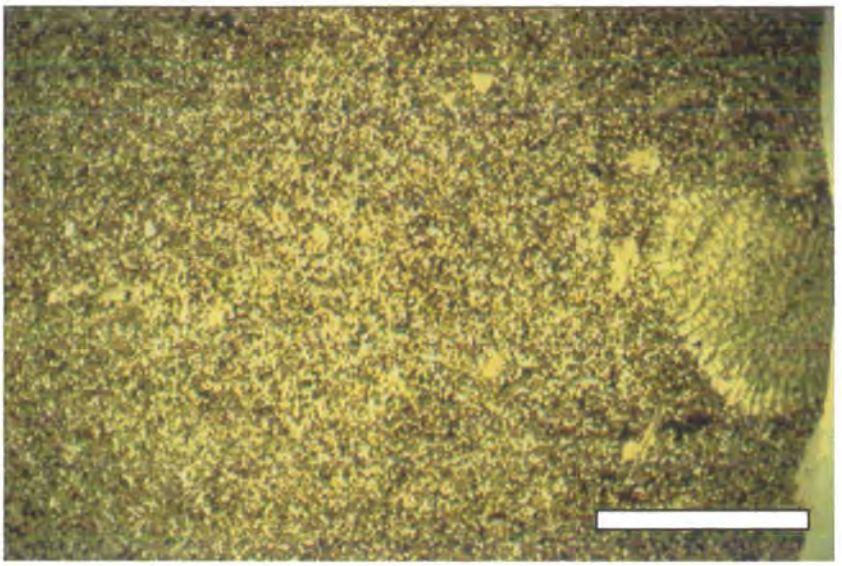

Text-Figure 2.8.4 Photomicrograph of sample 589 in thin section under plane polarised light. Scale bar = 5mm.

Formation

Gaer Fawr Formation (Sample above 588) Sample number 589 (see Text-figures 2.8.2 & 2.8.4)

Grains

The grains in this sample include quartz (both strained quartz and polycrystalline quartz > 50%) plus common feldspar (~20%) and rare muscovite mica (<10%). This sample also contains bioclast grains including fragments of brachiopod valves and spines, trilobites and echinoderm plates and spines.

Matrix

The matrix is composed dominantly of clay with additional feldspar and rare pyrite.

Texture

The quartz and feldspar grains are sub-angular in shape and well sorted. There is no alignment of the grains or bioclasts. Many grains are sutured at their contacts suggesting a degree of compaction within the sediment forming this sample. This sample also shows signs of bioturbation in the form of branching micrite-filled burrows.

Classification

Because of the composition and amount of clay matrix within this sediment (>15%) the sample has been classified as a greywacke.

Environmental Interpretation

The angularity of the grains and the faunal composition of this sediment indicate that deposition occurred in a shelf setting. The presence of angular feldspars within this sample indicates that it has not been greatly reworked or altered or transported any great distance from its source. In addition, several well -formed crystals of feldspar were found as a grain-forming component of this rock. This may indicate that the rock was deposited on a shelf close to an area of recent volcanic activity. Polycrystalline quartz also indicates that the terrigenous components of this sediment have an igneous (or metamorphic) source.

This evidence suggests that the environment of deposition was on the continental shelf close to a source area of terrigenous sediments with a recent volcanic influence.

2.8.3 Sample 590

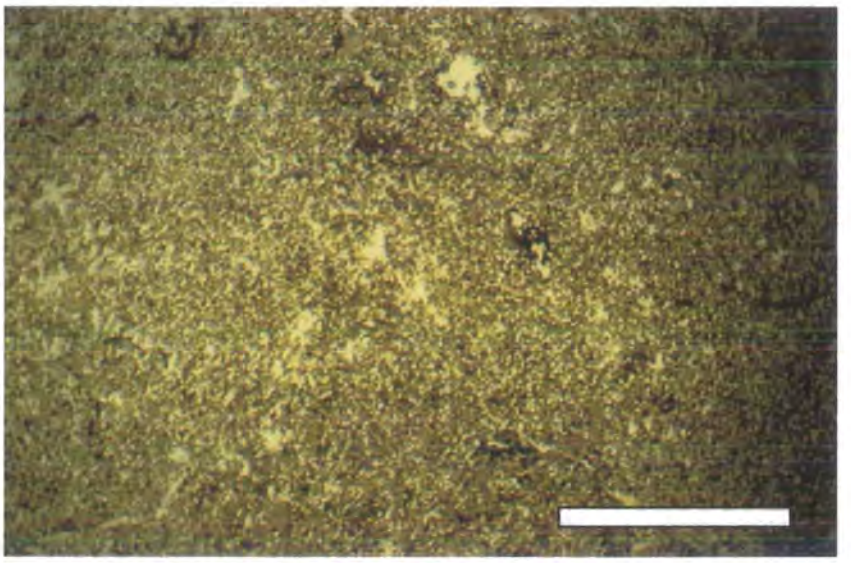

Text-Figure 2.8.5. Photomicrograph of sample 590 in thin section under plane polarised light. Scale bar = 5mm

Formation

Gaer Fawr (above 589) Sample number 590 (see Text-figures 2.8.2 & 2.8.5)

Grains

This sample is similar to that of 589 and the grains those of quartz, feldspar, mica and glauconite. The grains are sub-angular in shape. Bioclasts are common (>20%) and include fragments of echinoderms, trilobites and brachiopods. Brachiopod fragments are however, notably less abundant in this sample than in those below it.

Matrix

The matrix is composed of fine-grained clay and is slightly more abundant in this sample than was observed in sample 589. It contains abundant small (<1mm) branching burrows.

Texture

The bioclasts are well preserved but commonly fragmented. There is no alignment of the bioclasts within this sample. The matrix is found infilling some of the skeletal material.

Classification

Although there is a higher proportion of matrix to bioclasts in this sediment it has also been classified as a greywacke on the basis of the percentage of clay minerals in the matrix (>15%).

Environmental Interpretation

The faunal composition, fragmented nature of the skeletal material and the presence of glauconite all indicate deposition in shallow waters, particularly the continental shelf environment. The presence of large bioclasts and bioturbation indicates that this was a well-oxygenated environment. The occurrence of feldspar grains within the sample indicates it was not subject to long transport distances and that the depositional area was close to a source of terrigenous clastic sediments.

2.8.4 Sample 591

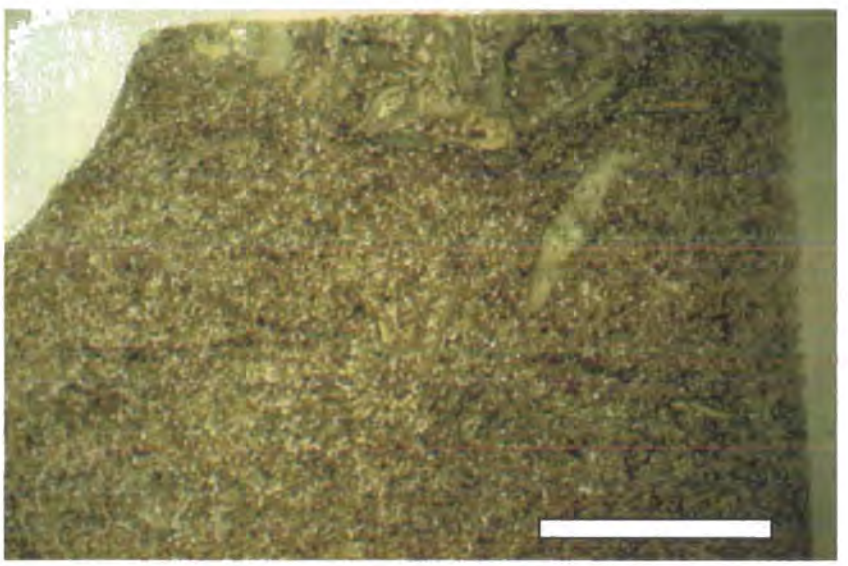

Text-Figure 2.8.6. Photomicrograph of sample 591 in thin section under plane polarised light. Scale bar = 5mm.

Formation

Gaer Fawr (sample above 590) Sample number 591 (see Text-figures, 2.8.2 & 2.8.6)

Grains

This sample has quartz and feldspar grains plus abundant bioclasts. The quartz and feldspar grains are similar to those described in previous samples in that they are angular in shape. The bioclasts are commonly broken and include fragments of brachiopod valves and spines and bryozoa.

Matrix

The matrix of this sample is dominated by clay minerals. The matrix is more abundant than observed in the samples described previously.

Texture

The individual grains of quartz and feldspar are sub-angular. The bioclasts occur throughout the sample usually in small pockets but show no alignment.

Classification

Because of the higher proportion of bioclasts still within a >15% clay matrix within this sample it has been classified as a bioclastic greywacke.

Environmental Interpretation

Because the quartz and feldspar grains are less abundant than in previous samples it is likely that this sample represents deposition further away from terrigenous source rocks. However, the presence of fauna such as brachiopods and bryozoans which are slightly fragmented suggests that this rock was still deposited in an environment subject to moderate energy levels. This would therefore be indicative of deposition on the continental shelf environment.

2.8.5 Sample 587

Formation

Gaer Fawr Formation Sample number 587 (see Text-figures 2.8.2 & 2.8.7).

Grains

Sample 587 has 5-10% quartz grains with rare pyrite (as cubic crystals) and glauconite grains. Other grains include brachiopod fragments such as disarticulated valves and spines, trilobite fragments and echinoderm plates and spines. Sponge spicules are present with quartz crystals apparent on the external margins. Fragments of bryozoa (~1mm across) are also present and have spherical chambers possessing concentric layered walls. Some bryozoa and other bioclasts are infilled with calcite. Peloids (<1mm) are also found among the grains.

The external margins of many of the bioclasts are pitted suggesting the activity of small boring organisms. The grains have well preserved margins but are commonly fragmentary.

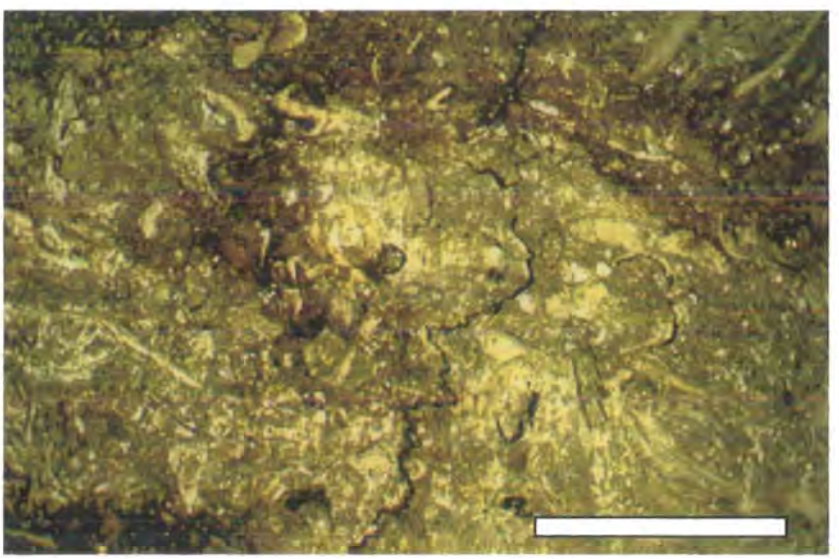

Text Figure 2.8.7. Photomicrograph of sample 587 in thin section under plane polarised light. Scale bar = 5mm.

Matrix

The matrix is dominantly micritic, much of which has been recrystallised. Compaction features include stylolites with a concentration of pyrite. Within the matrix there are small but pervasive patches of brown material. This does not affect the fossils and represents phosphatisation of the matrix.

Texture

There is no alignment of constituent grains. However, the bioclastic grains are largely fragmented but well preserved.

Classification

Packstone (grain supported) limestone

Environmental Interpretation

Deposition on a moderate energy shelf setting further away from the influence of clastic terrigenous input than the previous samples. The presence of phosphate has considerable palaeo-oceanographic implications for this section and will be discussed in section 2.9.

2.8.6 Sample 592

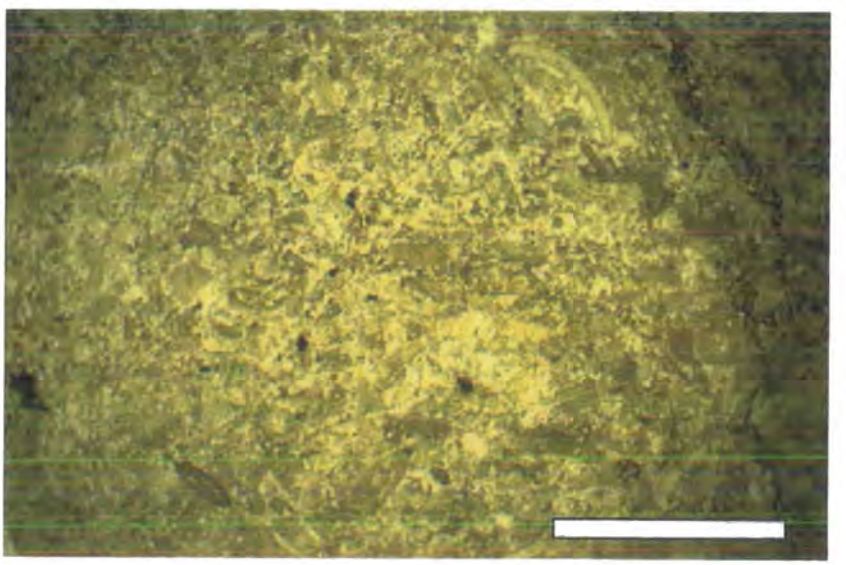

Text Figure 2.8.8. Photomicrograph of sample 592 in thin section under plane polarised light. Scale bar = 5mm.

Formation

Gaer Fawr Formation (uppermost sample) Sample number 592 (see Text-figures 2.8.2 & 2.8.8).

Grains

This sample contains quartz grains but much less feldspar than in all the lower samples. The mineral grains are well sorted and angular. Bioclasts are common and include the valves and spines of brachiopods, trilobite fragments and fragments of bryozoa. The bioclasts are hard to distinguish in this sample as it is heavily recrystallised.

Matrix

The matrix is highly recrystallised with diagenetic calcite and differs significantly from all previous samples, which possessed clay a dominated matrix. This is a recrystallised carbonate mud matrix.

Texture

Recrystallised texture with abundant syntaxial overgrowth structures. These are evident in the matrix when calcite crystals grow in optical continuity with previously deposited echinoderm fragments. These crystal overgrowths may be a result of the circulation of either burial or meteoric waters. The bioclasts are not aligned within this sample indicating that strong unidirectional currents were not operating in the environment of deposition.

Classification

This sample has also been classified as a bioclastic greywacke although it has been subject to much diagenetic alteration and recrystallisation.

Environmental Interpretation

The proportions of quartz and feldspar within this sample are significantly lower than those observed in the lower samples. This may indicate that the depositional area was further away from the source of terrigenous clastic material reaching this area. The faunal composition and fragmentation of the fossils does however, indicate that the environment of deposition was subject to moderate energy conditions, probably those on the continental shelf.

2.8.7 Sample 593

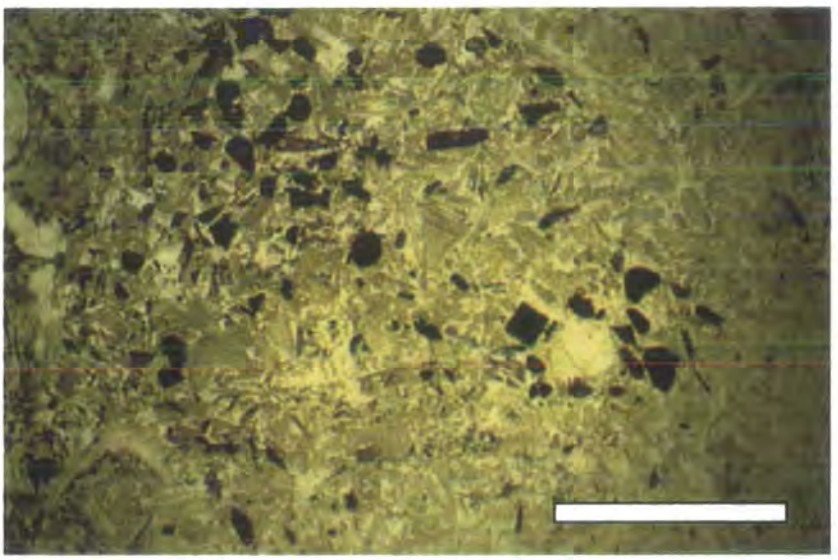

Text Figure 2.8.9. Photomicrograph of sample 593 in thin section under plane polarised light. Scale bar = 5mn

Formation

Nod Glas (above 592) Sample number 593 (see Text-figures 2.8.2 & 2.8.9)

Grains

There are abundant (>70%) bioclastic fragments including the skeletal remains of echinoderms, sponges, brachiopods and trilobites. Less abundant grains include those of quartz, feldspar and pyrite. A good example of a pyrite grain (opaque, square) can be seen towards the middle right of the section (Text-figure 2.8.9). Clasts of phosphate are also apparent in hand specimens of this sample.

Matrix

Patches of phosphate dominate the matrix of this sample. Phosphatisation of the grains is evident to the left side of the photomicrograph where there is abundant material causing a brown colouration. Phosphatisation has preferentially affected the bioclasts such as the echinoderm fragments and the sponges. This may be due to differences in porosity between bioclasts. There has been some recrystallisation of

this sample where calcite crystals can be observed to grow in optical continuity with bioclasts such as echinoderm plates. There is therefore calcitic cement between many of the grains.

Texture

The bioclastic grains are only slightly abraded and often well preserved. There is no distinct alignment of the bioclasts and the sample is poorly sorted.

Classification

Wackestone - Packstone

Environmental Interpretation

From the evidence it is inferred that the order of formation of this sample is as follows.

1. Deposition of grains (bioclasts, quartz etc)
2. Overgrowth of calcite cement
3. Phosphate precipitation

Because of the wide range of fossil types and the fragmentation they have undergone it is likely that the environment of deposition was of moderate energy in a continental shelf setting.

2.8.8 Sample 586

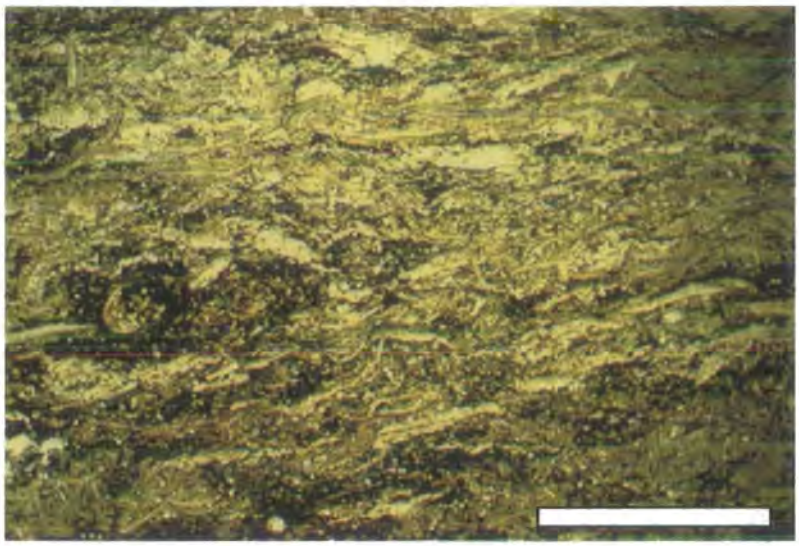

Text-Figure 2.8.10. Photomicrograph of sample 586 in thin section under plane polarised light. Scale bar = 5mm.

Formation

Nod Glas (sample above 593) Sample number 586 (see Text-figure 2.8.10)

Grains

The grains in this sample are dominantly bioclasts including fragments of brachiopod valves and spines, ostracode valves, bryozoa and trilobites. Echinoderm fragments can still be observed (as in lower samples) although they are much less abundant whereas the most common bioclasts in this sample are ostracodes and trilobites. This sample contains a notably higher abundance of trilobites than any other samples collected from this locality. Many of the skeletal fragments are phosphatised. In addition to skeletal debris there are rare (<10%) quartz grains.

Cement

A dark brown to black phosphate cement is pervasive.

Texture

Unlike all the lower samples the bioclasts are well aligned in sample 586.

Classification

This sample can be classified as a packstone as it is bioclast supported. The presence of a high number of trilobite fragments and phosphatisation could lead to a more precise classification of the sample e.g. phosphatised, trilobite packstone.

Environmental Interpretation

The abundance of unfragmented skeletal debris and alignment within this sample indicates deposition in a low-energy environment. Additionally, the highly bioclastic nature of this sample indicates that the sedimentation rate was low and therefore this is sample is condensed.

This sample therefore represents the deepest conditions within the section. Deposition most likely occurred on the outer shelf or the upper continental slope area.

2.8.9 Sample 585

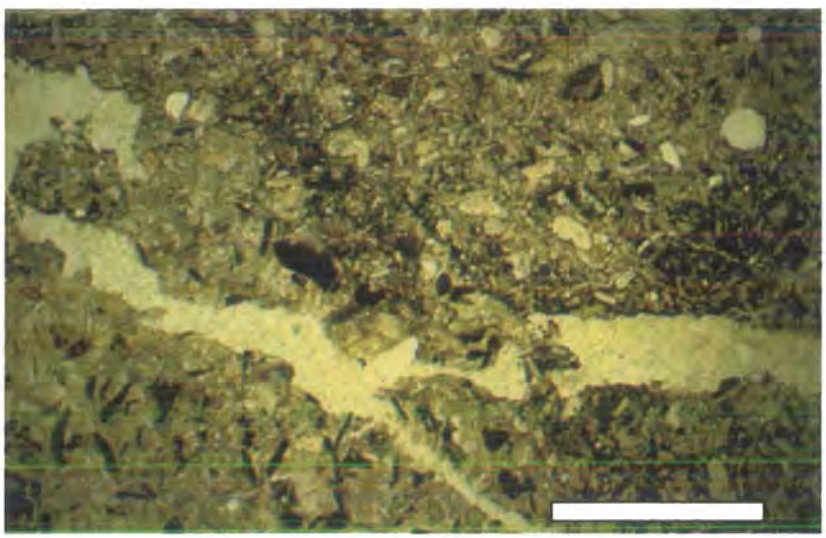

Text-Figure 2.8.11. Photomicrograph of sample 585 in thin section under plane polarised light. Scale bar = 5mm

Formation

Nod Glas (sample above 586) Sample number 585 (see Text-figures 2.8.2 & 2.8.11)

Grains

This sample is composed dominantly of bioclastic grains with rare quartz grains. Bioclasts include fragments of echinoderms, trilobites, brachiopods and bryozoa. Many of the grains are bored on their external margins. There are also detrital grains of phosphate (dark areas) within this sample which may indicate re-working of older phosphorites.

Cement

Phosphate occurs between the grains and also altering some of the echinoderm fragments. This preferential phosphatisation may be due to differences in porosity between the constituent bioclasts of this sediment.

Texture

This sample is poorly sorted in texture and the grains show no distinct alignment. There is a high degree of calcitic mineralisation seen on this section.

Classification

Packstone

Environmental Interpretation

The diverse fauna and composition indicates that this sample was deposited in a moderate energy environment most likely to be that of the outer shelf to upper slope.

2.8.10 Sample 584

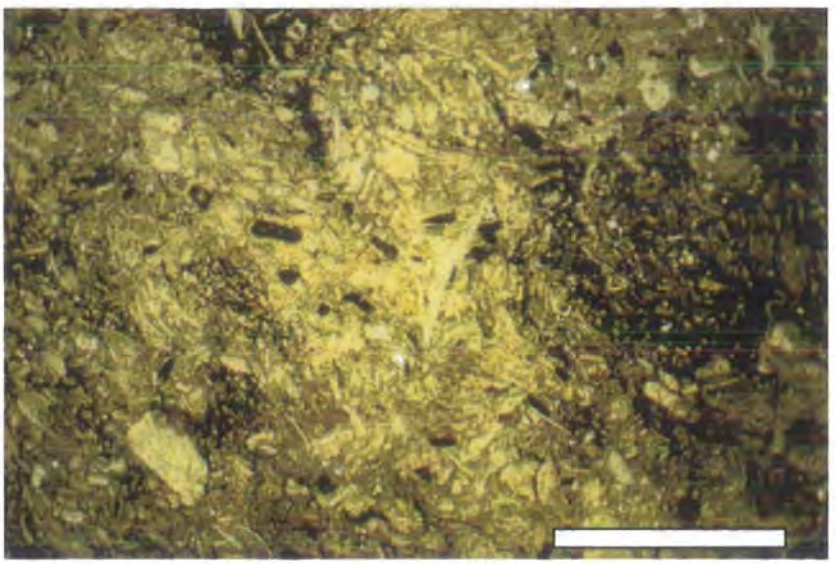

Text-Figure 2.8.12. Photomicrograph of sample 584 in thin section under plane polarised light. The darker areas to the right of the picture show the areas of phosphatisation between grains and skeletal fragments. Small phosphatic clasts can be seen in the centre section as elongated dark brown grains. Scale bar = 5mm

Formation Nod Glas (sample above 585) Sample number 584 (see Text-figure 2.8.12)

Grains

Sample 584 is similar to Sample 585 although bioclasts are more abundant. The skeletal grains include echinoderm plates and spines, trilobite fragments, brachiopod valves and spines. The smaller, thinner ellipses (Text-figure 2.8.12, bottom right) are disarticulated ostracode valves.

Cement

This sample has a phosphate cement between the grains. On the thin section, this is seen as dark brown areas (Text-figure 2.8.12). The phosphate alters, and replaces, some of the grains and the majority of phosphate material appears between the skeletal grains. The phosphatisation was a later event and occurred after deposition of all grains.

Texture

There is no alignment of the grains within this sample and it has a poorly sorted texture. The bioclasts are clustered in pockets and are not evenly distributed throughout the fabric of the rock.

Classification

Packstone

Environmental Interpretation

The faunal composition and sedimentology (especially the phosphate content) indicates a low to moderate energy environment of deposition. It is postulated that this sample was also deposited on the upper areas of the continental slope.

2.9 Interpretation

The Gaer Fawr Formation is composed of greywackes, with some higher bioclastic calcareous wackestones. It is both shelly and bioturbated in its upper part and so is thought to be the result of shelf deposition (Cave & Price, 1978). During subsequent deposition of the Nod Glas Formation, Welshpool was situated on the upper slope - outer shelf of the Welsh Basin. The Nod Glas Formation therefore marks a change in depositional conditions within the basin. The occurrence of phosphate-rich sediments within the lower Nod Glas Formation has considerable implications for the sequence stratigraphical and palaeo-environmental interpretation of this section.

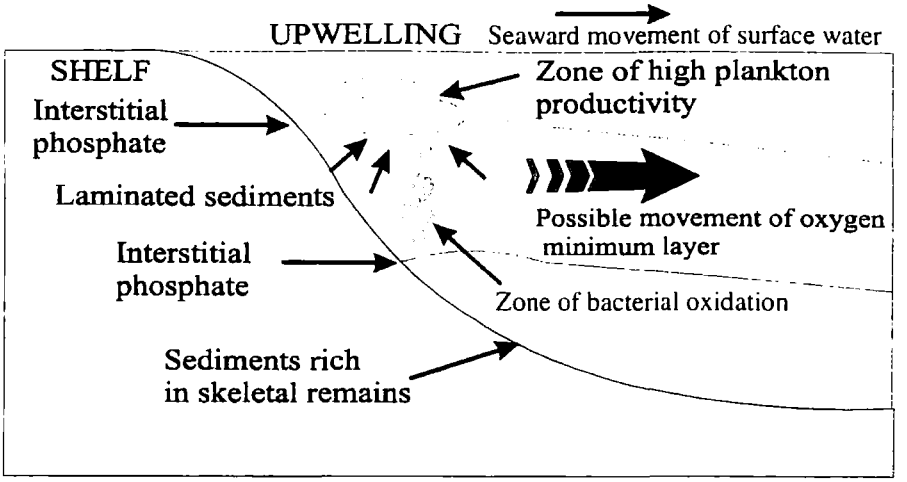

Text-Figure 2.9.1. The oceanic conditions required for phosphate formation (adapted from Jenkyns, 1989).

Within a systems tract, phosphatic deposits are usually found at the point of initial transgression and form the deposits of the maximum flooding surface (Jenkyns, 1989). Phosphate deposition in modern oceans occurs mainly at either shallow or pelagic depths. Phosphate deposition is characteristic of slow sedimentation, deposition on topographic highs and at areas of upwelling (Jenkyns, 1989). Most phosphates in the geological record have been shown to be associated with shelf dwelling calcareous organisms, cross bedding or reef building algae (Johnson & Baldwin, 1989). However, some modern phosphates have been shown to reach maximum development in the outer shelf to basin transition (Jenkyns, 1989). Phosphate-rich waters are usually found in zones of coastal upwelling. Phosphate rich waters therefore can result in the direct precipitation of calcium phosphate as nodules or laminae or replacement of calcium carbonate.

Pelagic sediments are composed of microscopic skeletal remains of planktonic animals. Biogenous sediments are deposited more rapidly below areas of high productivity. Such areas are often a result of oceanic upwelling events that bring nutrient-rich waters to the surface of the oceans causing a 'bloom' in the microscopic planktonic organisms in the surface waters. This results in the development of an oxygen minimum layer where phosphates are produced at the upper and lower boundaries (Text-figure 2.9.1.). In modern oceans these processes dominate depths

between 300 and 1500 metres and are characterised by a CO_2, nutrient, phosphate and nitrate maximum (Jenkyns, 1989, Johnson & Baldwin, 1989). Phosphates are therefore often attributed to the upper and lower levels of an oxygen minimum zone and these processes contribute to an abundant skeletal sedimentary record below such oceanographic features.

The phosphatic limestones of the Nod Glas Formation may therefore indicate that processes of upwelling were operating in the Welsh basin in the late Caradoc. The subsequent development of extensive shale units above the phosphatic lower member therefore indicates that deepening of the basin was also occurring during this time.

Geochemical studies (Temple & Cave, 1992) by XRD and ICP-AES have reported potential anoxic bottom water conditions prevailed during deposition of the Nod Glas Formation. This is supported by both the absence of bioturbation and presence of the well preserved graptolite faunas. The sedimentological transition from the Gaer Fawr to the Nod Glas Formation therefore indicates significant changes in palaeoenvironment and oceanography were occurring at this time. The deepening of the Welsh Basin in this area and changing of conditions within the water column may therefore have had an effect on the conodont faunas appearing within the Nod Glas Formation. It has been proposed that this transgression was related to volcanotectonic rather than eustatic events (Woodcock, 1990).

The deposition of the Gaer Fawr Formation (Woolstonian) represents that of inner to outer shelf environments close to an area of terrigenous input and recent volcanic activity. The initial deposition involved that of shelf bioclast dominated limestones (Text-figure 2.9.2A). The subsequent input of terrestrial clastic material produced greywackes (Text-figure 2.9.2B). The fossils contained within this formation often show signs of transportation but not over any great distance as many are still intact.

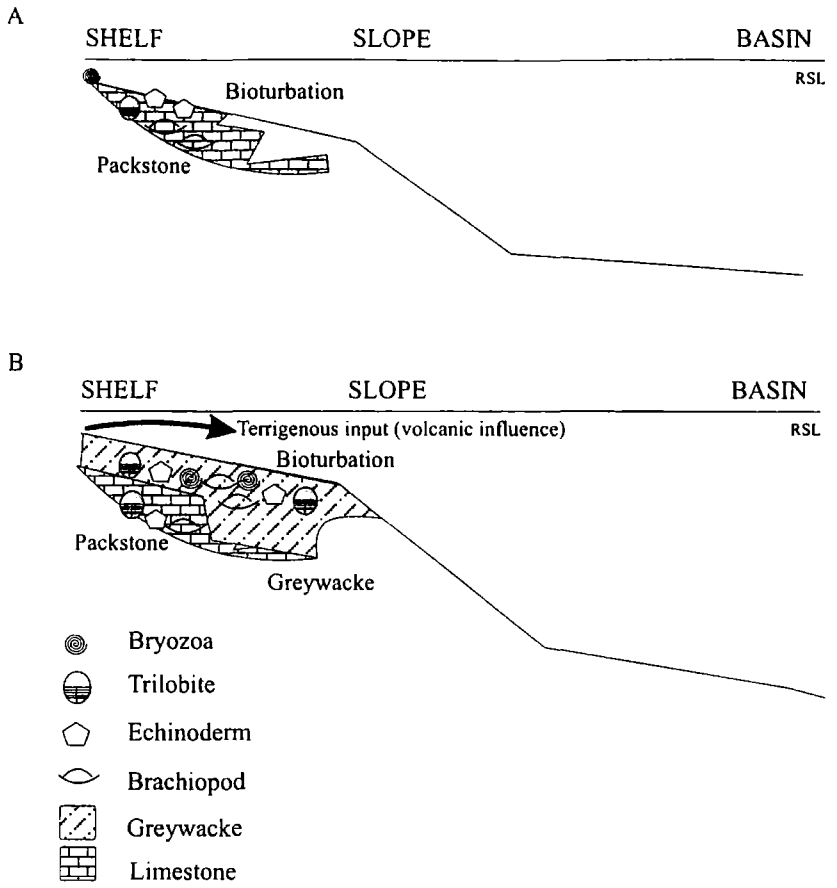

Text-Figure 2.9.2. Proposed development of the Gaer Fawr Formation at Gwern-y-Brain Stream, Guilsfield, Welshpool. A. Shows the development of the packstones of the Gaer Fawr Formation on the shelf. B. Shows subsequent deposition of the greywackes overlying the packstones.

However, oceanic conditions in the late Caradoc changed with the deepening of the basin, which promoted upwelling, and the development of a well formed oxygen minimum zone (OMZ). The oceanic conditions within such an upwelling area and associated OMZ are ideal for deposition of phosphatic material within the oceanic sediments as previously described. This is clearly shown by the samples 593, 586, 584 and 585 where there is both high skeletal abundance and widespread phosphate development. In addition, the phosphatisation of the upper Gaer Fawr Formation sediments (e.g. sample 587) may indicate later phosphatisation of continental shelf sediments by the transgression induced impingement of the OMZ (Text-Figure 2.9.3).

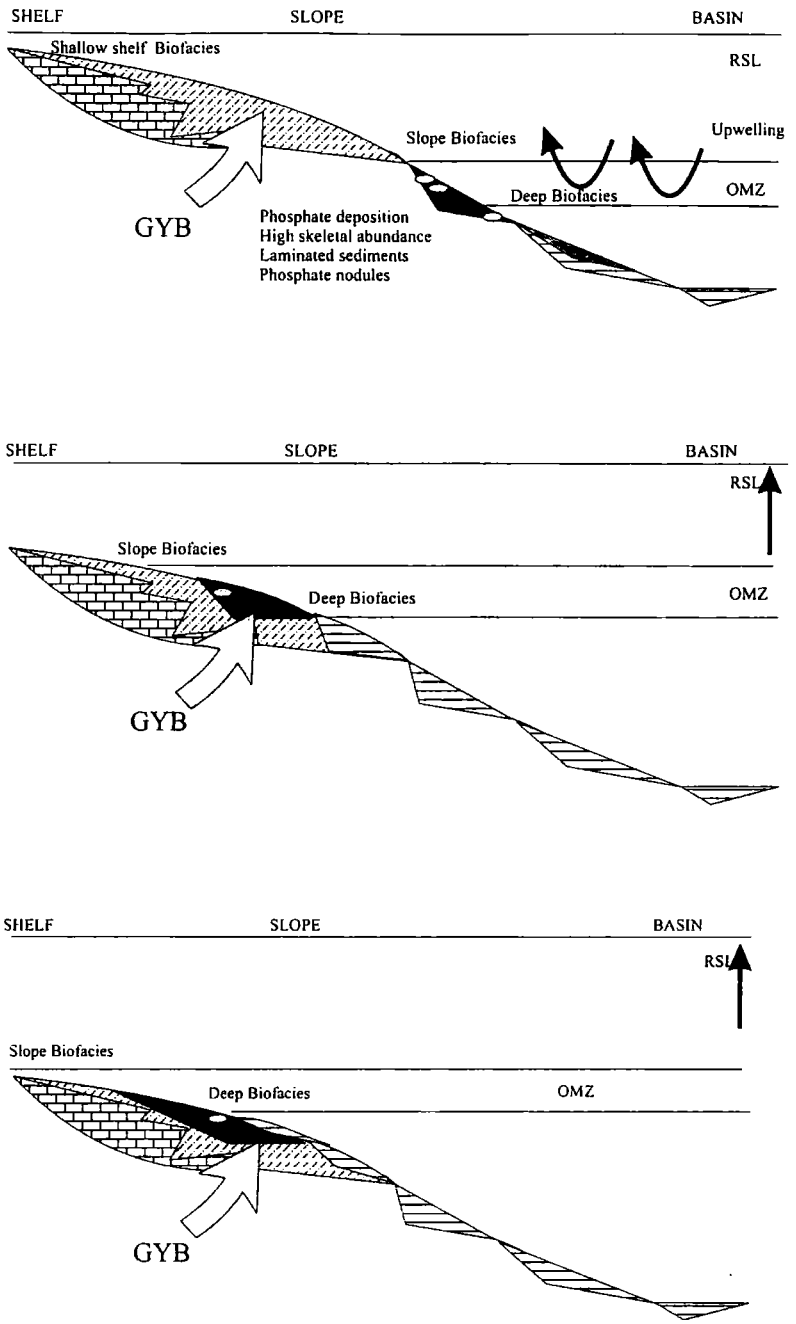

Text-Figure 2.9.3. The deposition of the Nod Glas Formation. Top. Shows the initial development of the OMZ and the position of phosphate deposition. Middle. shows the possible movement of the OMZ as the sea-level rises. Bottom. Shows how the OMZ may impinge upon the continental shelf as the transgression continues. Large grey arrow marks the position of the section at Gwern-y-Brain (GYB), Welshpool. GYB = Gwern-y-Brain, RSL = relative sea-level. OMZ = Oxygen minimum zone

Text–figure 2.9.3 (top) shows the initial development of upwelling at the margins of the Welsh Basin. This upwelling is postulated to cause an increase in the amount of nutrient reaching the upper parts of the water column. In turn, this may promote a faunal bloom and lead to the development of an oxygen minimum zone (OMZ) at an outer shelf position. Such oceanographic conditions are therefore responsible for the deposition of large amounts of phosphate within the sediments of the Lower Nod Glas Formation. The following stage of development (Text-figure 2.9.3 middle) shows a small increase in the relative sea-level. At this stage it is inferred that such a sea-level increase would promote and enhance upwelling processes whilst causing a relative upwards shift in the position of the OMZ. It is now possible that the OMZ could impinge upon the shelf environment. A further increase in the relative sea-level (Text–figure 2.9.3, bottom) would shift the OMZ upwards in the water column and onto the continental shelf and the deepening of the basin would lead to the extensive development of black shales over a wide area (Text-figure 2.9.4). Impingement of the OMZ onto the shelf environment may also explain the later phosphatisation observed in the upper Gaer Fawr sediments on the continental shelf.

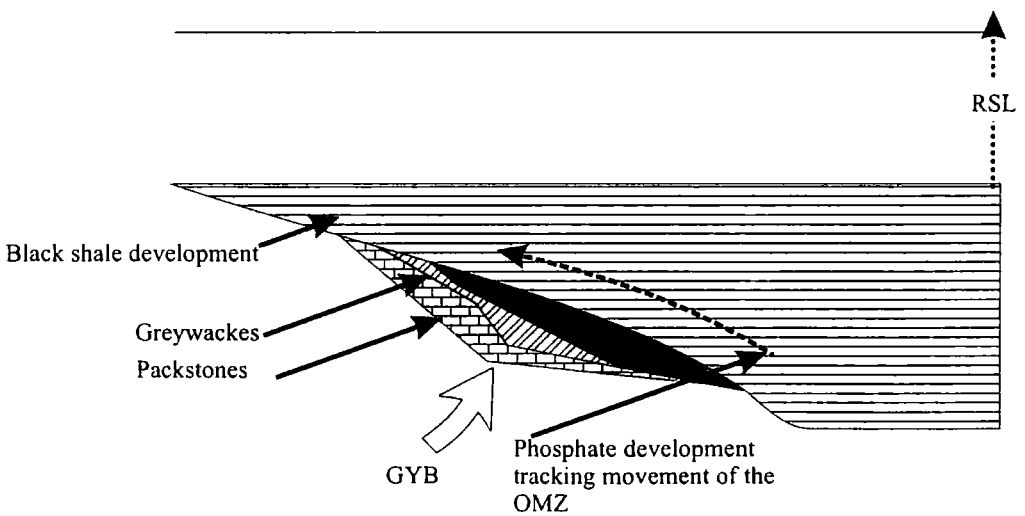

Text-Figure 2.9.4. The development of the Nod Glas Formation. GYB = Gwern-y-Brain, RSL = relative sea-level. OMZ = Oxygen minimum zone

The sedimentology of the Nod Glas Formation therefore represents significant deepening of the Welsh Basin and the sediments of the Nod Glas Formation are indicative of deposition on the uppermost continental slope close to the shelf-slope break. Furthermore, it is predicted that, as sea-level increased the OMZ would have moved upwards within the water column and impinged on the continental shelf environments in a similar way to that described by Cooper (1999) in his discussion on graptolite biofacies (see Part 1, Chapter 1). This impingement of the OMZ on the continental slope may have had a significant effect on conodont faunas occupying the Welsh Basin in the late Caradoc.

Text-figure 2.9.5 illustrates the proposed oceanographic conditions required for the facies interpretation as shown. It shows the position of the OMZ, based on Reading (1991). It is proposed that the upper layer of the end Caradoc ocean (above storm wave base) was oxygenated and well mixed lying above the well-developed OMZ. Within the OMZ, oxygen levels were variable and higher both at the top and bottom regions. The process of upwelling causes the higher and lower levels of the OMZ to consist of cooler water masses. Overall, these two layers of the ocean became cooler with increasing depth. However, the lower layer of the ocean was anoxic, warmer and highly saline.

Sample 586 is distinctive, has a laminated texture and abundant skeletal remains forming the middle layer of the OMZ. Samples 593 and 584/5 are similar to each other and the phosphate is distributed throughout the sediment within the matrix or as small nodules. Both these features characterise deposition in an oxygen minimum zone.

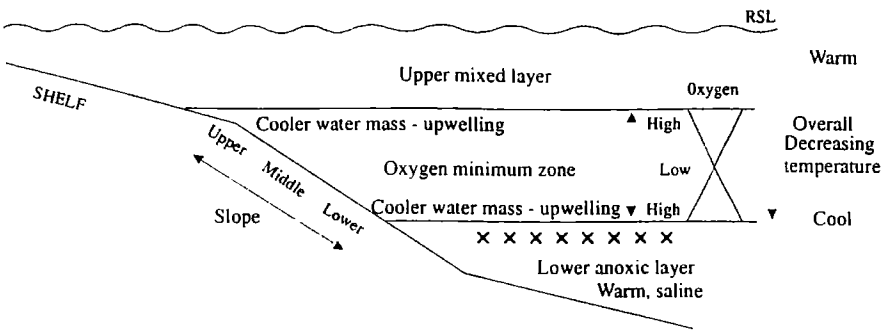

Text-Figure 2.9.5. The proposed ocean state for the Nod Glas Formation, Gwern-y-Brain, Welshpool.

2.10 Conodont sample preparation

Conodont samples were taken at several points within the phosphatic horizons of the lower member of the Nod Glas Formation and from the Gaer Fawr Formation. The samples were typically between 1 and 2 kilograms in weight and were processed for conodonts using unbuffered acetic acid and a 63μm sieve. Residues were large and therefore magnetically separated prior to heavy liquid separation in bromoform. Although these two techniques were employed prior to picking, final residues remained unusually large and conodonts rare within these. The conodonts are reasonably well preserved although commonly slightly fragmented and are black in colour. This is indicative of burial to 10-12 km and heating to in excess of 300 degrees (Epstein *et al.*, 1977). Most specimens were easily studied by the use of a light-reflecting microscope.

2.11 Conodont faunas of the upper Gaer Fawr Formation and lower Nod Glas Formation

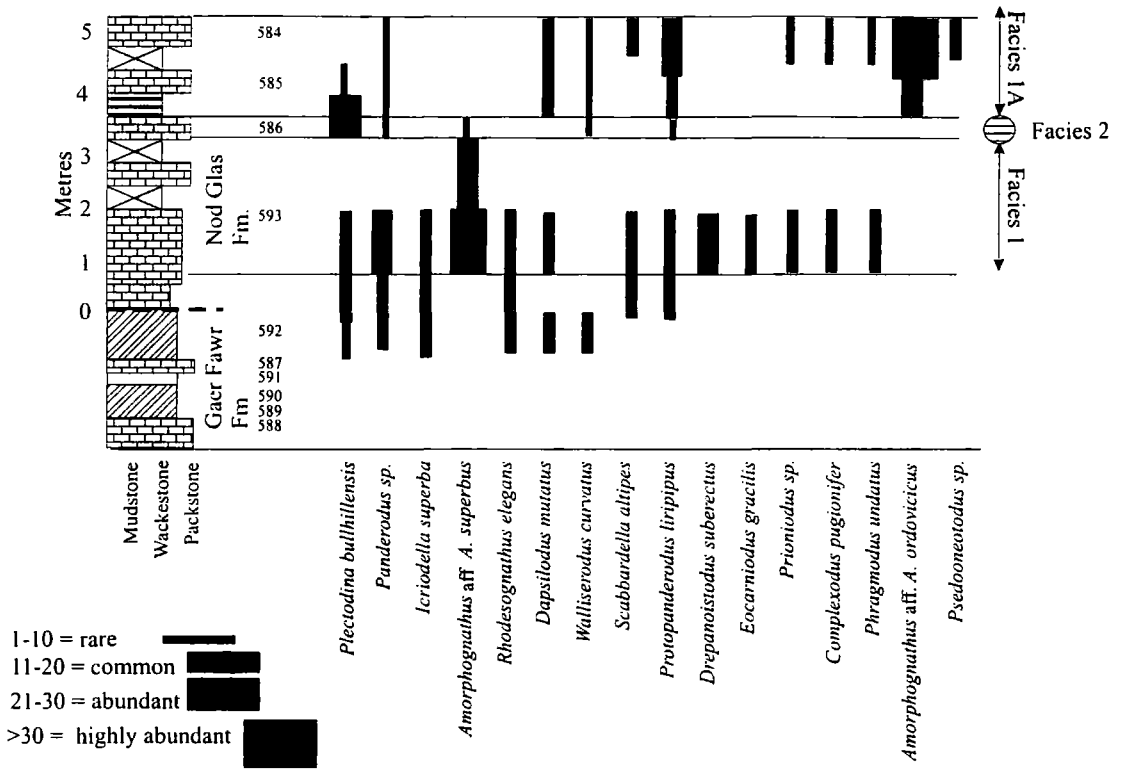

Text-Figure 2.11.1. The conodonts from the upper Gaer Fawr Formation and lower Nod Glas Formation, Gwern-y-Brain Stream, Welshpool extracted during this present study. Thicker bars represent samples of greater abundance as indicated on the diagram.

Text-figure 2.11.1 shows the conodont occurrences within the upper part of the Gaer Fawr Formation and lower Nod Glas phosphorites. Samples 587 to 592 were all taken from the Gaer Fawr Formation. Samples 588, 589, 590 and 591 represent the lowest samples from this section and were collected from a small quarry downstream of the contact between the Gaer Fawr and Nod Glas Formation. The lower turbidites did not yield a conodont fauna when processed.

Sample 587 was taken from the upper part of the Gaer Fawr Formation and yielded a sparse but varied conodont fauna including representatives of *Plectodina bullhillensis*, *Icriodella superba*, *Panderodus* sp. and *Amorphognathus* sp. Generic and particularly species names are given tentatively as the majority of material is

either poorly preserved or fragmented. *Icriodella superba* is represented by two incomplete Pa elements, distinctive in that they contain a double row of denticles on the lateral process. *Panderodus unicostatus* specimens are complete, although not all elements from the apparatus have been recovered. All elements of *Amorphognathus* are extremely poor and show only the tips of Pa element processes. Again, the diagnostic element (in this case the M element) is not present within this sample so classification can only be given to generic level. Specimens of *Plectodina bullhillensis* include incomplete Sc, Sa and Pa elements. This species is characterised by a very small Pa element and an unusually large Pb element (Savage & Bassett, 1985). Although the material is fragmentary, specimens in sample 587 appear to show these characteristic features. A further fragmented element is present within this sample and appears to be coniform with a large, almost circular cavity. Its generic or species identity remains enigmatic.

Sample 592 represents the highest sample taken from the Gaer Fawr Formation and yielded a slightly more diverse and abundant fauna than sample 587. Sample 592 was taken ~30 cm above sample 587 and is a slightly darker colour in hand specimen. The fauna extracted from this sample was again poorly preserved and generally fragmented. Many of the complete elements are extremely delicate and show few signs of reworking. The presence of *Panderodus unicostatus* is again noted in this sample but the elements recovered do not include a diagnostic falciform element leaving the species name tentative. Other coniform elements include those of *Dapsilodus mutatus* a species distinguished by its characteristically flared basal margin. Two other coniform genera are also present. A coniform element with a large circular basal cavity, similar to that found in 587 is more complete and may belong in *Walliserodus*. The second coniform has a distinct indentation in the basal margin and no distinct basal cavity or striations. The element is laterally compressed and has been identified as belonging to *Scabbardella altipes*. *Plectodina bullhillensis* appears as both S and P elements, the former are commonly fragmented reflecting the delicate nature of this element. Pa elements are rare. Fragments of *Amorphognathus* include no Pa elements but Pb elements are evident along with the remains of several delicate and often fragmented S elements. Again, the lack of a diagnostic M element from this sample leaves the conodont identified only to generic level. Sample 592 sees the first appearance of *Rhodesognathus elegans* where

abundant sinistral and dextral Pa elements are represented in conjunction with rare sinistral S elements.

2.12 Conodonts from the Nod Glas Formation

It is possible to divide the lithologies of the Nod Glas Formation into three facies. The first represents sample 593, the second sample 586, and the third both the samples 585 and 584 (Text-figure 2.11.1). The information provided in the text is summarised in Table 2.12.

Facies 1 (sample 593 from the basal Nod Glas Phosphorites)

This is a distinct sedimentary facies in the lower Nod Glas Phosphorites and it yielded has 13 conodont species. The phosphate within this sample occurs mainly as small (< 10mm) nodules although there is a small amount of interstitial phosphate within the matrix. This sample yields a more diverse and abundant conodont fauna than all samples from the underlying Gaer Fawr Formation. Conodont elements extracted were generally complete and well preserved and show little sign of re-working. Sample 593 is marked by the low numbers of species such as *Plectodina bullhillensis*, *Panderodus unicostatus*, *Icriodella superba* and *Phragmodus undatus*. This horizon records the first appearance of several other species such as *Protopanderodus liripipus* characterised by deep latitudinal grooves and the upward flare to the basal cavity. A notable addition is that of the appearance of *Drepanoistodus suberectus* in appreciable numbers. *Rhodesognathus elegans* is abundant and represented by both sinistral and dextral P and S elements. Examples of *Amorphognathus* are well represented in this sample with Pa, Pb and M elements common to abundant. Unfortunately, many of the Pa elements are fragmented and only one diagnostic M element has been recovered and assigned to *Amorphognathus* aff. *A. superbus* (for a full discussion see Part I, Chapter 4). Two Pa morphotypes resembling those of *Amorphognathus* are present in sample 593. Fragmentary specimens of *Complexodus pugionifer* are distinguished from *Amorphognathus* in possessing a large posteriorly directed cusp. *Complexodus pugionifer* has not previously been recognised from the Nod Glas Formation.

The identification and implications of *Amorphognathus* occurrence in the Nod Glas Formation will be discussed in Part I, Chapter 4.

Facies 2 (sample 586)

This sample was collected from a horizon approximately 1.5 metres above sample 593. Facies 2 is the most distinctive sedimentary microfacies within the lower Nod Glas Phosphorites and has a strongly laminated texture with a high percentage of interstitial phosphate and abundant skeletal debris.

The conodont fauna extracted from this sample was sparse compared to that seen in sample 593 but more abundant than in the samples beneath that and many of the taxa present prior to 586 no longer occur. A total of 5 species are represented in this facies. Fragments of *Amorphognathus* are present, although rare and are identified as *Amorphognathus* aff. *A. superbus.* Compared to Facies 1, elements of *Rhodesognathus elegans* are rare in this sample but *Plectodina bullhillensis* is more abundant. Coniform taxa include those belonging *Protopanderodus liripipus*, *Panderodus unicostatus* and *Walliserodus curvatus.* Facies 2 does not yield *Dapsilodus mutatus*, *Drepanoistodus suberectus*, *Prioniodus* sp., *Complexodus pugionifer* and *Phragmodus undatus.*

Facies 1A (sample 584/585)

This facies is of similar lithology to Facies 1. There is no alignment of grains in either facies 1 or 1A and the phosphate occurs both in the matrix and as isolated nodules or clasts. Facies 1A comprises the top two samples taken from the lower Nod Glas Formation. The lithology of these two samples is very similar with the phosphate being dominantly interstitial. Facies 1A sees the first appearance of *Amorphognathus* aff. *A. ordovicicus* and *Pseudooneotodus.* When compared to Facies 2, *Dapsilodus mutatus* is again present, but *Walliserodus curvatus* is very rare. A total of 10 species occur in this facies.

In detail, sample 585 shows a slight decrease in both conodont diversity and abundance. *Panderodus unicostatus*, *Protopanderodus liripipus* and *Dapsilodus mutatus* are common. *Amorphognathus* elements are generally higher in abundance although there are no complete Pa elements. Sample 584 however, yielded a sample of higher diversity and abundance than that fauna from Facies 2. Coniform elements are particularly abundant and diverse including examples of *Panderodus unicostatus* *Protopanderodus liripipus* and *Dapsilodus mutatus.* As in the sample 585, *Amorphognathus* elements are more robust but mostly occur as fragments. Abundant

Pa, Pb and S elements can be seen. *Plectodina bullhillensis* is extremely rare and only occurs at the base of this facies (i.e. only in sample 585).

Table 2.12.

Formation	Sample numbers	Facies	*Plectodina bullhillensis*	*Panderodus unicostatus*	*Icriodella superba*	*Amorphognathus A*	*Rhodesognathus eleg.*	*Dapsilodus mutatus*	*Walliserodus curvatus*	*Scabbardella altipes*	*Protopanderodus liri.*	*Drepanoistodus sub.*	*Eocarniodus gracilis*	*Prioniodus sp.*	*Complexodus pugionif.*	*Phragmodus undatus*	*Amorphognathus B*	*Pseudooneotodus sp.*	Total number
Nod Glas	584/5	Facies 1A	×	×				×	×	×	×			×		×	×	×	10
	586	Facies 2	×	×		×			×		×								5
	593	Facies 1	×	×	×	×	×	×		×	×	×	×	×	×	×			13

Table 2.12. The conodont species of the three Facies (as described in the text) in the lower Nod Glas Formation. ***Amorphognathus*** **A =** ***Amorphognathus*** **aff.** ***A. superbus*** **and B =** ***Amorphognathus*** **aff.** ***A. ordovicicus.***

This information on the Nod Glas facies divisions and conodont occurrences is summarised on Text-figure 2.12.3 that illustrates these microfacies divisions in terms of lithology and conodont species diversity.

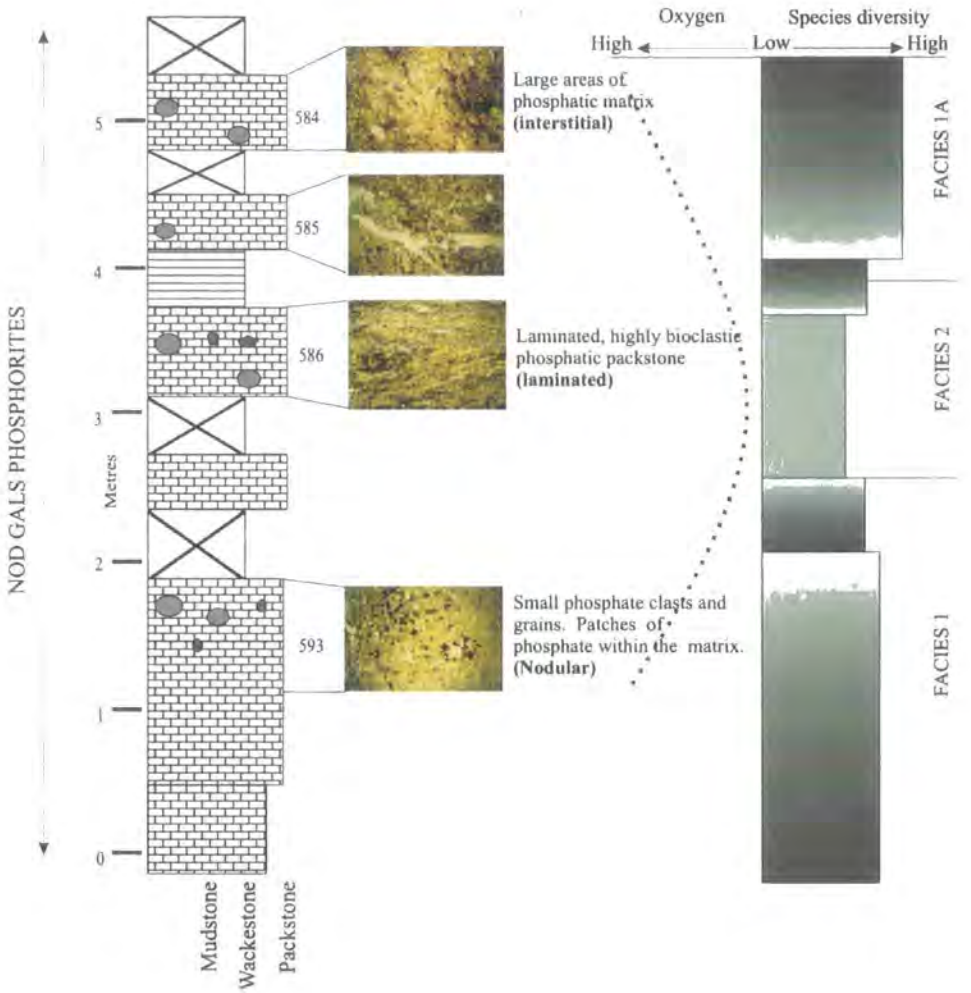

Text-Figure 2.12.3. The three facies of the Nod Glas Formation and relative species diversity in each.

2.13 Faunal similarity in the Nod Glas Formation

The similarity between two related faunas can be measured in terms of the Simpson Coefficient of Similarity (S), where S is the number of species in common between the two faunas divided by the total number of species in the smallest fauna expressed as a percentage (Armstrong & Owen, 1998). Faunal similarity analyses have therefore been conducted to compare the three facies and find the percentage similarity of species occurring in each (Table 2.13).

$$\text{Simpson: } \frac{C}{N1} x100$$

Table 2.13

Sample/facies	C	N1	% Similarity
1 & 2	4	5	80
1 & 1A	6	10	60
2 & 1A	4	5	80

Using this method the faunal similarity of conodont species belonging Facies 1 and 2 is 80 whilst between facies 1 and 1A a value of 60% is calculated. However, when facies 2 and 1A (3) are compared there is a 80% similarity at conodont species level.

The Simpson Coefficient of Similarity is sample size dependent and due to low numbers of species, similarity was also measured using the Jaccard (Table 2.13A) and Dice (Table 2.13B) coefficients. These methods show lower values of percentage similarity but indicate a greater similarity between Facies 2 and 1A.

$$\text{Jaccard: } \frac{C}{N1 + N2 - C} x100$$

Table 2.13A

Sample/facies	C	N1	N2	% similarity
1 & 2	4	5	13	29
1 & 1A	6	10	13	36
2 & 1A	4	5	10	37

$$\text{Dice: } \frac{2C}{N1 + N2} x100$$

Table 2.13B

Sample/facies	2C	N1	N2	% similarity
1 & 2	8	5	13	44
1 & 1A	12	10	13	52
2 & 1A	8	5	10	53

2.14 Interpretation and characterisation of conodonts

Facies 1 contains *Amorphognathus*, *Rhodesognathus*, *Complexodus* and *Phragmodus* and these are interpreted to represent nektobenthic genera. It also includes the coniform genera *Panderodus*, *Dapsilodus*, *Scabbardella*, *Drepanoistodus* and *Protopanderodus*.

Facies 2 contains abundant *Plectodina*, alongside *Amorphognathus* both are interpreted to be nektobenthic. The coniform genera of Facies 2 are *Panderodus*, *Walliserodus* and *Protopanderodus*.

Facies 1A contains *Amorphognathus* and *Phragmodus*. The coniform genera include *Panderodus*, *Dapsilodus*, *Walliserodus*, *Scabbardella* and *Protopanderodus*.

GAER FAWR	FACIES 1	FACIES 2	FACIES 1A	BIOFACIES	*Dapsilodus*	*Walliserodus*	*Scabbardella*	*Protopanderodus*	*Drepanoistodus*	*Panderodus*
Plectodina	*Amorphognathus*	*Plectodina*	*Amorphognathus*							

Text-Figure 2.14.1. The distribution of coniform taxa in the Gaer Fawr and Nod Gas Formations.

The only coniform conodonts independent of facies in the Nod Gas Formation are *Panderodus*, *Walliserodus* and *Protopanderodus*. There appears to be no simple pattern to the majority of coniform taxa in this section apart from *Walliserodus* and *Protopanderodus* which occur across the OMZ. It is likely that these two are nektonic.

Text-figure 2.14.2 illustrates the occurrence of conodonts in relation to the OMZ. Because of the relative abundance of *Amorphognathus* and *Plectodina* and *Amorphognathus* in Facies 1, 2 and 1A respectively these have be used to name each nektobenthic biofacies. In addition, the coniform taxa appearing with each major biofacies is noted.

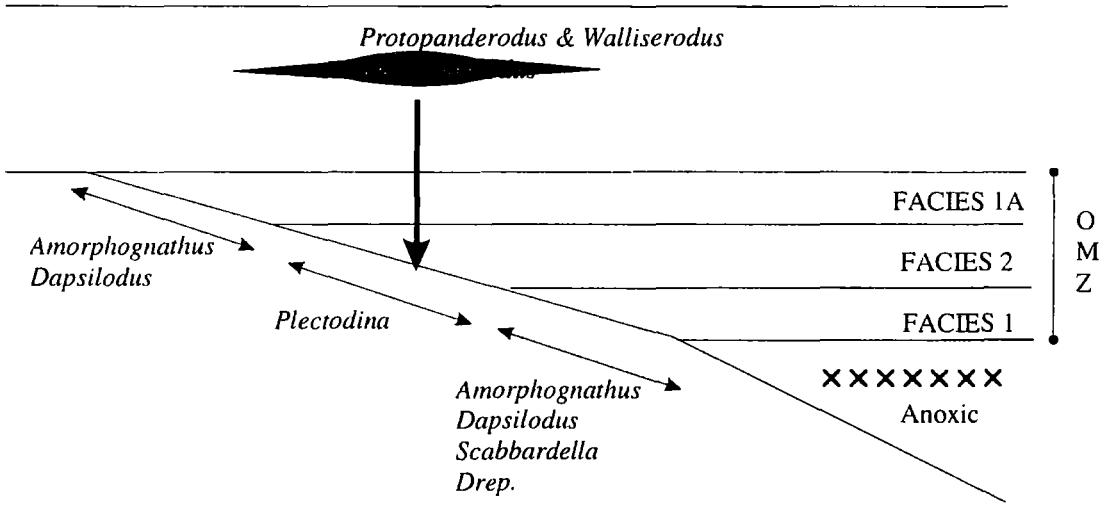

Text-figure 2.14.2. The distribution of biofacies in the Nod Glas Formation. OMZ = oxygen minimum zone.

2.15 Conclusions

- At the Nod Glas the classic Sweet & Bergström (1984) model applies over the whole section i.e. a change from *Plectodina* to *Amorphognathus* Biofacies occurs from the Gaer Fawr Formation to the Nod Glas Formation.
- Conodont species diversity is highest in Facies 1 and 1A.
- The distribution of biofacies reflect subtle environmental differences in the OMZ

- Temperature is postulated to be the main control on biofacies distribution.
- The *Amorphognathus* biofacies probably reflects the cooler base and top of the OMZ. In the Sweet & Bergström (1984) model, *Plectodina* biofacies occur above the seasonal thermocline in well oxygenated, warmer water.
- Only *Walliserodus*, *Panderodus* and *Protopanderodus* appear to be facies independent and are therefore interpreted as nektonic.
- There is no clear distribution pattern for other coniform taxa
- Mixing of all biofacies may occur at the boundaries
- The sedimentary interpretation indicates classic OMZ phosphates with a low oxygen area in the mid-part of the zone and conodont species diversity parallels the interpreted oxygen content within the OMZ.
- The appearance of *Plectodina* in the mid-OMZ is anomalous, i.e. it should coincide with the return of shallow, oxygen-rich waters (and be on the shelf).

There is therefore some conflict in interpretation between conodont biofacies and lithofacies in terms of the occurrence of *Plectodina* within Facies 2. In order to explain this anomaly three possible hypotheses can be constructed.

1. Storm events on the shelf bring shallow water species into the mid-OMZ.
2. *Plectodina* biofacies represent a low oxygen, high nutrient adapted fauna close to the shelf break.
3. The middle zone of the OMZ is an area of warmer water bounded by cooler bands brought in by upwelling processes at the margins of the basin.

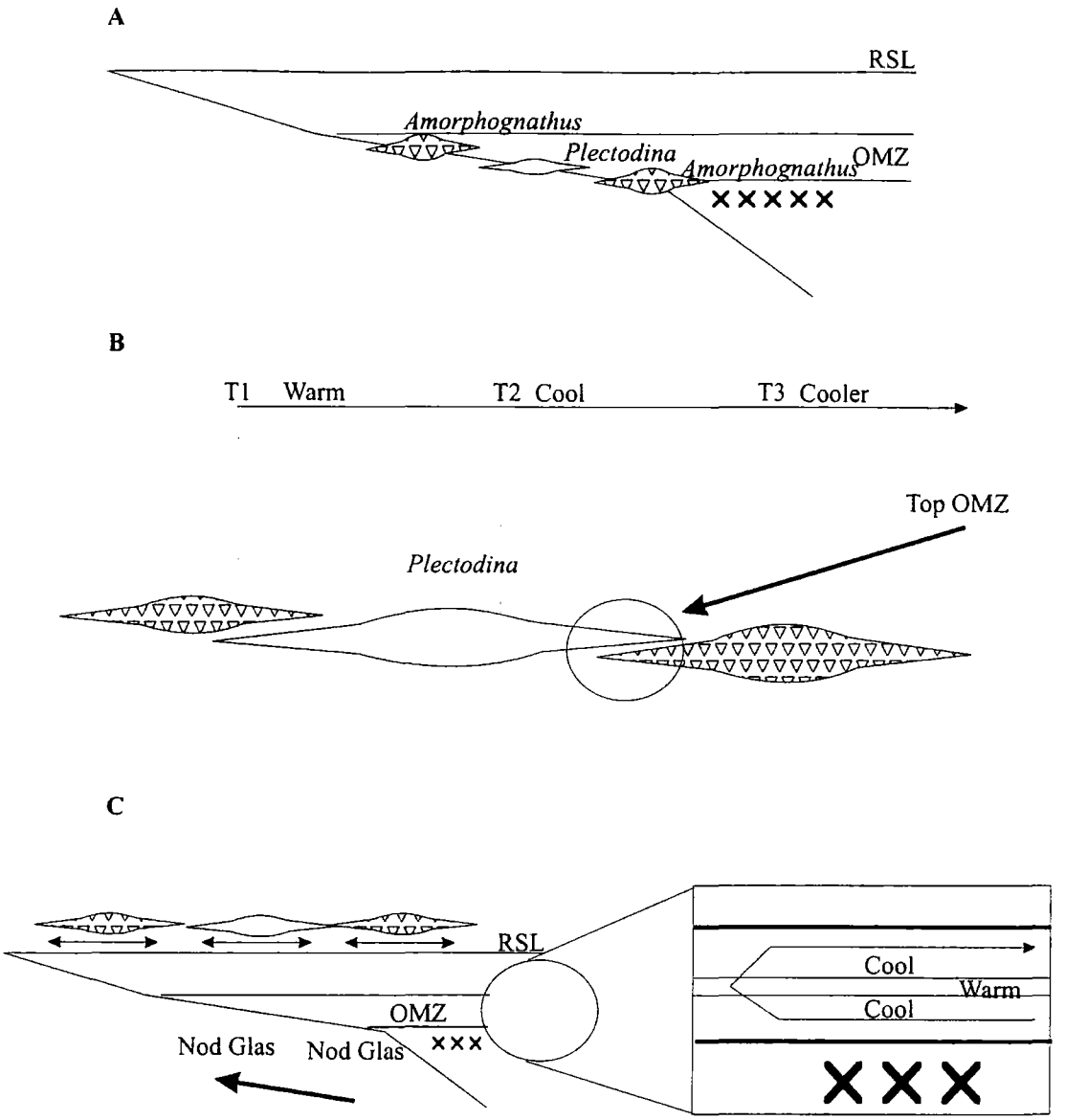

Text-figure 2.16.1. The occurrence of *Plectodina* biofacies in the Nod Glas Formation. A. shows the biofacies occurrences in the OMZ. *Amorphognathus* species dominate the biofacies at the boundaries of the OMZ. B. Represents the temperature gradient within the OMZ. C. Illustrates the warm water band in the centre of the OMZ. Cooler water at the upper and lower boundaries of the Nod Glas Formation is a result of upwelling processes. Anoxic, warm waters lie beneath the OMZ. The warm water layer at the centre of the OMZ is dominated by *Plectodina bullhillensis*, which is postulated to favour a warmer water environment.

Hypothesis three is favoured. The conodont biofacies occurrences of the Nod Glas Formation can therefore be explained in terms of their adaptation to the subtle environmental conditions of the oxygen minimum zone.

Part I - Chapter 3

3. Ashgill conodonts from the Lake District and the Oslo Graben

3.1 Introduction

From the Llanvirn to the Ashgill (Ordovician), the English Lake District formed a part of the Avalon terrane. It lay on the southern side of the Iapetus Ocean in temperate latitudes (Trench & Torsvik, 1992). Evidence suggests that, during the late Ordovician, Avalonia drifted northwards towards Laurentia during closure of the Iapetus Ocean (Cocks *et al.*, 1997).

Rhodes (1955), Orchard (1980) and more recently Armstrong *et al.* (1996) have previously described conodonts from this area of Britain. As part of this study the lower section of the Dent Group has been logged and sampled for conodonts. The upper Caradoc – Ashgill Dent Group was previously termed the Coniston Limestone but was renamed by Kneller *et al.* (1994). Ingham & McNamara (1978) and Lawrence *et al.* (1986) provide full descriptions of the Dent Group.

The present chapter also discusses upper Ordovician conodont biofacies of the Oslo Graben. During the early Palaeozoic this Oslo Region was a cratonic basin (Worsley *et al.*, 1983). It has been demonstrated that Baltica collided with Avalonia in the late Ordovician (Cocks *et al.*, 1997) and with Laurentia in the middle to late Silurian (Cocks & Fortey, 1998). Evidence suggests that during the Ordovician Baltica underwent a slow northward movement into lower latitudes through time and also indicates that the climate was warm in Baltica during the mid-Ordovician and was closer to the equator (like Laurentia) by the end of the Ordovician (Bruton *et al.*, 1985).

3.2 Aims

1. To document the occurrence of conodont biofacies in Avalonia and the Oslo Graben.
2. To assess the factors affecting the distribution of conodont biofacies with particular regard to phylogenetic emergence models.

3.3 The Dent Group

The Dent Group conodont faunas have been comprehensively described by Armstrong *et al.* (1996) who documented faunas from the formation at Hartley Ground (SD 2145 8975), Broughton in Furness, Cumbria where the mixed clastic carbonate succession lies unconformably on the Borrowdale Volcanic Group.

A faunal list is provided by Armstrong *et al.* (1996, Table 1, p. 11) who identified the succession to lie within the *Amorphognathus ordovicicus* Zone and assigned a late Rawtheyan age for this part of the Dent Group (Table 3.3). In addition, Armstrong *et al.* (1996) compiled conodont occurrence data based on the work of Orchard (1980), Ingham (1977) and Kneller *et al.* (1994) to demonstrate the species within the Ashgill Series of the Ordovician. This is illustrated in Text Figure 3.3.1.

Table 3.3

	HG1	HG2	HG3	HG4
A. ordovicicus				
Birksfeldia circumplicata				
?Dapsilodus sp.				
Drepanoistodus suberectus				
Eocarniodus gracilis				
Hamarodus europeaus				
Panderodus unicostatus				
? Prioniodus?				
Protopanderodus liripius				
Scabbardella altipes				
Strachanognathus parvus				
Walliserodus amplissimus				
Walliserodus cf. *amplissimus*				

Table 3.3. The conodont occurrences at Hartley Ground, Broughton in Furness, Cumbria from the data of Armstrong et al. (1996).

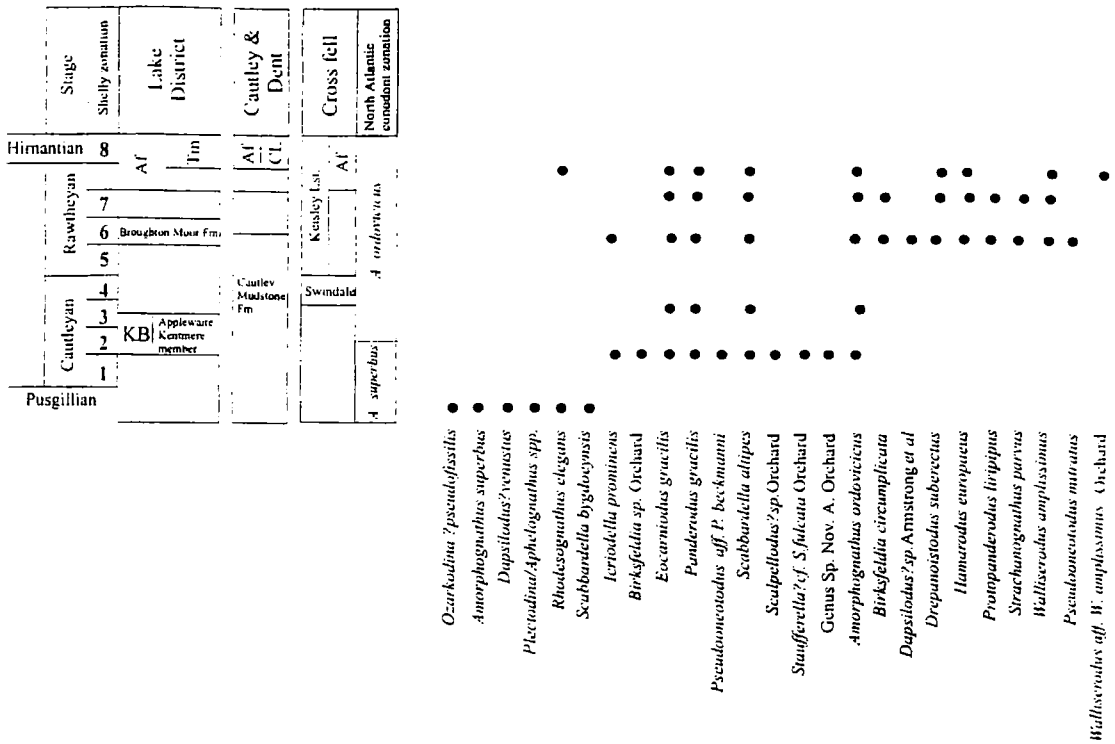

Text Figure 3.3.1. The conodont species occurrences from the Ashgill Series of northern Britain compiled from the data of Orchard (1980) and redrawn from Armstrong *et al.* (1996)

3.4 Greenscoe Road Cutting (Broughton in Furness)

Samples were collected and processed for conodonts from a new road cutting at Greenscoe (Grid reference, SD 221 756, Text-figure 3.4.1). The north-south road cutting exposes a complete section of the Dent Group, approximately 40 metres in length and consisting of steeply dipping limestones with interbedded volcanics (Text-figure 3.4.2). The sharp contact of the Dent Group and the underlying Skiddaw Slates can be seen at the northern end of the outcrop.

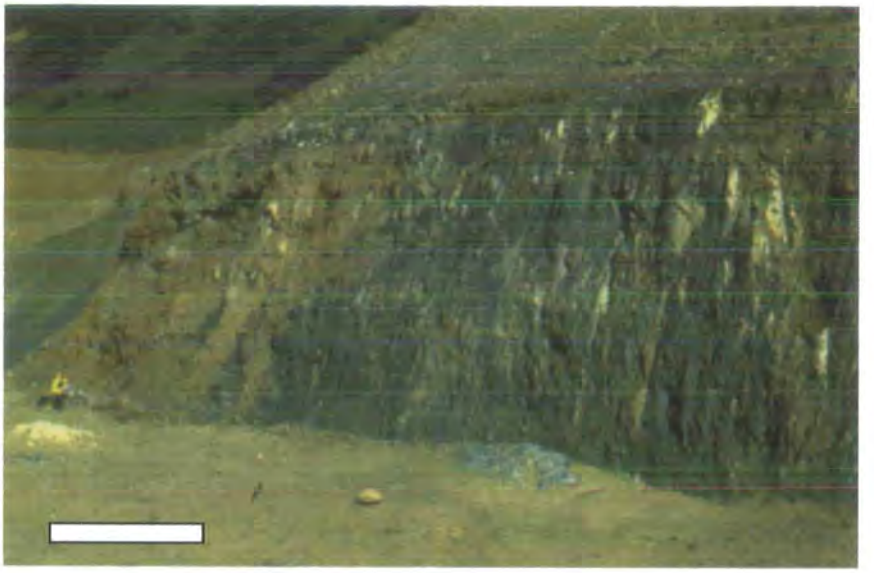

Text Figure 3.4.1. Field photograph of the northern side of the exposed Dent Group at Greenscoe - the lower part of the unit showing thinly bedded limestones. Scale bar = ~10m

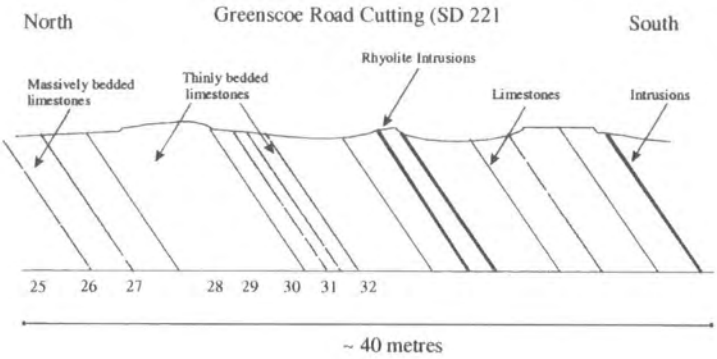

Text Figure 3.4.2. The relationship between the major units in cross-section. Numbers (25-32 relate to conodont samples D725-D732) along the base of the section show levels from which productive conodont samples were obtained.

The sedimentary log of the complete outcrop is shown in Text-figure 3.4.3

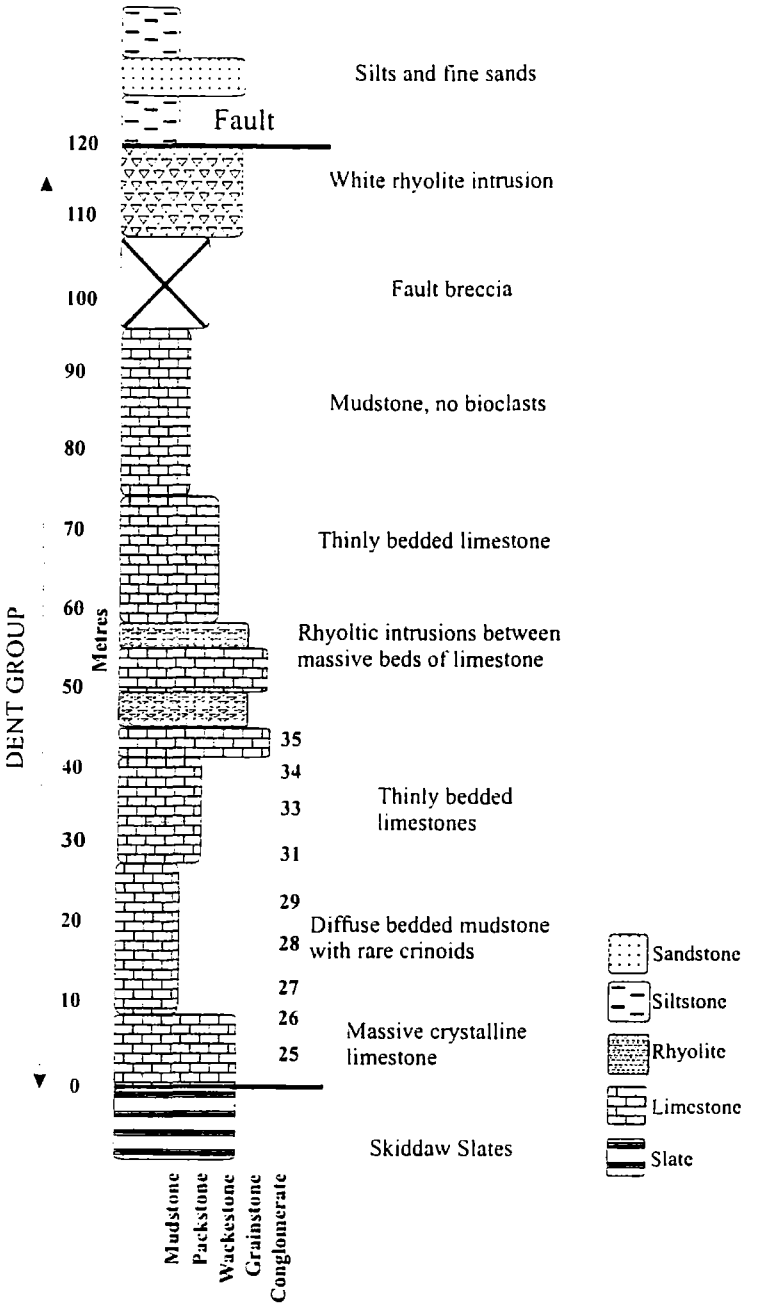

Text Figure 3.4.3. Complete sedimentary log of the Dent Group at Greenscoe (SD 221 756)

The basal three metres of the Dent Group comprise a micritic mudstone with isolated, rare crinoid and pelmatozoan fragments. The beds dip at a constant 70° SSE. Within the lower part of the section there is abundant mineralisation, veining and infilled vugs are common. The three metres above this are extremely weathered with intense brown discoloration. From 6 to 10 metres within the section a finer

grained grey calcareous mudstone yields rare-common crinoid fragments. The bedding in this unit is massive and between 15 cm to 1 metre in thickness. Above the massive limestone units, individual beds became much thinner up to about the 22 metres level. From this horizon to ~ 40 metres the limestone beds are increasingly massive and towards the upper limits are interbedded with rhyolitic intrusions which are white in colour. The limestone units above these intrusions are more massively bedded and muddy with few or no bioclasts. At ~ 80 metres the section is interrupted by a fault and the occurrence of ~ 5 metres of tectonic gouge breccia. Above this horizon a large white rhyolitic intrusion is persistent to a vertical level of ~100 metres. Above this igneous horizon, siltstone lithologies are dominant.

3.5 Sedimentology

Standard size (2"x3") thin sections were made from several samples collected from the Dent Group, Greenscoe. The positions of these samples are indicated on the schematic sedimentary log (Text-figure 3.3.4).

GC 26

This sample is a fine-grained crystalline limestone. The sparite cement forms larger crystals than those of micrite and is seen between the skeletal grains and infilling pores. There are rare bioclasts within the micritic matrix, consisting of isolated, disarticulated brachiopod valves, which show no alignment. In addition, there are isolated pockets of finer grained micrite. Mineralisation (calcite veins) are visible in the thin section and in hand specimen.

GC 31

This sample is similar to that of GC 26 and is a fine-grained crystalline limestone. This sample however, has a higher proportion of bioclasts within the matrix including disarticulated but unfragmented, unaligned brachiopod valves and crinoid ossicles. The bioclasts occur in small isolated pockets. This limestone therefore has a wackestone texture.

GC 33

Sample GC 33 is darker grey in colour than both of the previous samples and is composed dominantly of fine-grained micrite. There are few (<5%) large bioclasts such as disarticulated brachiopod valves within this dominantly micritic matrix The matrix does however, contain abundant complete crinoid ossicles and crinoid ossicle fragments. The brachiopods are disarticulated but not fragmented and not aligned. The sample has been classified as a wackestone.

GC34

Sample 34 is highly bioclastic (>40% bioclasts) which are dominated by crinoid ossicles and brachiopod valves. The surrounding matrix is fine grained micritic mud. The bioclasts occur as pockets (layers?) within the micritic matrix. As with previous samples the larger disarticulated brachiopod valves are not aligned and unfragmented.

GC 36 (sampled from above the first rhyolitic intrusions)

This fine-grained, micritic mudstone contains few bioclasts (<10%) such as disarticulated brachiopod shells. There is no alignment of bioclasts but they occur as layers or pockets within the muddy matrix.

GC37

Sample 37 is a fine grained micritic mudstone containing few (<10%) bioclasts including ovate peloids and brachiopod skeletal fragments. There is no alignment or clustering of these bioclasts. This sample is crosscut by extensive post-depositional calcite mineralisation.

3.6 Environmental interpretation

Carbonate deposition on the continental shelf is related to two main factors; relative lack of siliciclastic sediment and high organic productivity. The transition from dominantly crystalline limestones to those composed largely of micritic mud indicates a slight deepening occurred within this section. The presence of pockets and layers of bioclasts within the micritic matrix indicates that there has been post-mortem transport and sorting, most likely caused by storm events. The environment

of deposition is therefore likely to be on an open shelf. The presence of sand sized sediment and irregular patches of shell hash are indicative of central shelf conditions, lime mud (micrite) is often attributed to deeper outer shelf (foreslope) settings (Sellwood, 1989).

3.7 Conodonts

Samples were collected along the total horizontal length (~ 40 metres) of the outcrop and processed for conodonts.

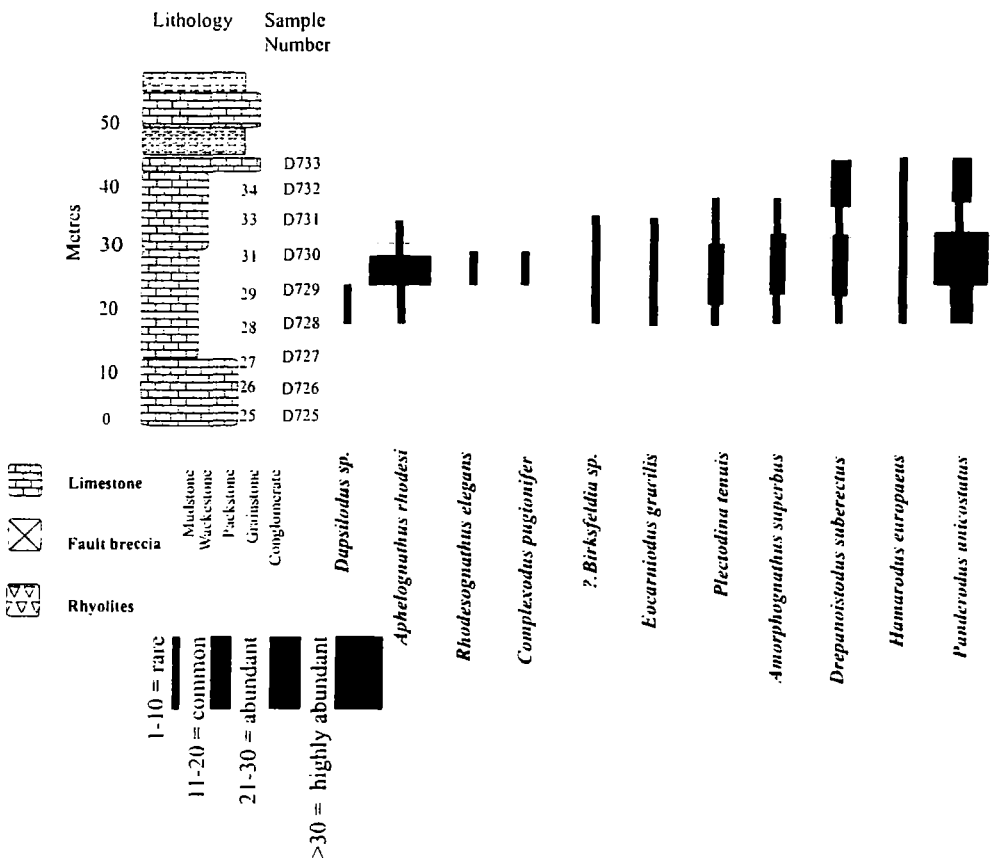

Text-Figure 3.7.1. Conodont abundances from the basal 40 metres of the Dent Group at Greenscoe Road cutting. The key is shown on the bottom left of the figure.

Although the samples collected represented a vertical thickness of ~110 metres, only samples from the basal 40 metres (samples 728 – 732) yielded conodont faunas. Conodont occurrences are shown in Text-figure 3.7.1. These five samples came from the thinly bedded micritic limestones at the base of the section. It may be that the high degree of dolomitisation has altered the majority of the sampled limestones so processing did not yield a conodont fauna. The conodont elements have a colour alteration index (CAI) of 5, which is consistent with heating to 300-400° C. The fauna is generally poorly preserved.

In reference to the Dent Group as documented by Armstrong (1995) and Armstrong *et al.* (1996) a similar conodont fauna has been found within this section at Greenscoe. However, in addition to the fauna documented by Armstrong *et al.* (1996) the conodont species *Aphelognathus rhodesi*, *Plectodina tenuis* and *Rhodesognathus elegans* are present in the Dent Group sediments at Greenscoe. Other genera discussed described by Armstrong *et al.* (1996) are missing from this section; most notably the coniform genera *Walliserodus*, *Strachanognathus* and *Scabbardella.*

The lowermost sample (728) yielded a poorly preserved fauna of both low abundance and diversity. The numerically dominant conodont species is *Panderodus unicostatus*. There are several fragments of what appear to be the Pa elements of *Amorphognathus* but the species name can not be confirmed as this sample did not yield any diagnostic M elements. Other taxa are also named tentatively due to poor preservation of samples and comprise examples of *Birksfeldia circumplicata Dapsilodus mutatus* and *Drepanoistodus suberectus* (Text-figure 3.7.1).

Sample 729 yielded a more abundant and diverse conodont fauna. This sample sees the appearance of conodonts such as *Aphelognathus rhodesi*, *Plectodina tenuis*, *Eocarniodus gracilis*, *Rhodesognathus elegans*, ?*Complexodus* sp. and *Hamarodus europeaus*. *Aphelognathus* is particularly abundant. In addition M elements of *Amorphognathus superbus* are present (Text-figure 3.7.1).

Sample 730 yielded a less diverse and abundant collection than 729. Within this sample much of the conodont fauna is fragmented and poorly preserved. Elements of *Panderodus unicostatus* are again common alongside rare examples of fragments of *Amorphognathus* sp., *Birksfeldia circumplicata* and *Eocarniodus*

gracilis. *Amorphognathus* elements can not be given a species name as there are no diagnostic elements present within this sample.

Sample 731 yielded an extremely low abundance, low diversity and poorly preserved conodont fauna. This fauna is dominated by coniform elements of *Drepanoistodus suberectus* and *Panderodus unicostatus* and contains only two *Amorphognathus* fragments and few examples of *Eocarniodus gracilis*. This represents the lowest conodont diversity and abundance of all samples from this section.

Sample 732 yielded a sparse conodont fauna including representatives of *Drepanoistodus suberectus*, *Plectodina tenuis*, *Panderodus unicostatus*, *Hamarodus europaeus* and *Rhodesognathus elegans*. Coniform elements are more abundant than ramiform elements within this sample.

3.8 Conodont Biofacies at Greenscoe, Cumbria

At Hartley Ground the Lunholm Member of the Dent Group is represented by calcareous mudstone and siltstones at the base, nodular limestones, calcareous siltstones and a clast supported debris flow deposit (Armstrong *et al.*, 1996). In contrast, the exposure of the Dent Group at the Greenscoe locality is composed of sparry limestones grading into fine grained micritic mudstones. This suggests that the Dent Group is diachronous and is onlapping the Borrowdale Volcanic Group. The conodont faunas from the two localities differ in that the base of the latter yields a conodont fauna characteristic of shallow shelf deposits following the Biofacies scheme of Sweet & Bergström (1984).

Moreover, the tentative identification of the conodont species *Amorphognathus superbus* within the Greenscoe samples indicates that the fauna is older (Pusgillian to early Cautleyan) than the *A. ordovicicus* zone in the Lunholm Member at Harley Ground.

The large numbers of *Aphelognathus* specimens at Greenscoe in conjunction with elements of *Plectodina* indicates that this fauna represents a shelf or shallow water biofacies as defined by Sweet & Bergström (1984). *Amorphognathus* biofacies taxa also appear within this section and include the eponymous genus in

addition to *Rhodesognathus elegans*, *Dapsilodus mutatus* and *Drepanoistodus suberectus*. *Panderodus unicostatus* appears in large numbers throughout.

3.9 Conodont Biofacies (northern England) end Caradoc-Hirnantian

By utilising the Dent Group data collected for this study and the data collated by Armstrong *et al.* (1996) it is possible to divide the Ashgill conodont occurrences from parts of northern England. During the Ashgill, a series of transgressions occurred over a relatively short duration. Therefore, these sections are ideal to test the model of phylogenetic emergence and conodont Biofacies distribution as discussed earlier in Part I.

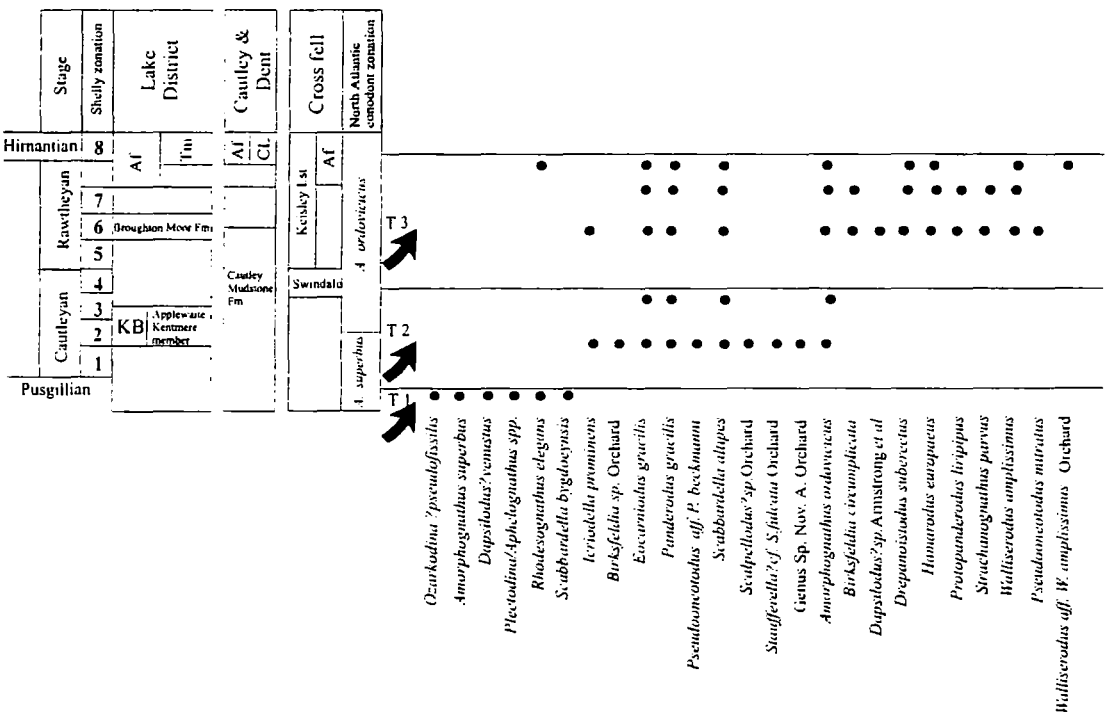

Text-Figure 3.9.1 Conodont occurrences in Northern England and corresponding transgressional episodes (adapted from Armstrong *et al.*, 1996). T1= Pusgillian, T2 = Cautleyan 2, T3= Rawtheyan 6.

Text-figure 3.9.1 shows the conodont occurrences from the Pusgillian to the Rawtheyan. This data can be divided into three distinct sections which, coincide with the Pusgillian, Cautleyan (Zone 2) and Rawtheyan (Zone 6) transgressive events respectively.

Sweet & Bergström (1984) identified conodont biofacies believed to occupy the shelf in the Upper Ordovician including both the *Aphelognathus* Biofacies (where *Aphelognathus* represented >40% of the fauna) and *Plectodina* Biofacies. Furthermore, they identified a shelf edge *Amorphognathus superbus – Amorphognathus ordovicicus* Biofacies. Within this Biofacies, elements of *Amorphognathus* comprised 16-63% of the fauna. Other elements within this Biofacies could also reach high abundance (e.g. *Plectodina* and *Phragmodus* 27% and 19% respectively, and *Panderodus* 30%). Sweet & Bergström (1984) also included the coniform genera *Drepanoistodus*, *Dapsilodus* and *Protopanderodus* in the *Amorphognathus* Biofacies. The deep-water *Dapsilodus mutatus – Periodon grandis* Biofacies was identified close to the Carbonate Compensation Depth. *Dapsilodus mutatus* and *Periodon grandis*, with percentage abundance values of 38% and 18% respectively, dominated the fauna comprising this Biofacies (Sweet & Bergström, 1984). Other taxa assigned to this Biofacies included *Phragmodus undatus* (<1%), *Icriodella superba* (<1%) and the coniform taxa of the *Amorphognathus* Biofacies as listed above.

The Pusgillian conodont faunas of northern England are indicative of the shallow water, shelf biofacies (as defined by Sweet & Bergström, 1984) comprising both *Aphelognathus* and *Plectodina*. Although it is unclear from the data from Armstrong *et al.*, (1996) as to the percentage abundance of each genus in samples from the Pusgillian, these can be obtained from the Pusgillian section of the Dent Group at Greenscoe (as described in section 3.8). In this section, *Aphelognathus* forms approximately 80% of the genera in sample D729 and is therefore chosen as the type genus of the Biofacies.

However, members of the typically shelf edge *Amorphognathus* Biofacies also occur on the shelf in the Pusgillian of northern England, notably *Amorphognathus superbus*, *Rhodesognathus elegans* and coniform taxa such as *Scabbardella altipes*, *Panderodus unicostatus* and *Dapsilodus mutatus*.

During the Cautleyan, members of the typically shelf edge *Amorphognathus* Biofacies are again found in the shelf sediments of Northern England (see Text-figure 3.9.1). Members of the *Amorphognathus* biofacies in northern England are postulated to also include the genera *Eocarniodus*, *Birksfeldia*, *Scabbardella* and *Panderodus*.

Notably, the Pusgillian shallow water biofacies comprising dominantly *Aphelognathus* and *Plectodina* no longer appears on the shelf by low Cautleyan times. Additionally, the species of *Amorphognathus* present in the Cautleyan is *Amorphognathus ordovicicus*.

In the Rawtheyan, genera typical to the *Amorphognathus* Biofacies are still present in the shelf sediments of Northern England (Text-figure 3.9.1). The *Amorphognathus* species present is *Amorphognathus ordovicicus*. Furthermore, other conodont genera also appear in shelf sediments during the Rawtheyan particularly *Icriodella* and *Hamarodus*. The coniform genera include *Dapsilodus*, *Drepanoistodus*, *Strachanognathus*, *Protopanderodus* and *Walliserodus* most of which are coniform genera belonging to Sweet & Bergström's (1984) *Dapsilodus – Periodon* deep-water conodont biofacies.

3.10 Implications

During the Pusgillian the Earth shifted from a greenhouse to an icehouse climate and deep-ocean circulation/ventilation resumed (e.g. Armstrong & Coe, 1997). As a result, ocean states changed and salinity-stratified oceans became thermally stratified and ocean waters are postulated to have decreased in temperature with depth.

The Pusgillian to Rawtheyan shelf sediments of Northern England record the change in conodont biofacies during three major transgressive episodes. The Pusgillian transgression results in the impingement of the normally outer shelf/ slope *Amorphognathus* (*superbus*) biofacies onto the shelf. Although the biofacies during the Pusgillian dominantly comprise typically warm water shelf taxa (e.g. *Aphelognathus/Plectodina*) the transgression is postulated to have caused the

movement of a deeper and cooler water mass onto the shelf, bringing with it species typical of the *Amorphognathus* shelf-edge to slope biofacies (Text-figure 3.10.1 top).

The shelf sediments of the Cautleyan in northern England are dominated by taxa belonging to the *Amorphognathus* biofacies. However, following the Cautleyan 2 sea-level rise, the species of *Amorphognathus* is no longer *Amorphognathus superbus* but *Amorphognathus ordovicicus*. The typical shelf genera (e.g. *Aphelognathus/Plectodina*) are no longer present on the shelf environment and appear to have been replaced by dominantly shelf edge/ slope conodont taxa (Text-figure 3.10.1 middle).

Following the Rawtheyan (Zone 6) transgression shelf sediments record the appearance of deeper-water conodont genera. These include *Icriodella* and *Dapsilodus*. *Protopanderodus* and *Walliserodus* also occur on the shelf although these genera are inferred herein to belong to an off-shore nektonic biofacies which moved inshore during the transgression. Species of *Panderodus* are common to the sediments of the Pusgillian, Cautleyan and Rawtheyan and are also inferred here to be facies independent and most likely nektonic in habit.

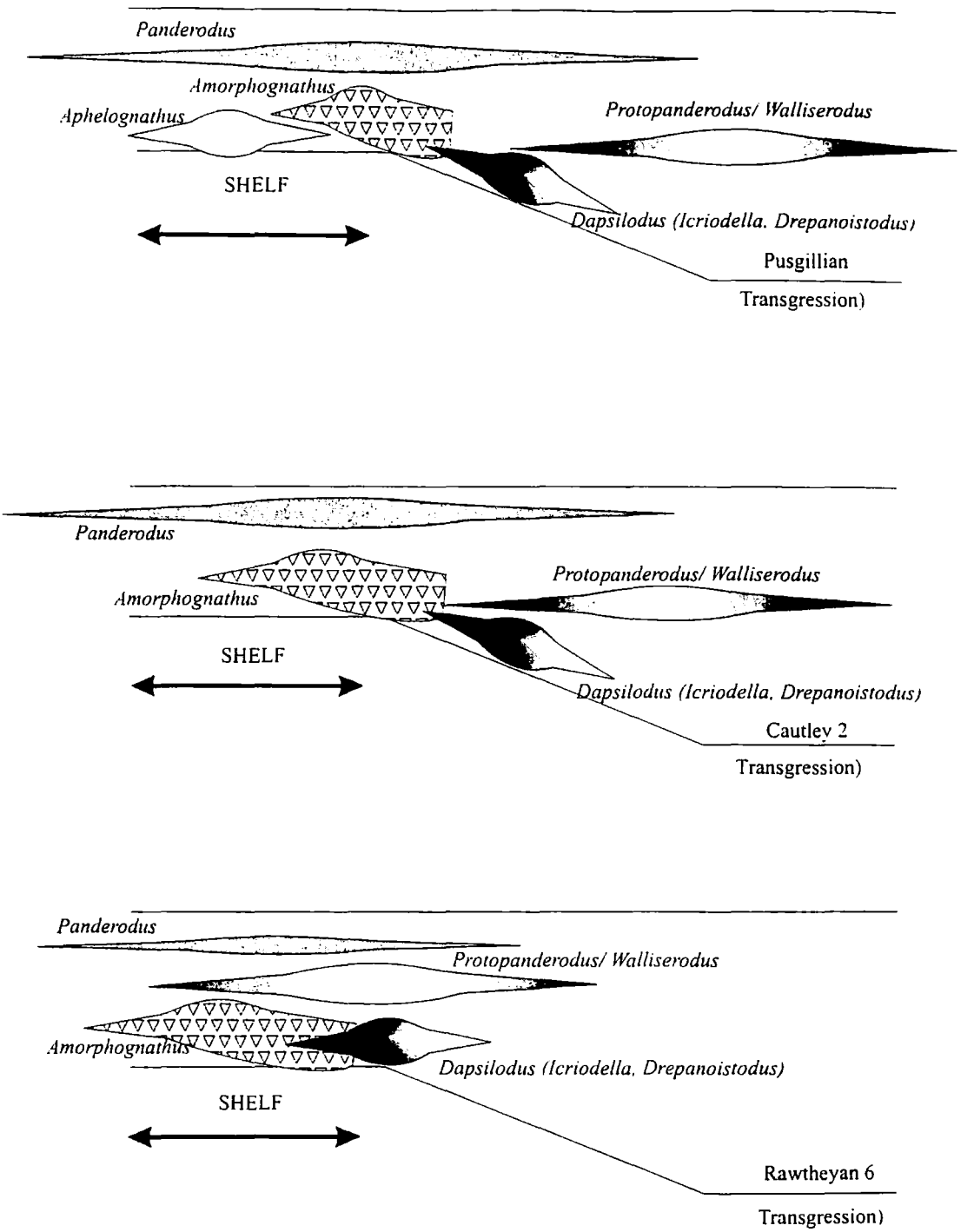

Text-Figure 3.10.1. The appearance of conodont biofacies from the Pusgillian to the Rawtheyan (from the data of Armstrong *et al.*, 1996). Top – the Pusgillian transgression and biofacies, middle – the Cautleyan (Zone 2) transgression and biofacies, bottom – the Rawtheyan (zone 6) transgression and biofacies. The arrow marks the depositional area of the shelf.

3.11 Conclusions

The eustatic transgressive episodes during the upper Ordovician caused the movement of deeper-water biofacies into shallower shelf conditions. This is exemplified by the progressive appearance of the *Amorphognathus* and the *Dapsilodus – Protopanderodus* Biofacies in the shelf sediments of northern England. This indicates that along the southern margins of the Iapetus Ocean, cooler water masses impinged on the shelf at times of transgression. The shore-wards movement of the *Protopanderodus - Walliserodus* planktonic Biofacies may be a result of increased accommodation space in the water column brought about by the increase in sea-level allowing biofacies expansion.

3.12 Conodont biofacies in the Oslo Graben

The Oslo Region was defined by Størmer (1953) to comprise eleven districts in a NNE-SSW trending strip of southern Norway (Owen *et al.*, 1990). During the early Palaeozoic this area was a cratonic basin (Worsley *et al.*, 1983) and the Cambrian to Silurian sections are thicker than is seen on contemporaneous platform sequences elsewhere on the Baltic craton (Bruton *et al.*, 1985). The Ordovician rocks of the Oslo Region comprise alternating shale and limestone formations (Owen *et al.*, 1990) indicative of deposition on the outer shelf.

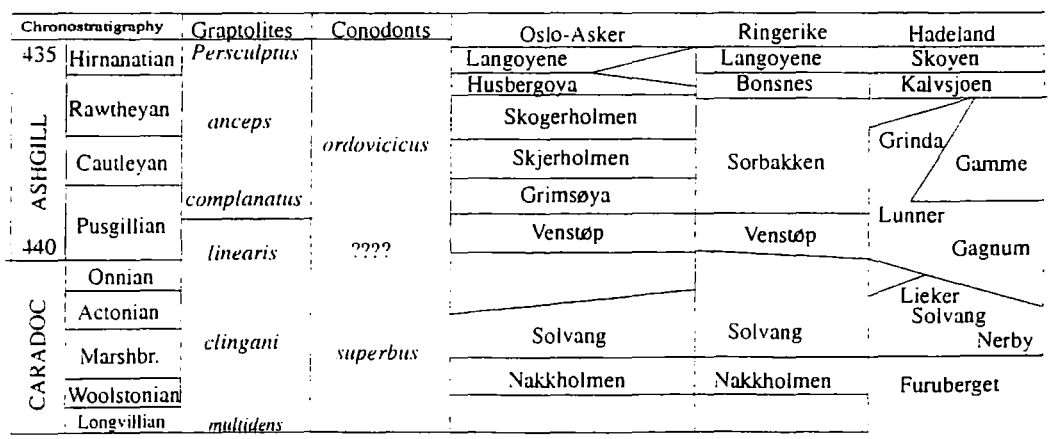

Text Figure 3.12.1. The Stratigraphy and Formations of the Oslo Graben area showing part of the Ordovician succession from which conodonts are discussed herein. Adapted from Stouge & Rasmussen, 1995 and Owen *et al.*, 1990 using the revised British Ordovician chronostratigraphy of Fortey *et al.* (1995).

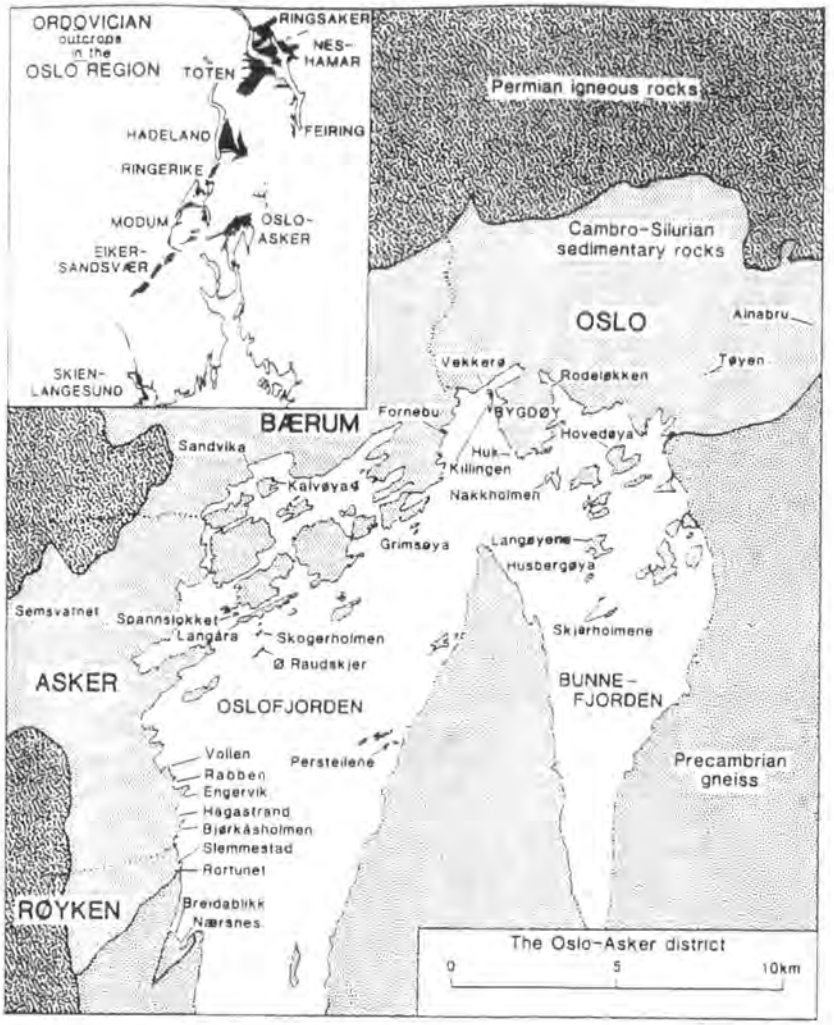

Text-figure 3.12.2. Map of the Oslo-Asker District showing the localities as mentioned in the text (from Owen *et al.*, 1990)

Hamar (1964, 1966) documented the conodont faunas from both the Oslo-Asker and Ringerike districts, including faunas from the Aurelucian Ampyx Limestone (now termed the Vollen Formation), the Upper Chasmops Limestone (now the Solvang Formation) and the Upper Chasmops Shale (the Nakkholmen Formation). Hamar (1966) described a large conodont fauna within the Solvang Formation (*linearis* zone) including genera such as *Amorphognathus*, *Drepanodus*, *Protopanderodus*, *Panderodus* and *Periodon*. He further described less diverse

faunas from the older Nakkholmen Formation (*multidens – clingani*) including *Panderodus*, *Protopanderodus* and *Drepanodus*.

A summary of the formations discussed in the present chapter is provided in Table 3.12 and a locality map is provided in Text-figure 3.12.2.

Table 3.12

Formation	Age/environment
Bønsnes	Shelly fauna indicates a Rawtheyan age for this formation. Shallow water deposition indicated by the presence of calcareous algae and other sedimentary evidence
Sørbakken	Owen (1979) noted that the occurrence of *Calymene* cf. *marginata* 40 metres above the base of this formation indicates a correlation with the lower Cautleyan Drummock group of Girvan. Trilobites in the upper part indicate correlation with the Rawtheyan units in Oslo-Asker and Hadeland.
Venstøp	Presence of *lineraris* zone graptolites, *Flexycalymene* and *Tretaspis* sp. indicates an early Ashgill (Pusgillian) age. Sediments indicate low energy conditions of deposition.
Solvang	Trilobites indicate an Actonian and Onnian age. *Tretaspis ceriodes* found in the shale near top has middle *clingani* zone fauna and *Amorphognathus complicatus* (Owen, 1979).
Nakkholmen	Graptolites such as *Amplexograptus rugosus*, *Climacograptus* indicate Lower *clingani* zone (Woolstonian – Marshbrookian)

Table 3.12. Summary of the ages of formations (from Owen, 1979; Owen *et al.*, 1990).

3.13 Sample Set 16881-1 (01-015) from North Raudskjer.

Table 3.13.

Sample Number	Formation	Sedimentology
16881-1 01 (2244g)	Nakkholmen Formation	Grey silty micrite
16881-1 02 (2305g)	Solvang Formation (base)	Grey silty micrite
16881-1 03 (2043g)	Solvang Formation	Grey silty bio-micrite
16881-1 04 (2177g)	Solvang Formation	Grey silty bio-micrite
16881-1 05 (2617g)	Solvang Formation	Slity bio-micrite some spar
16881-1 06 (2466g)	Solvang Formation	Mid-grey, shelly silty limestone
16881-1 07 (2985g)	Solvang Formation (top)	Limestone nodules in shale unit
16881-1 08 (2441g)	Venstøp Formation (base)	Limestone nodules in shale unit
16881-1 09 (2610g)	Above the Venstøp Formation	Grey silty micrite
16881-1 010 (1885g)	Grimsøya Formation	Grey silty micrite
16881-1 011 (2096g)	Grimsøya Formation	Grey silty micrite
16881-1 012 (1589g)	Grimsøya Formation	Grey silty micrite
16881-1 013 (3378g)	Grimsøya Formation	Grey silty micrite
16881-1 014 (1958g)	Grimsøya Formation	Grey silty micrite
16881-1 015 (2095g)	Grimsøya Formation (upper units)	Grey silty micrite

Table 3.13. Details for Sample Set (16881-1). Numbers in brackets indicates the amount of sample dissolved not counting the acid resistant residues.

Samples from North Raudskjer (~ to the western part of Oslo-Asker) were provided by Dr. M.P. Smith (University of Birmingham) from the Nakkholmen, Solvang, Venstøp and Grimsøya formations (Table 3.13). The following section reviews the lithologies and age diagnostic fossils from each formation.

3.14 Nakkholmen Formation

Owen *et al.* (1990) described the Nakkholmen Formation as comprised dominantly of shale lithologies with occasional black limestone nodules. The formation is present in Oslo-Asker and Ringerike and is more calcareous in its western part (including Raudskjer), the nodular horizons becoming more common and the shales thinning and becoming paler. The brachiopod and trilobite fauna increases in diversity westwards (Harper *et al.*, 1985).

3.15 Solvang Formation

The Solvang Formation is dominantly composed of nodular and more planar bedded limestones interbedded with shales. It is one of the most fossiliferous units in

the Oslo region (Owen *et al.*, 1990) and is largely Actonian-Onnian in age. The uppermost part of the formation on Ringerike contains trilobites which Owen (1979) interpreted as being low Ashgill in age (Pusgillian).

Bruton & Owen (1979) used faunal logs to demonstrate the progressive immigration of trilobite species and an increase in diversity in the Solvang Formation in Oslo-Asker and Raudskjer followed by a major faunal shift at the base of the overlying shales (Venstøp Formation). Bruton & Owen (1979) postulated that the distribution of species within the Solvang Formation indicated a gradual incoming of species, the later stages of which were accompanied by the initiation of dominantly shale deposition to the east.

3.16 The Venstøp Formation

The Venstøp Formation has been documented by Owen *et al.* (1990) to be 7.4 metres in thickness in Oslo-Asker in contrast to the 26 metres vertical thickness at Ringerike (north-west Frognøya). In all districts, this dominantly shale lithology, has been found bounded by limestones. In Oslo-Asker Owen *et al.* (1990) documented the presence of a thin phosphatic conglomerate at the base of the Venstøp Formation. The phosphatic horizon was previously described by Williams & Bruton (1983) who believed that it represented a hiatus or time interval spanning the late *clingani* and early *linearis* graptolite biozones.

Graptolites are common in some horizons of the Venstøp Formation, as are trilobites, and combined evidence from these two indicates an early Ashgill (Pusgillian) age (*linearis* zone). Shelly faunas are abundant but low in diversity and show a higher degree of articulation than other formations in the region. This, together with an association of *Chondrites*, indicates a low energy environment of deposition (Owen, 1979; Owen *et al.*, 1990).

3.17 Grimsøya Formation

The basal part of the Grimsøya Formation contains thin limestone nodules among faint shale partings. The upper section consists of interbedded limestones and shales and the unit thins towards the east. Much of the formation is unfossiliferous

(Owen *et al.*, 1990); however, trilobites, corals and cephalopods have been documented from certain parts of the sections. The Grimsøya Formation is of Ashgill age but its fauna is not more specifically age diagnostic.

3.18 Summary (log, graptolite zones and conodont samples, 16881-1)

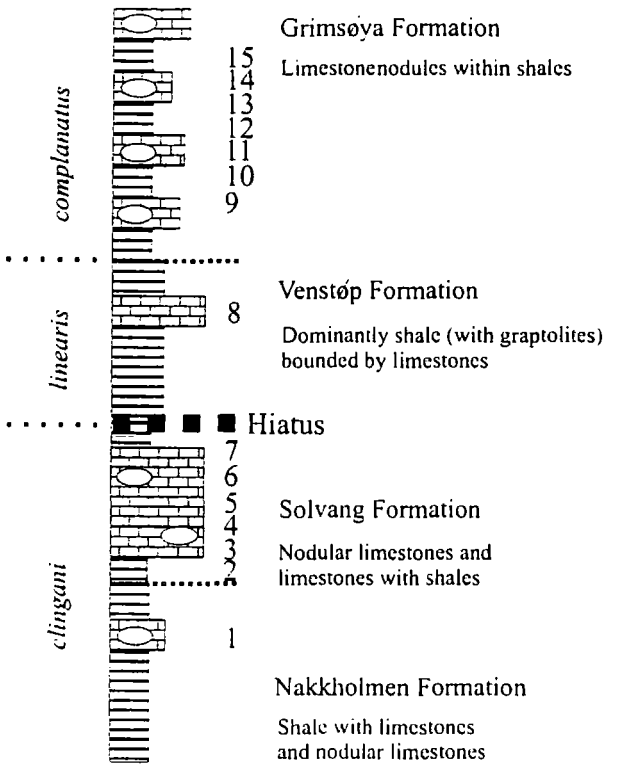

Text Figure 3.18.1. Schematic log of the formations at north Raudskjer, Oslo-Asker. The numbers indicate the approximate positions of conodont samples.

Text-figure 3.18.1 shows a schematic log of formations at North Raudskjer. The lower part of this section (to the lower part of the Venstøp Formation) is shown in detail in Owen *et al.* (1990). Sedimentological evidence indicates that the Nakkholmen Formation was deposited on the outer shelf - upper slope environment. The subsequent development of limestone beds comprising the Solvang Formation suggests a slight shallowing of the section. The phosphatic conglomerate at the base

of the Nakkholmen Formation (Owen *et al.*, 1990) shows initial deepening of the section occurred at this point and may further suggest the development of an oxygen minimum zone. The overlying widespread shale development of the Venstøp Formation is indicative of significant transgression. This sedimentological change bears a similarity to that of the Nod Glas Formation as described in Part I, Chapter 2.

3.19 Conodonts (Sample Set 16881-1)

Text-figure 3.19.1 illustrates the key used to demonstrate the number of conodont species in specimens from the Oslo Graben.

Text-Figure 3.19.1. Key for abundance charts used for the Oslo conodont samples.

Samples 01-04, 06, 08,09 and 011-015 are low in both conodont abundance and diversity. Samples 05 and 07 however, yielded a more abundant conodont fauna. Both these samples lie towards the top of the Solvang Formation (Text-figure 3.19.2).

Amorphognathus superbus occurs at the top of the Solvang Formation. Higher in the section (the Grimsøya Formation), the lack of M elements makes diagnosis difficult but it is assumed that the *Amorphognathus* elements belong to *Amorphognathus ordovicicus*.

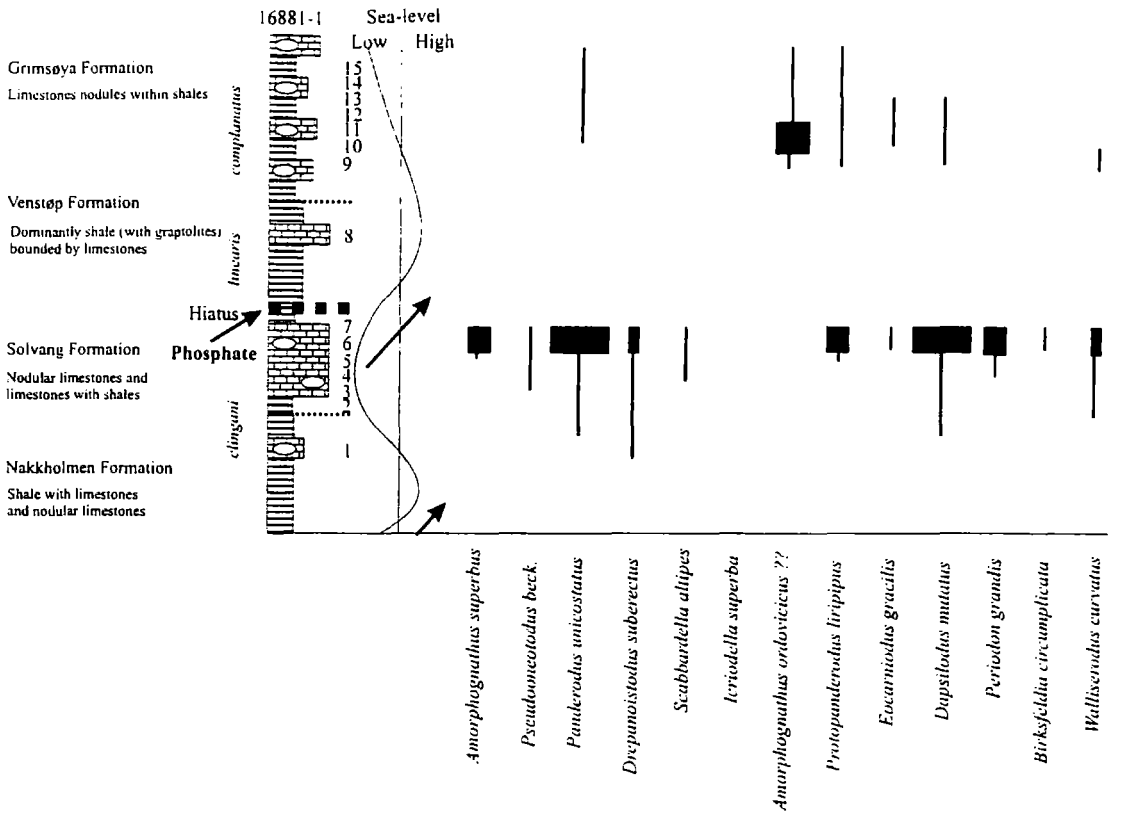

Text-Figure 3.19.2. Conodont range chart for sample set 16881-1. The interpreted sea-level curve is shown to the right of the sedimentary log. Major sea-level rises are marked by arrows on the sea-level curve.

3.20 Conodont Biofacies

As illustrated in Text-figure 3.19.2 the conodont faunas of North Raudskjer are dominated by genera belonging to both the *Amorphognathus* and *Dapsilodus-Periodon* Biofacies (as defined by Sweet & Bergström, 1984).

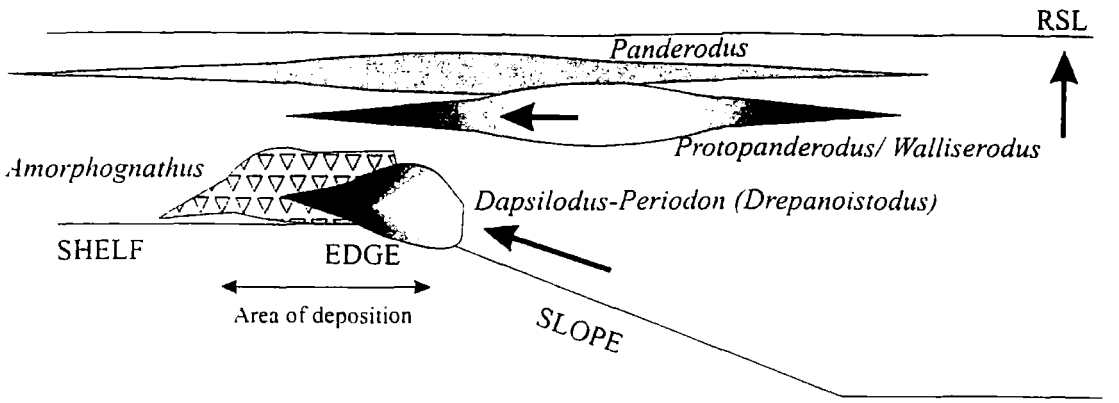

Text-Figure 3.20.1. The position of the conodont biofacies in North Raudskjer (sample set 16881-1). Arrows indicate movement of conodont biofacies.

Text-figure 3.20.1 illustrates the conodont biofacies present on North Raudskjer as elucidated from sample set 16881-1. The sedimentology of the Nakkhlomen Formation indicates deposition on the outer edge of the shelf or the upper slope. However, conodont occurrences are most abundant in the shelf edge deposits of the Solvang Formation.

The top of the Solvang Formation coincides with the beginning of a sea-level rise (see Text-figure 3.19.2). This is postulated to have resulted in the impingement of the cooler deeper-water *Dapsilodus-Periodon* biofacies into a shallower shelf-edge position (Text-figure 3.20.1). The sea-level rise also results in the appearance of the nektonic, off-shore *Protopanderodus-Walliserodus* Biofacies towards the top of the Solvang Formation.

The sample (16881-1 08) from a limestone horizon within the shale dominated Venstøp Formation was barren of conodonts. However, the overlying Grimsøya Formation did yield conodonts albeit in low abundance.

3.21 Sample Set (Frognøya)7881-1 (01-012)

Frognøya is a small island SW of Noderhov (Text-figure 3.21.2). The Ringerike district is situated NW of Oslo (Størmer, 1953) and the local Lower Palaeozoic succession in this region has a NE-SW strike and youngs toward the

south-east (Owen, 1979). For a full review of this area see Owen (1979). The succession of Ordovician rocks is well developed on the north and west coasts of the island (Frognøya). Hamar (1966) first described the conodont fauna from the Solvang Formation in the Ringerike District.

Dr. M. P. Smith (University of Birmingham) collected sample set 7881-1 from the Island of Frognøya in Ringerike. The conodont samples analyses are from the Solvang, Venstøp, Sørbakken and Bønsnes formations (Text-figure 3.21.1).

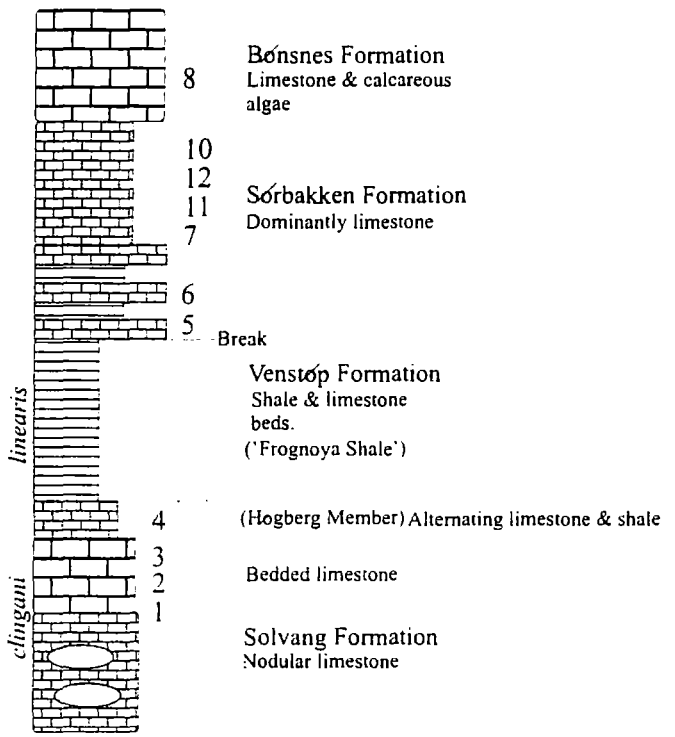

Text Figure 3.21.1. Schematic diagram of the successions at Ringerike, Frognøya (adapted from information in Owen, 1979; Owen *et al.*, 1990).

Table 3.21

Sample number	Formation	Sedimentology
7881-1 01 (1893g)	5m below top Solvang	Pale grey silty micrite
7881-1 02 (2139g)	2.9 m below top Solvang	Pale grey silty micrite
7881-1 03 (1474g)	Solvang Fm. (Høgberg Mmb.)	Pale grey silty micrite
7881-1 03a (1307g)	Solvang Fm. (Høgberg Mmb.)	Pale grey shelly micrite
7881-1 04 (2370g)	Solvang Fm. (Høgberg Mmb.)	Mid-grey silty micrite
7881-1 05 (1946g)	4m above Frognøya Shale H. mmb.)	Dark-grey silty limestone
7881-1 06 (2077g)	7.5 m below top of Frognøya Shale	Dark grey calcareous siltstone
7881-1 07 (1837g)	Base of Sørbakken Formation	Mid-grey silty micrite
7881-1 08 (2703g)	Base of Bønsnes Formation	Mid-grey silty micrite
7881-1 09 (2456g)	17m below top Sørbakken Fm.	Mid-grey silty micrite
7881-1 010 (2183g)	Top Sørbakken Formation	Mid-grey silty micrite
7881-1 011 (1960g)	Sørbakken Fm	Mid-grey silty micrite
7881-1 012 (2170g)	16m above base of Sørbakken Fm	Mid-grey silty micrite

Table 3.21 Details of sample set 7881-1 (01-1012)

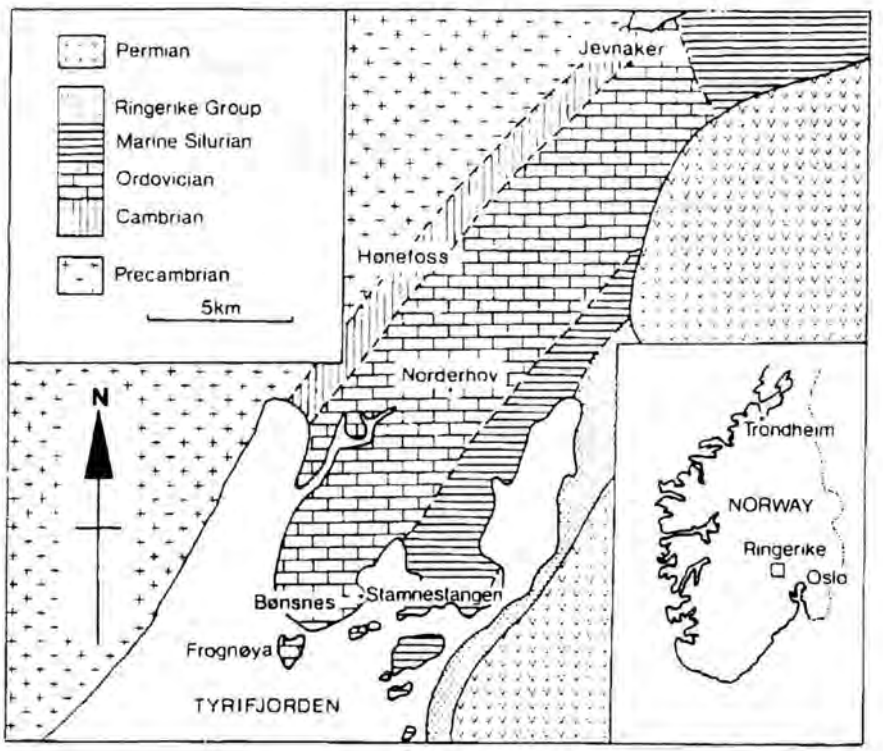

Text Figure 3.21.2. Simplified geological map of the Ringerike District showing the position of Frognøya Island (from Owen, 1979)

The Solvang Formation is exposed in the NW of the island (Owen, 1979) and its lower 4 metres consists of nodular limestones with thin shale partings whereas the upper 3 metres is composed of alternating bedded limestones and shales formerly termed the Høgberg Member (see Owen *et al.*, 1990, p.24). Faunal evidence indicates that the 'Høgberg Member' is probably younger than the top of the Solvang Formation elsewhere (Owen *et al.*, 1990).

3.22 The Venstøp Formation

The lowest 4-5 metres on Frognøya was noted by Owen *et al.* (1990) to be composed entirely of shale and is succeeded by 5 metres of shale with some limestone beds and isolated limestone nodules. The remaining 15 metres of the unit consists of limestone beds with some nodules. Many of the limestone beds are argillaceous and some are strongly bioturbated. Fossils in the shale are often fragmentary but include graptolites. Some of these are preserved in three dimensions in the limestone beds (see also Williams & Bruton, 1983).

3.23 The Sørbakken Formation on Frognøya

The Sørbakken Formation (previously termed the Trinucleus limestone) was estimated by Owen (1979) to be approximately 100 metres thick. No complete section is available through the Sørbakken Formation although there is no structural, sedimentological or palaeontological evidence for any hiatus in it (Owen, 1979). Its base marks a distinctive change from shale to limestone deposition. The top of this unit is marked by the appearance of calcareous algae in the basal beds of the overlying Bønsnes Formation. With the exception of the basal few metres the Sørbakken Limestone has a very diverse fauna of trilobites and brachiopods. The lithology of this unit is dominated by limestones, nodular limestones, and intervening calcareous shales. Toward the top of the unit the limestones are platy and almost black in colour (Owen *et al.*, 1990).

The diverse fauna of the upper part of this formation is indicative of a Cautleyan age.

3.24 The Bønsnes Formation on Frognøya

Only the lower part of this unit is exposed on Frognøya. The lower beds have a fauna of brachiopods and trilobites whereas the upper coral beds have no other shelly fossils. The lowest part of the Bønsnes Formation is dominantly composed of calcareous algal beds. Trilobite faunas in this formation indicate a Rawtheyan age (Owen, 1979). The Formation appears to represent deposition in significantly shallower water than all the previously described formations herein and the samples collected are barren of conodonts.

3.25 Conodonts (Sample set 7881-1)

The sedimentology of the section on Frøgnoya indicates that the Solvang Formation was deposited in an outer shelf or slope setting. The Venstöp Formation ("Frognøya Shale") indicates a deepening. The sequence stratigraphy of this part of the succession correlates with the transition from the Solvang to the Venstøp Formation in North Raudsker indicating that the phosphate layer in the latter is equivalent to the 'Høgberg Member' on Frøgnoya (Text-figure 3.25.1).

Above the Venstøp Formation deposition of the Sorbakken Limestone is indicative of a relative sea-level fall. The algal limestones of the Bonsnes Formation indicate that this shallowing continued upwards (Text-figure 3.25.1).

Conodont samples at Frognøya are from the upper part of the Solvang Formation, the lower Venstøp Formation and the Sorbakken Formation. Samples 1-4 (Text-figure 3.25.2) yielded a low diversity, low abundance conodont fauna. Samples 6 and 7 come from the Sorbakken Formation and yield a lower diversity but higher abundance conodont fauna. Samples 12, 10 and 8 are all barren with the exception of the tentative identification of *Walliserodus* in sample 08.

The transition from the Solvang to the Venstøp Formation indicates significant deepening of the section on Frognøya during the low Pusgillian (Text-figure 3.25.2).

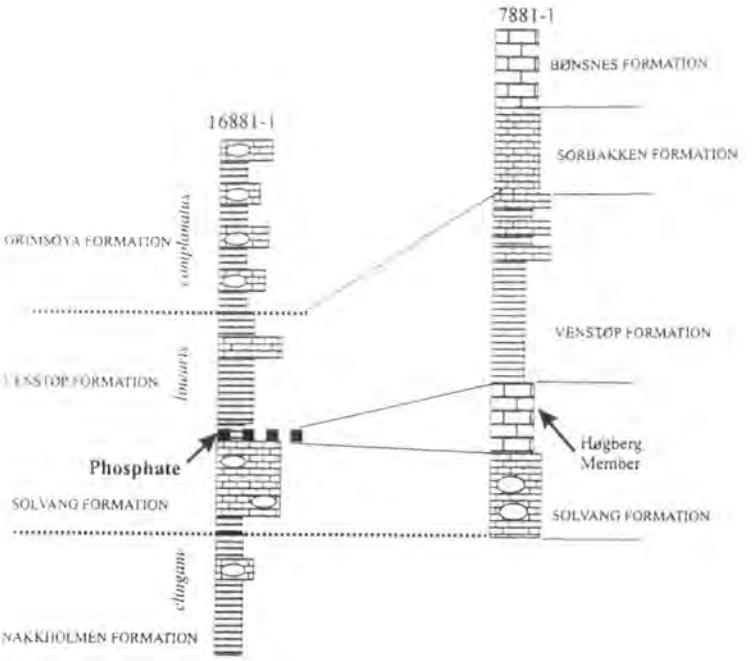

Text-figure 3.25.1. Correlation of the formations on North Raudskjer and Frognøya. The sequence stratigraphy on Frognøya correlates to the transition from the Solvang to Venstøp Formation in North Raudskjer. The phosphate layer is therefore equivalent to the Høgberg Member.

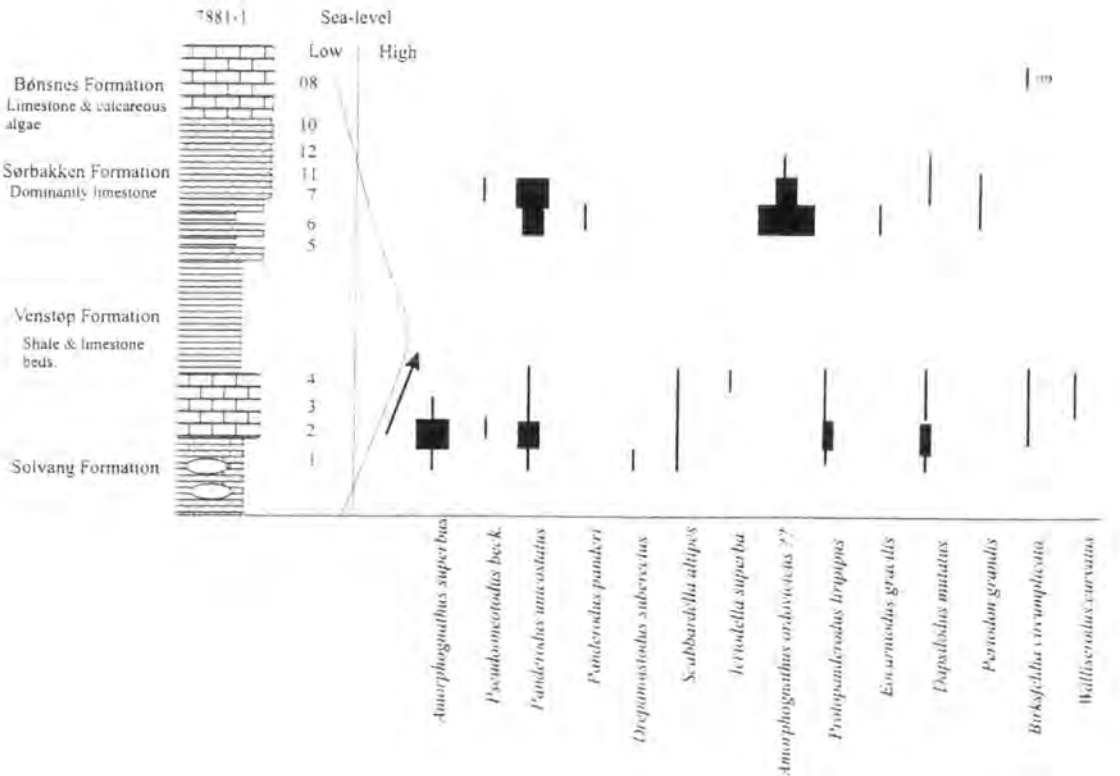

Text-figure 3.25.2. Abundance chart of conodonts from sample 7881-1, Frognøya.

3.26 Conodont Biofacies

The conodont faunas on Frognøya can be divided into members of two nektobenthic biofacies. The association of *Amorphognathus superbus*, *Scabbardella altipes* and *Birksfeldia circumplicata* in the Solvang formation is indicative of the upper slope *Amorphognathus* Biofacies. *Birskfeldia* is assigned to the *Amorphognathus* Biofacies both here and in northern England which is an additional genus to those assigned by Sweet & Bergström (1984). The *Amorphognathus* Biofacies is present in the Solvang and lower Venstøp Formations and is mixed with members of the deeper water *Dapsilodus-Periodon* Biofacies (Text-figure 3.26.1). The transgression therefore brings these characteristically deeper – water biofacies onto the shelf.

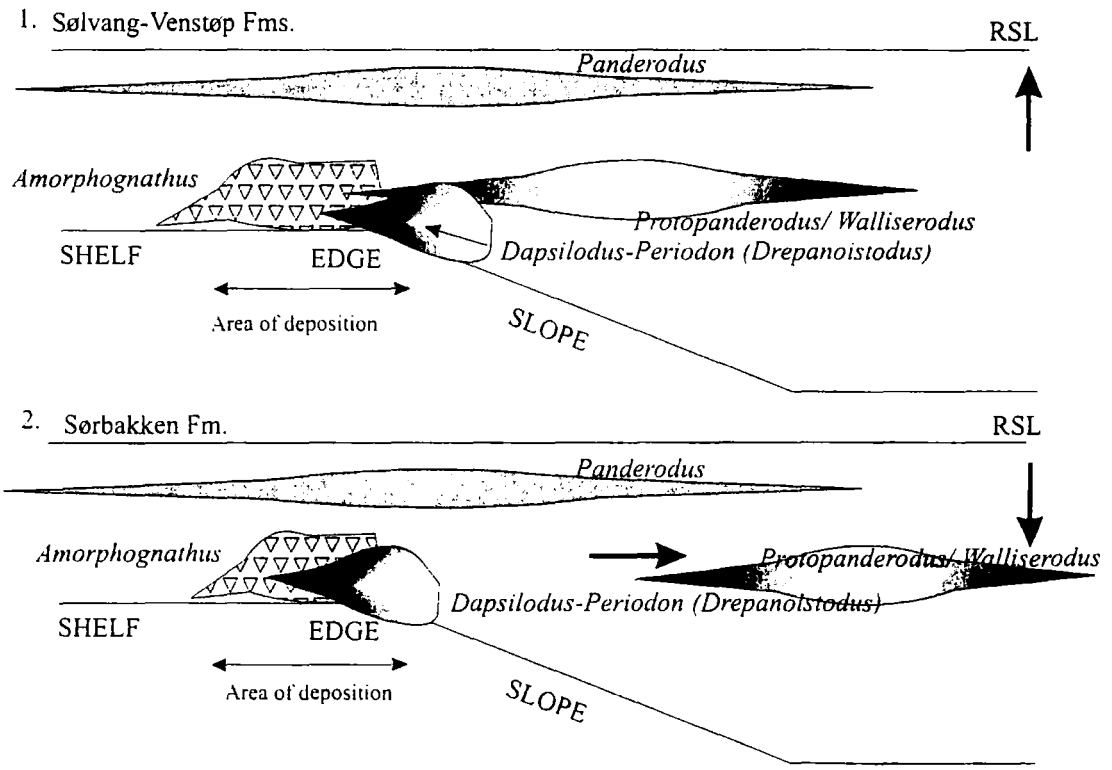

Text-Figure 3.26.1. Conodont Biofacies of Frøgnoya (samples 7881-1). Arrows indicate movement of conodont biofacies. 1. The conodont biofacies in the lower part of the section (Solvang Fm.). 2. The biofacies in the Sørbakken Formation.

The *Panderodus* and *Walliserodus-Protopanderodus* Biofacies are both interpreted to be nektonic. It is inferred that during the initial sea-level rise the colder deeper water biofacies move into an outer shelf position and the nektonic coniform biofacies move shorewards (Text-figure 3.26.1 (1)). As sea-level fell, the *Protopanderodus-Walliserodus* Biofacies moved into a more offshore position and its members were therefore not deposited in the shelf sediments of the Sørbakken Formation.

3.27 Sample Set 13881-1 (01-013)

This collection was made by Dr. M.P Smith (University of Birmingham) in the Hadeland district. The relationship between the successions of this region, from which samples were collected, are summarised in Table 3.27 and Text Figure 3.28.1.

Table 3.27

Sample Number	Formation	Sedimentology
13881-1 01 (2125g)	Solvang Formation	Mid-grey silty micrite
13881-1 02 (2419g)	Solvang Formation	Mid-grey silty micrite
13881-1 03 (2472g)	Solvang Formation	Mid-grey silty micrite
13881-1 04 (518g)	Lunner Formation	Nodular horizon within shale
13881-1 05 (2272g)	Gagnum Lst. (Gamme Fm.)	Mid-grey silty micrite
13881-1 06 (2152g)	Gagnum Lst. (Gamme Fm.)	Mid-grey silty micrite
13881-1 07 (2679g)	Gagnum Lst. (Gamme Fm.)	Mid-grey silty micrite
13881-1 08 (2302g)	Gagnum Lst. (Gamme Fm.)	Mid-grey silty micrite
13881-1 09 (2177g)	Gagnum Lst. (Gamme Fm.)	Mid-grey silty micrite
13881-1 010 (2420g)	Gagnum Lst. (Gamme Fm.)	Mid-grey silty micrite
13881-1 011 (2268g)	Gagnum Lst. (Gamme Fm.)	Mid-grey silty micrite
13881-1 012 (2155g)	Gagnum Lst. (Gamme Fm.)	Mid-grey silty micrite
13881-1 013 (2450g)	Gagnum Lst. (Gamme Fm.)	Mid-grey silty micrite

Table 3.27. Sample set 13881-1 details

The majority of samples from set 13881-1 were collected from the Gagnum Limestone (see Text-Figures 3.2.1 & 3.27.2). The Gagnum Limestone is now termed the Gamme Formation (Owen *et al.*, 1990). The main lithology of this formation is nodular limestone and the base can be seen to show an abrupt change from the shales of the underlying formation. Much of the formation is unfossiliferous, but where fauna is present trilobites dominate. The shelly fauna indicates an age from Pusgillian to early Rawtheyan (Owen, 1979).

The Nerby Member lies in the *clingani* Graptolite Biozone and the Gamme Limestone is between the lower *complanatus* and upper *anceps* graptolite Biozones and therefore is Pusgillian – Rawtheyan in age (Owen *et al.*, 1990). The Lunner formation was previously termed the Tretaspis Shale or the Gagnum Shale (Owen, 1990) and reported to be composed dominantly of shales approximately 185 metres thick in the south east of Hadeland. However, the Lunner Formation thins and splits into two (divided by the Gagnum Formation) in a North-Westwards direction. It has a nodular base and intermittent siltstone horizons. The Lunner Formation has a low diversity fauna which indicates an age in the north slightly older than that in the south estimated as late Caradoc – Rawtheyan(?) by Owen (1979). The transition from the Nerby Member to the Lunner Formation indicates an increase in water depth.

3.28 Conodonts in Hadeland

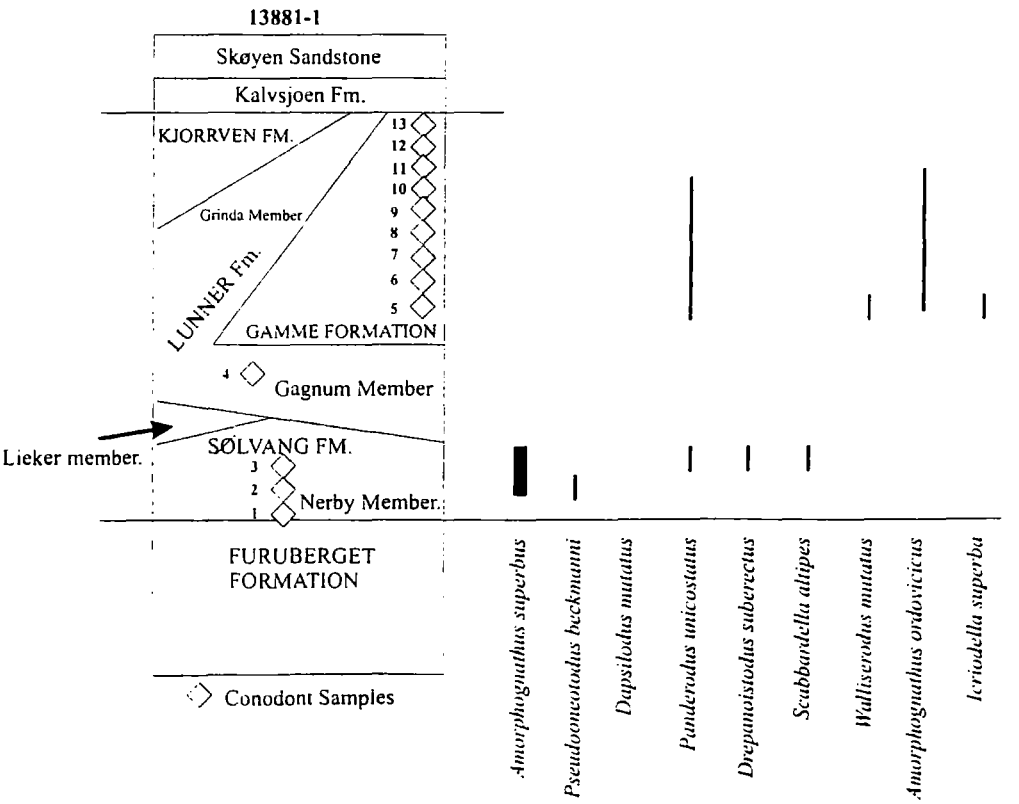

Text-figure 3.28.1. Abundance of conodonts from sample set 1338-1

Samples yield a low diversity, poorly preserved conodont fauna (as illustrated in Text-figure 3.28.1) dominated by members of the *Amorphognathus* biofacies. Conodont faunas from the Nerby Member of the Solvang Formation include *Amorphognathus superbus*, *Pseudooneotodus beckmanni*, *Panderodus unicostatus*, and *Drepanoistodus suberectus* and *Scabbardella altipes*. The fauna is poorly preserved and low in abundance which has resulted in tentative species names. The Gamme Formation yields a similar conodont fauna with the exception of the absence of *Drepanoistodus mutatus* and *Scabbardella altipes* which are both missing from this section.

The transition from the Nerby Member (Solvang Fm.) to the Lunner Formation represents an increase in relative sea-level and coincides with the appearance of *Amorphognathus ordovicicus* in this section.

3.29 Conclusions

The sections of the Oslo Graben were deposited in outer-shelf to upper slope conditions. *Amorphognathus* biofacies taxa are therefore dominant in the sections discussed from the Oslo Graben. However, the data indicates that the relative sea-rises occurring during the upper Ordovician in this Region caused the movement of deeper-water conodont facies into shallower outer-shelf conditions i.e. the emergence of the *Dapsilodus-Periodon* Biofacies. Moreover, the appearance of a new *Amorphognathus* species in the Oslo Graben is also related to transgressive episodes indicating the impingement of cooler water masses onto the shelf at times of transgression. Species of *Panderodus* are common to all the sections discussed and this genus is therefore interpreted as nektonic. The *Walliserodus-Protopanderodus* Biofacies also appears in shelf sediments when sea-level rises and these genera are also interpreted as being nektonic, but occupying an off-shore position. As sea-level increases, this biofacies moves into a near-shore position and its members are therefore deposited in outer-shelf sediments.

Part 1 - Chapter 4

4. Evolution and biostratigraphical utility of *Amorphognathus* along the southern margin of the Iapetus Ocean

4.1 Introduction

The *Amorphognathus* lineage is, in north-west Europe, the basis of the conodont biozonation of the Caradoc - Ashgill. The first appearance of *Amorphognathus tvaerensis* is in the mid-late Aurelucian (Caradoc) whilst *Amorphognathus superbus* first appears in the upper Soudleyan. Recent work of the IGCP to define the base of the Ashgill has favoured that the first appearance of *Amorphognathus ordovicicus* was in the upper Caradoc *linearis* graptolite zone (Fortey *et al.*, 1995).

The present study has indicated, that in Britain and Oslo, *Amorphognathus* is facies controlled, reflecting the occurrence along the southern margin of the Iapetus ocean of a cool (slope) water mass which impinged on the shelf during eustatic transgressive events. The coincidence and cause of the appearance of *Amorphognathus* species on transgression is further investigated here. This has implications for the biostratigraphical utility of members of the *Amorphognathus* lineage.

4.2 Aims

1. To investigate the occurrence and evolution of the *Amorphognathus* lineage during the Ordovician and its role in more accurately placing the *Amorphognathus superbus – Amorphognathus ordovicicus* biozone boundary.

Caradoc and Ashgill conodont faunas in Wales and the Welsh borders were documented by Rhodes (1953) and more recently by Savage & Bassett (1985). Other studies included those of Lindström (1959), Bergström (1964) and Orchard (1980). Although much of the evidence from these studies implies that the *A. superbus – A. ordovicicus* boundary lies in Ashgill strata (e.g. Orchard, 1980, Bergström & Orchard, 1985), Savage & Bassett (1985) reported the early occurrence

of *Amorphognathus ordovicicus* in Onnian Strata from the Welsh Borders (Nod Glas Formation, Welshpool). This was contrary to the report of this boundary in the low Cautleyan (Orchard, 1980)

Because the species diagnostic M elements were poorly preserved in the samples he studied, Orchard (1980) postulated that the lower limit of the *ordovicicus* zone could be inferred from the changing character of faunas at this level. This M element is rarely found, and when present, appears to be of variable morphology within samples (see Text-figure 4.5.1). The M element of *Amorphognathus tvaerensis* has a long anterior process and several apical denticles and an indistinct cusp. *Amorphognathus superbus* has an M element with apical denticles and three distinct, often denticulated processes. The M element of *Amorphognathus ordovicicus* has a single apical denticle, often with a small denticle on its inner lateral edge. The outer lateral process is reduced when compared to those of *Amorphognathus tvaerensis* and *Amorphognathus superbus*.

4.3 The first appearance of *Amorphognathus*

Savage & Bassett (1985) reported *A. ordovicicus* from the Robeston Wathen Limestone (Haverfordwest) but samples from the laterally equivalent Sholeshook Limestone were barren. Barnes *et al.* (1999) in a restudy of the conodonts of the basal part of the Sholeshook Limestone at Whitland, found samples from the base of the section to contain abundant M elements of *Amorphognathus ordovicicus*. In addition to *A. ordovicicus*, they reported *A. superbus*, *A. ventilatus* and *A. lindstroemi* and confirmed a lower Ashgill age for the Sholeshook Limestone. Shelly fauna from the Sholeshook and Robeston Wathen limestones indicate that they range from the Cautleyan Zone 2 to the Rawtheyan Zone 5 (Price, 1973, 1974, 1977, 1980, 1980a). Moreover, the transitional beds at the base of the Sholeshook Limestone at Whitland may be a little older than the base of the formation elsewhere (Zalasiewicz *et al.*, 1995, p. 615). The Cautleyan and Rawtheyan stages in south Wales correlate with at least two major highstands (see sea-level curve, Part I, Chapter 1).

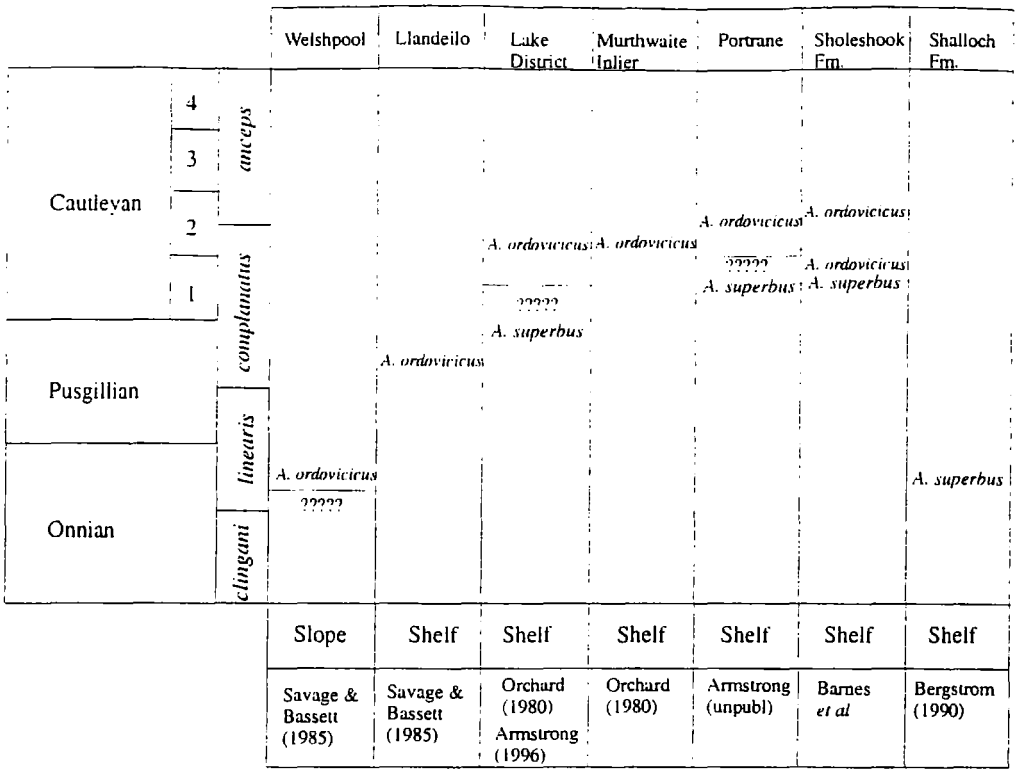

Text-figure 4.2.1 shows the occurrence of *Amorphognathus superbus* and *ordovicicus* in Britain (see text for explanation). Chronostratigraphy and graptolite zones based on Fortey *et al.*, (1995).

Savage & Bassett (1985) reported *A. ordovicicus* (based on Pb element morphology) in the Birdshill Limestone. Price (1973, p224; 1984, p. 103) summarised the shelly faunas and proposed a Pusgillian – early Cautleyan age for the Birdshill and Crûg limestones (see also Owens, 1973, p. 48). Bergström (1971) and Orchard (1980) discussed the correlation of these limestones based on the occurrence of conodonts which they placed within the *superbus* Biozone, although Orchard (1980, p.13) did suggest that the Crûg Limestone may be slightly younger and therefore, close to the *superbus – ordovicicus* boundary. This was on the basis of specimens, which he considered to be transitional to *Amorphognathus ordovicicus*.

Orchard (1980) stated that the conodont faunas from the Rhiwlas Limestone and Abercwmeiddaw Beds sections lay in the *A. ordovicicus* Biozone. Both the Rhiwlas Limestone and the Abercwmeiddaw Formation have been dated on the basis of macrofauna and found to be early Rawtheyan (Williams, *et al.*, 1972)

In Northern England *Amorphognathus ordovicicus* first appears in a fauna from Cautleyan Zone 2 in Sally Beck in the Murthwaite Inlier (Orchard, 1980). Orchard also documented abundant *A. ordovicicus* in the late Rawtheyan Cystoid Limestone in the Cautley area. As summarised in Part I, Chapter 3 (Text-figure 3.3.1) in the north of England *Amorphognathus ordovicicus* first appears in the lower Cautleyan (Armstrong *et al.*, 1996).

Bergström (1990) recorded *A. superbus* in the Cascade Grits in Penwhapple Burn in the Girvan region and tentatively placed the base of the *superbus* zone much lower in the Ardwell Group. Here the species occurs with *D. clingani* Zone graptolites (Bergström, 1990, figure 7). *Amorphognathus ordovicicus* was documented from the upper Shalloch Formation, Girvan (Bergström, 1990, figure 5), (Whitehouse Group). Rare detrital carbonates have yielded a lower Ashgill shelly fauna and graptolites indicate the *D. complanatus* Biozone (Pusgillian – Cautleyan Zone 2). Higher levels of the Shalloch Formation, probably lie within the *D. anceps* graptolite Biozone which ranges from Cautleyan Zone 2 to the end of the Rawtheyan (Ingham, 1992: Fortey *et al.*, 1995). The first appearance of *A. ordovicicus* in Scotland could therefore be as low as the Pusgillian.

4.4 Wales - the Nod Glas Formation

The presence of the conodonts *Plectodina bullhillensis* and *Amorphognathus tvaerensis* within the basal 50cm of the phosphorite led Savage & Bassett (1985) to suggest a Woolstonian age for this part of the Nod Glas Formation. Savage & Bassett (1985) noted the appearance of *A. ordovicicus* towards the top of the phosphorites and documented the occurrence of two distinctive faunas within the Nod Glas Formation. They recorded *Amorphognathus* aff. *A. tvaerensis* at the base of the Nod Glas phosphorites (Sample 77 of Savage & Bassett) whereas the upper 30cm of the phosphorites yielded abundant specimens ascribed to *Amorphognathus ordovicicus*. In addition, they noted the rarity of the M element and preferred to base their concept of *A. ordovicicus* on the character of the Pb element, which they proposed in *A. ordovicicus* was smaller and more robust than the same element in *A. superbus*. This distinction could not be rigorously confirmed in the study of *Amorphognathus* Pb elements obtained from the collections made for this thesis (see

also Bergström & Massa, 1992; Feretti & Barnes, 1997). It should be stressed that no M elements of *A. ordovicicus* from Nod Glas samples were figured in the work of Savage & Bassett (1985) therefore this identification cannot be rigorously confirmed nor has this study been able to duplicate their findings.

Bergström & Orchard (1985) reported the presence of two *Amorphognathus - Rhodesgnathus* bearing faunules from low and high in the Nod Glas Formation. They attributed specimens of *Amorphognathus* in the upper part of the section to *Amorphognathus cf. A. complicatus.*

Re-collection of samples from the lower 5 metres of the Nod Glas Formation in the present study has revealed the presence of two *Amorphognathus* species M elements. The first was from an upper horizon sample (584) and the second from a lower horizon (593). The former is attributed to *Amorphognathus aff. A. ordovicicus* and the latter to *Amorphognathus aff. A. superbus.* The positions of these samples are shown on the range chart in Part 1 Chapter 2 (Text-figure 2.11.1). Scanning electron images of the *Amorphognathus* M elements from the Nod Glas phosphorites are shown below (Text-figures 4.4.1 & 4.4.2). For comparison, an M element of *Amorphognathus ordovicicus* (from Oslo) is also illustrated in Text-figure 4.4.3.

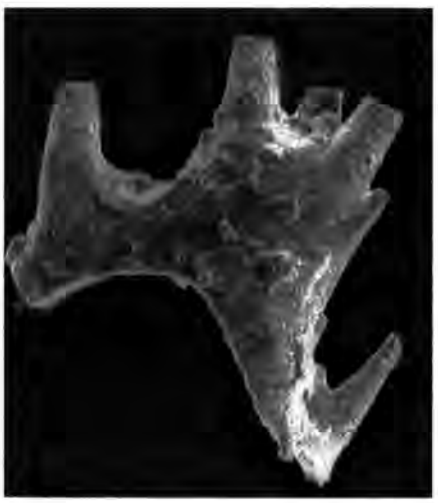

Text-Figure 4.4.1 M element from the Nod Glas Formation sample 593 (*Amorphognathus aff.* A. *superbus*, x200)

Text-Figure 4.4.2 *Amorphognathus* M element from the Nod Gas Formation sample number 584 (*Amorphognathus aff. A. ordovicicus x* 180).

Figure 4.4.3. Example of the *A. ordovicicus* M element from the Oslo Graben (Frøgnoya, lower Sorbakken Formation - Pusgillian x180).

The M element of *Amorphognathus aff. A. superbus* (Text-figure 4.4.1) bears only superficial resemblance to that of *Amorphognathus tvaerensis* in that the denticles adjacent to the cusp are fused to it. The difference between this element and the M elements of both *A. tvaerensis* and *A. superbus* is the presence of well-developed clearly denticulated lateral processes. Savage & Bassett (1985) suggested that this could represent a new species (their *Amorphognathus* aff. *A. tvaerensis*)

Insufficient specimens do not allow final designation and the taxon is retained in open nomenclature and it is named herein as *Amorphognathus aff. A. superbus*.

A single specimen of *Amorphognathus aff. A. ordovicicus* (M element) has been recovered from the top of the phosphorite beds (Sample 584, Text-Figure 4.4.2). This element has a single prominent denticle on the outer lateral process and incipient denticles on the inner edge of the cusp. The M element of *A. ordovicicus sensu stricto* (Text-figure 4.4.3. from Oslo) lacks the incipient denticles. The Nod Glas specimen is compared to *A. ordovicicus* until further specimens can be obtained.

Thus the section at Gwern-y-Brain would appear to contain either new species of *Amorphognathus* or ecophenotypes of the eponymous species bearing in each case an additional lateral process. This study therefore refutes the positioning of the *superbus-ordovicicus* biozone boundary within the Nod Gas Formation. The following section provides a review of the occurrence of *Amorphognathus ordovicicus* in light of the contradictory evidence discussed above.

4.5 Biostratigraphical conclusions

- The base of the *Amorphognathus ordovicicus* biozone cannot be identified in the Nod Glas Formation. Therefore its reported occurrence in the late Caradoc is extremely tentative.
- *Amorphognathus superbus* ranges up into the low Ashgill in the Birdshill Limestone (central Wales) and northern England.
- A form transitional between *A. superbus* and *A. ordovicicus* may occur in the Pusgillian to lower Cautleyan, Birdshill, Crûg and Sholeshook Limestones.
- *Amorphognathus ordovicicus* first appears unequivocally within Cautleyan Zone 2 in the Dent Group of the Murthwaite Inlier and close to the base of the Ashgill in Scotland.
- *Amorphognathus ordovicicus* ranges into the Upper Ashgill (Hirnantian) when conodonts disappear from the British succession.

In the British succession *Amorphognathus ordovicicus* can not be considered indicative of the base of the Ashgill as currently defined.

4.6 Sequence stratigraphy, sea-level changes and the evolution and occurrence of *Amorphognathus*.

Species of *Amorphognathus* are widespread in both the North Atlantic and Midcontinent Realms. The appearance of *Amorphognathus ordovicicus* in the British successions coincides with transgressive episodes (Text-figure 4.6.1).

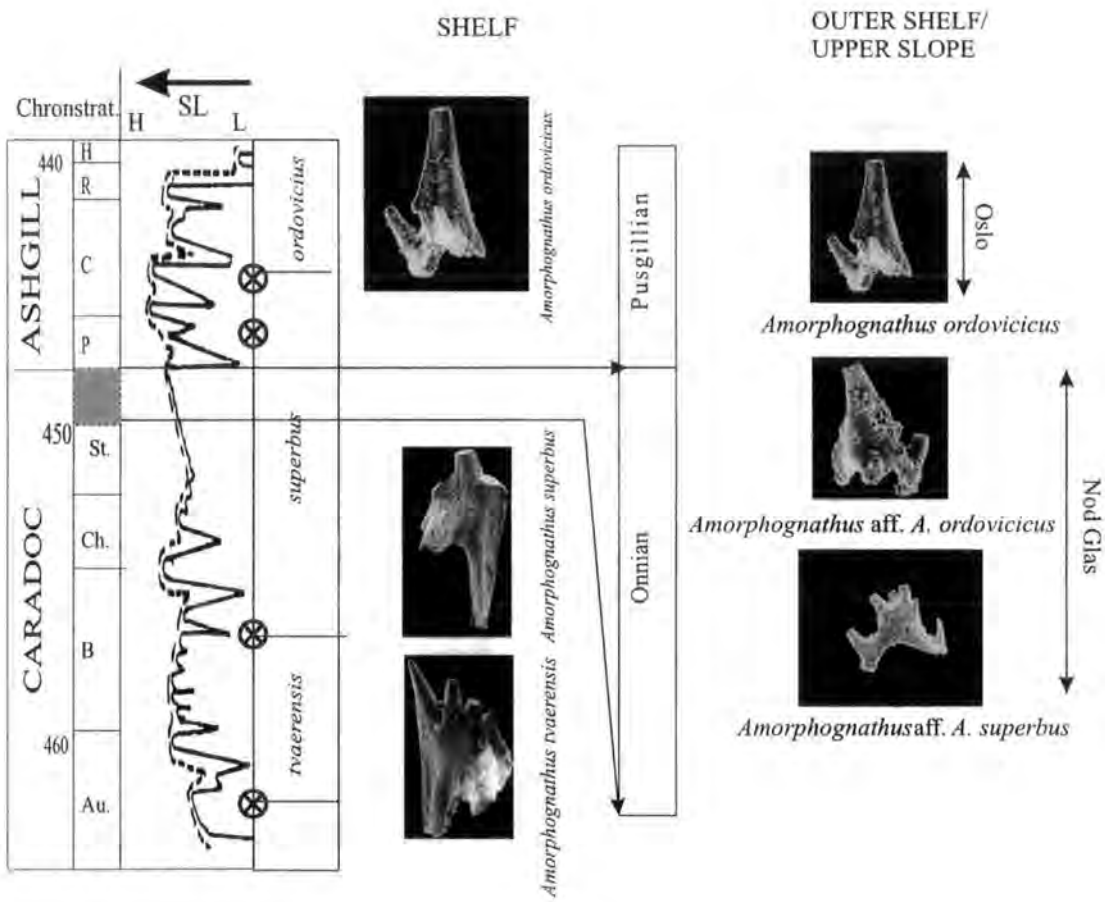

Text-Figure 4.6.1. The occurrence of *Amorphognathus*. Figures of *A. tvaerensis* and *A. superbus* are adapted from Bergström & Orchard (1985). Other element specimens were collected and photographed by the author. Sea-level curve adapted from Ross & Ross (1992) and chronostratigraphy and biozones based on Fortey *et al.*, 1995 and data herein. Transgressions are marked by crosses next to the sea-level curve.

Within the *Amorphognathus* lineage the main evolutionary changes occur in the M element. The M element of *Amorphognathus tvaerensis* has a long anterior process and several apical denticles and an indistinct cusp. *Amorphognathus superbus* has an M element with apical denticles and three distinct, often denticulated processes. *Amorphognathus ordovicicus* differs from these species as it shows a reduction or loss of these denticulated processes.

The M elements recovered from the Nod Glas Formation are distinct and can be compared to *Amorphognathus superbus* and *Amorphognathus ordovicicus*. Text-figure 4.6.1 illustrates each of these specimens and further provides illustrations of the diagnostic M elements of *Amorphognathus tvaerensis*, *Amorphognathus superbus* and *Amorphognathus ordovicicus* and the appearance of each species with respect to the sea-level curve of the upper Caradoc and Ashgill.

4.7 The evolution of *Amorphognathus ordovicicus*

The morphological change between M elements of *A. tvaerensis* and A. *superbus* involves the development of a lateral process and possible increase in size of the three denticles adjacent to the cusp. Both these species dominate shelf environments from the Caradoc to the mid-Ashgill in northern England and Wales (section 4.1). However, at present, the ancestry of *Amorphognathus superbus* remains enigmatic or cryptic.

The sedimentological analysis of the lower Nod Glas Formation showed deposition occurred within the OMZ in a deep outer shelf - upper slope environment (Part I, Chapter 2). *Amorphognathus* aff *A. superbus* occupied the lower, deepest boundary of the OMZ whereas *Amorphognathus aff. A. ordovicicus* occupied the upper boundary. The evolutionary transition from *Amorphognathus superbus sensu stricto* to *Amorphognathus aff. A. superbus* appears to coincide with a faunal shift from the shallow shelf to slope environment. The regressive episode at the beginning of the Cheneyan (Text Figure 4.7.1) may have caused range expansion in the *A. superbus* shelf population into deeper shelf/slope environments.

During range expansion and submergence *A. superbus* acquired an increase in size of the denticles adjacent to the cusp and the development of a lateral process of the M element (Text-figure 4.7.2).

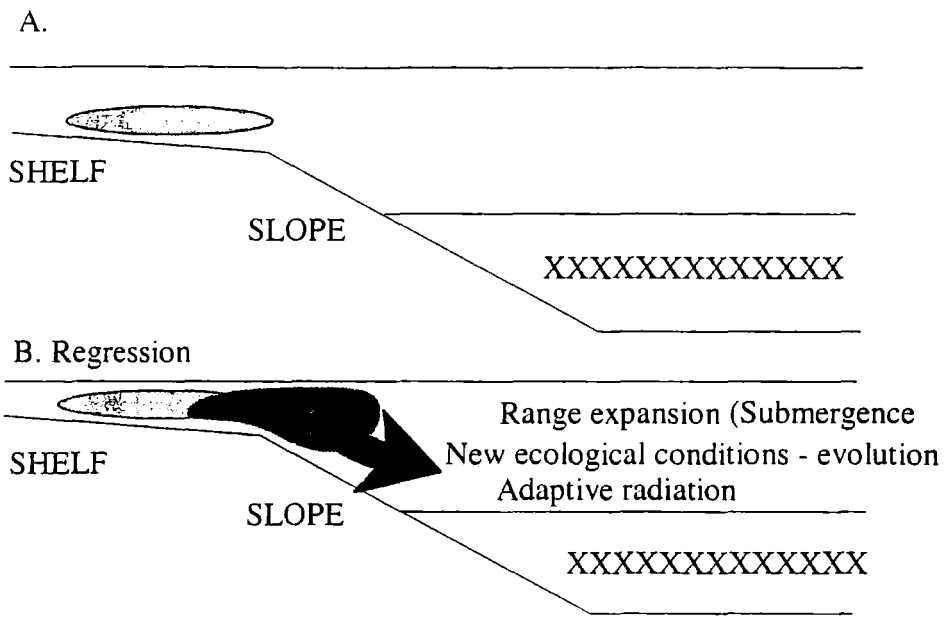

Text-figure 4.7.1. Conceptual model for the range expansion of *A. superbus* during the Cheneyan regressive episode. Note: the area of the slope ecozone is restricted due to greenhouse ocean bottom anoxia.

Once established in a deep-water setting *Amorphognathus aff. A. superbus* became the ancestor to *A. ordovicicus*. Evolution in the deep sea resulted in the loss of the cusp adjacent denticles and newly evolved inner and outer lateral processes.

The full evolutionary sequence is not present in the Nod Glas Formation. It is assumed that this also occurred in deep-water as *A. ordovicicus* occurs in Oslo in the Venstøp Formation, which was deposited in an outer shelf/slope area during the Pusgillian. However, the first appearance *of Amorphognathus ordovicicus* in Northern England and Wales is in younger shelf limestones. Therefore, it is suggested that *Amorphognathus ordovicicus* also evolved in an upper slope environment and appeared for the first time in shelf sediments as a result of phylogenetic emergence during the Pusgillian and lower Cautleyan transgressive

episodes (Text-Figure 4.6.1). It is unlikely that evolutionary processes were acting at the time of emergence as transitional forms of *Amorphognathus* have not been identified. Evolution therefore appears to have ceased prior to the transgressive episode (or as a result of the transgression). This is illustrated in Text-figure 4.7.2.

The observation that both *Amorphognathus superbus* and *Amorphognathus ordovicicus* can occur within the same sample suggests that some *Amorphognathus superbus* forms that stayed on the shelf did not change morphologically and evolve, only becoming extinct after competition from the newly emerged *Amorphognathus ordovicicus* species.

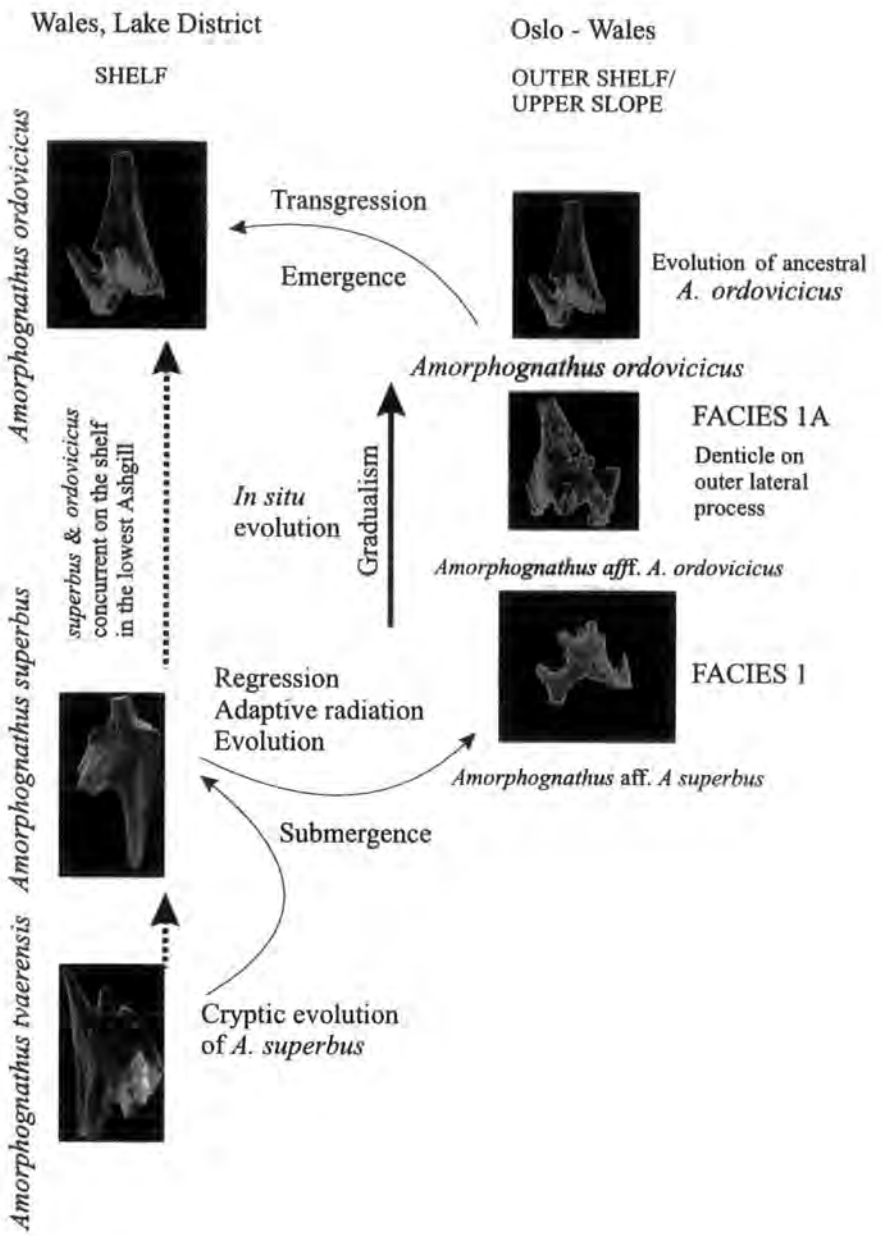

Text-Figure 4.7.2. The gradual evolution of *Amorphognathus*. Figures of *A. tvaerensis* and *A. superbus* are adapted from Bergström & Orchard (1985). Other element specimens were collected and photographed by the author.

4.8 Speciation models

Allopatric speciation occurs when a population becomes geographically isolated (Charlesworth, 1990). Sympatric speciation results from genetic isolation by preferential mating with a spatially heterogeneous population. Parapatric speciation occurs when two populations are only partially isolated (Skelton, 1993). The range expansion and subsequent evolution of *A. superbus* on the slope could be attributed to the latter as a result of the two populations only being partially isolated. The evolution of the *Amorphognathus* lineage may be a result of specific environmental triggers.

Shallow marine sediments provide most of the conodont fossil record because deep-sea sediments are rare in the geological record and conodonts difficult to extract from these lithologies. The Plus ça Change hypothesis predicts a tendency for continuous and gradual evolution in the narrowly fluctuating, relatively stable conditions of the deep-sea environment. In contrast, the model predicts stasis and occasional punctuations in shallow water environments (Sheldon, 1996). This is because in more stable environments organisms can be ecological specialists and suffer fewer time-averaged adaptations.

In specialist lineages, evolutionary change has to occur more continuously to avoid extinction events. As noted by Sheldon (1996), the organisms which are more sensitive to environmental change have a shorter duration than static species in a more widely fluctuating environment such as the shallow shelf. The evolution of *Amorphognathus* occurred in a deeper water slope environment and was gradual, therefore conforming to the predictions of the Plus ça Change hypothesis.

4.9 Conclusions

- The Nod Glas Formation provides a unique opportunity to observe deep-water conodont evolution.
- The evolution of *Amorphognathus* is gradual and therefore conforms to predictions made by the Plus ça change model.
- The evolution of the *Amorphognathus* (*tvaerensis – ordovicicus*) lineage on the southern margins of the Iapetus Ocean occurs as a result of specific environmental triggers.
- Evolution from *superbus* to *ordovicicus* occurs by adaptive radiation as a result of phylogenetic submergence to deeper-water environments, gradual evolution and subsequent phylogenetic emergence (Text-figure 4.9.1). The range expansion to new ecospace and subsequent evolution of *A. superbus* on the slope could be attributed to parapatric speciation as a result of the two populations being only partially isolated.

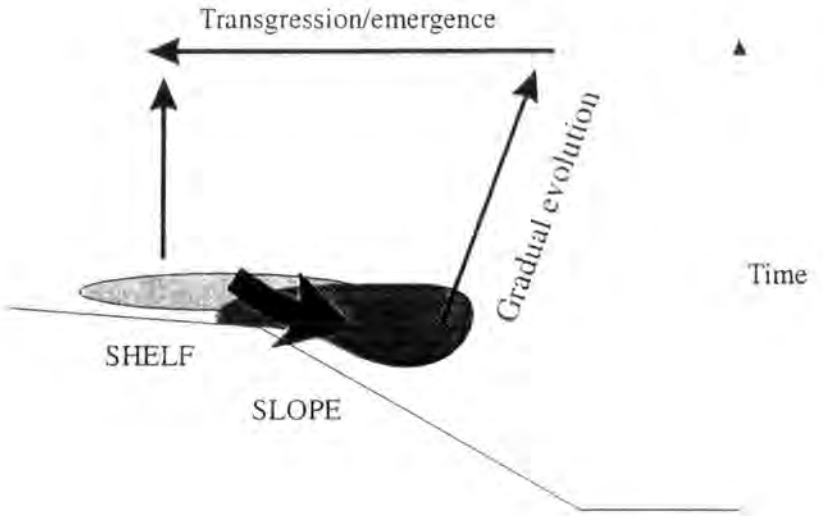

Text-Figure 4.9.1. The conceptual model linking evolution and appearance of faunas due to sea-level fluctuations.

- Phylogenetic emergence (i.e. the shelf-wards movement of the cooler water *Amorphognathus* biofacies during a transgression) results in the appearance of the newly evolved species which often occur alongside older species that were situated on the shelf and did not enter the slope environment (e.g. concurrent *A. superbus* and *A. ordovicicus*, Barnes *et al.*, 1999).
- Modern oceans display high species diversity on the slope (e.g. Wilson & Hessler, 1987) which is in contrast to low conodont species diversity on the slope of the upper Caradoc oceans. This may be due to the restriction of available bathyal ecozone. Restriction of this ecozone may be a result of deep-water anoxia in the greenhouse oceans of the Ordovician. Modern oceans are thermally stratified and therefore the larger bathyal ecozone may permit greater speciation.

Part I - Chapter 5

5. Part I Conclusions

The distinct shelf to deep-water conodont biofacies and generic associations of Sweet & Bergström (1984) can be recognised in sections representing shelf to upper slope deposition in both Avalonia and Baltica.

The phosphate-dominated sedimentology of the lower member of the Nod Gas Formation, Wales represents deposition in the oxygen minimum zone. Within this zone, *Amorphognathus* species dominate the upper and lower boundaries where it is inferred that the water was cooler as a result of marginal upwelling processes.

The *Plectodina* Biofacies is typically found on the shelf in the Upper Ordovician and therefore postulated to be adapted to warmer water conditions. The presence of the *Plectodina* Biofacies in the middle of the oxygen minimum zone, between the *Amorphognathus* Biofacies, indicates the presence of a warmer water layer. The low oxygen levels associated with this zone appear to play little part in the distribution of conodont biofacies but do lead to lower species diversity. Thus the distribution of conodont biofacies present in the OMZ more likely reflect the subtle variations in temperature within the water column.

The Nod Glas Formation has also provided a unique insight into the evolution of *Amorphognathus* in the deep-water environment. The appearance of new species of *Amorphognathus* on the shelf during the Caradoc and Ashgill coincides with eustatic marine transgressions thus implying cladogenesis in deep-water settings. The morphological change from *Amorphognathus superbus* to *Amorphognathus* cf. *A. superbus* can be correlated with range expansion and the change from salinity to thermally stratified oceanic conditions. The range expansion of *Amorphognathus superbus* resulted in the acquisition of lateral processes on the M element producing an ecophenotype or new species through parapatric speciation. From this ancestor, the gradual evolution of *Amorphognathus ordovicicus* progressed by the loss of the lateral process and cusp adjacent denticles. The initial transgression of the Ashgill brought this new taxon into the shelf setting alongside ancestral *Amorphognathus superbus* stock. This pattern of gradual evolution in deep-water is that predicted by the Plus ça Change model.

It is therefore postulated that the taxa of the *Amorphognathus* Biofacies are adapted to cooler water. The presence of this biofacies in the upper Ordovician of the Welsh Basin was predominantly temperature controlled. Although occupying the oxygen minimum zone during the end Caradoc, the taxa of the *Amorphognathus* Biofacies were present in open marine environments during the Ashgill in northern England.

Phylogenetic emergence is proposed as the mechanism by which the *Amorphognathus* and deeper-water *Dapsilodus-Periodon* Biofacies can appear on the shelf and slope sediments of Avalonia and Baltica. This 'faunal shift' occurs as a result of eustatic marine transgression. As sea-level rises, deeper cooler water masses impinge upon shallower shelf areas and the stenothermal occupants track this movement. The processes of phylogenetic emergence and submergence therefore have fundamental implications for the evolution of *Amorphognathus* and other deeper water conodont lineages and further explain the paradox of the appearance of deeper-water conodonts in shallow water limestones.

The fundamental controls on Upper Ordovician conodont biofacies along the southern margins of Iapetus were predicted to be oceanographic changes related to the northwards drift of both microcontinents and/or the widespread global cooling leading up to the end Ordovician glaciation. The former resulted in warm (equatorial) waters by the end Ashgill and the latter in cold (glacial) ocean conditions during the Ashgill.

The *Amorphognathus* and deeper-water conodont biofacies dominated the clastic Ashgill successions in Avalonia and Baltica and remained stable at generic level throughout the upper Ordovician. This indicates that the global cooling related to the onset of glaciation was the dominant control on biofacies distribution. Climatic factors were therefore dominant over the northwards drift of the microcontinents.

This has implications for the interpretation of Upper Ordovician North Atlantic Realm nektobenthic conodonts. Conodont biofacies distribution in the upper Ordovician was temperature controlled and nektobenthic genera were able to inhabit a range of oxygen conditions.

The patterns shown indicate that biofacies tracked temperature defined water masses during sea-level change. As shelf conditions cooled, these taxa were able to occupy the shallow shelf niches vacated by extinction/ecological displacement of the *Aphelognathus-Plectodina* Biofacies taxa.

Appendix 1A – Systematic palaeontology

Appendix 1A - Systematic Palaeontology

Introduction

Upper Ordovician conodont species are well documented by authors such as Orchard (1980), Savage & Bassettt (1985) and Armstrong *et al.* (1996). The conodonts from samples collected and analysed as part of this study were generally poorly preserved (CAI 5), and very low in abundance. For these reasons the systematic descriptions provided herein are largely abbreviated. The most complete apparatuses have only been recovered for species of *Amorphognathus*. Therefore, detailed systematic descriptions and synonymy lists are provided for this genus alone.

The conodont generic suprageneric classification used within the abbreviated systematic description below is that of Aldridge & Smith (1993). The terminology of Sweet (1988) is used to describe element morphology. Apparatus structure notation is that of Sweet & Schönlaub (1975) (as modified by Armstrong (1990) & extended by Aldridge *et al.* (1995).

Synonymy lists

Synonymy lists are abbreviated and annotated as advised by Matthews (1973). They include the first documentation of the species, major species concept revisions, first multielement descriptions and the most recent documentation.

Phylum CHORDATA Bateson, 1886

Class Conodonta Eichenberg, 1930 *sensu* Clark, 1981

Order PRIONIODONTIDA Dzik, 1976

Remarks

The apparatus of prioniodontid conodonts was regarded by Sweet (1988) as containing six or seven morphotypes. Aldridge *et al.* (1995) reconstructed the prioniodontid conodont apparatus after discovery of the prioniodontid animal (*Promissum pulchrum* Kovács-Endrödy) in the Soom Shale of South Africa. This reconstruction showed paired Pa, Pb, Pc, Pd, M, Sb_1, Sb_2, Sc and Sd elements with a single Sa element (see reconstruction, Part II, Chapter 1).

Family BALOGNATHIDAE Hass, 1959

Genus *Amorphognathus* Branson and Mehl, 1933c

Type Species

Amorphognathus ordovicica, Branson & Mehl, 1933c

Diagnosis

Refer to Bergström (1971 p. 131-134)

Remarks

Amorphognathus has an apparatus comprising Pa, Pb, Pc, M, Sa, Sb_1, Sb_2 (= Sd of previous reconstructions) and Sc elements and was considered by Armstrong *et al.* (1996) to have a prioniodontid apparatus plan similar to that of *Promissum pulchrum* (as documented by Aldridge *at al.*, 1995). Armstrong *et al.* (1996) included the platform elements Pa - Pc, a single M element plus Sa – Sd in the apparatus. Armstrong *et al.* (1996) also tentatively proposed the possible occurrence of a Pd element in the *A. ordovicicus* apparatus. Currently there is little evidence to support this view.

Methods of determining between species of *Amorphognathus* have proved problematical. Therefore, during the present study analysis has concentrated fundamentally on variations within the M element. The M element of *Amorphognathus* shows considerable morphological variation (Nowlan & Barnes,

1981). Other morphological variations previously considered for diagnosis have included the relative arching and the angle between processes of the Pb element. In addition, the sinuosity of the lower inner basal margin of the dextral Pb element was considered by Savage & Bassett (1985) to be indicative of the species *A. superbus.*

Amorphognathus superbus Rhodes, 1953
Plate 1, figs 1-9

**1953 Holodontus superbus* n.sp. Rhodes, p. 304, pl. 21 figs 125-127

1953 *Amorphognathus ordovicicus* Branson & Mehl; Rhodes, p. 283, pl. 20 figs 35-37

1953 *Ambolodus triangularis* Rhodes, p. 280, pl. 20 figs 35-37

1953 *Ligonodina elongata* n. sp. Rhodes, p. 305, pl. 21 figs 130&131

1953 *Trichonodella gracilis* n.sp. Rhodes, p. 314, pl. 21 figs 144, 147-150

1985 *Amorphognathus superbus* Rhodes; Savage & Bassettt, p.692, pl. 83 figs 1- 19

1985 *Amorphognathus superbus* Rhodes; Bergström & Orchard, p. 61 pl. 2.4 figs 1-4 & 8

1994 *Amorphognathus superbus* Rhodes, Dzik p. 93, pl. 23 figs 3-5

Holotype

Holodontus superbus Rhodes, 1953, p. 304, pl. 21 figs 125-127

Type locality

Gelli - grin Limestone (late Caradoc) Wales.

Diagnosis

Refer to Dzik (1994, p. 94)

Description

The Pa element of *A. superbus* is pastiniscaphate with a robust posterior process from which two pairs of lateral processes project from the antero-posterior midline. The two lateral processes vary in size between inner and outer sets, the latter being less prominent. Fused denticles present on processes though they are more pronounced on the anterior and posterior processes. Denticles are node-like and decrease in size away from the cusp. The basal cavity in Pa elements is pronounced and extends as a deep groove into all processes.

The Pb element is pyramidal and strongly arched with an anterior, posterior and outer lateral process. The anterior and posterior processes vary in length with the anterior process commonly longer than the posterior process. Six fused denticles are apparent on the anterior process and denticles are not easily seen on the posterior process. The cusp is slender, prominent but only slightly curved. Pb elements have a deep, wide basal cavity and the arching of the element varies within samples and is therefore not regarded as a useful diagnostic feature.

Amorphognathus superbus has a tertiopedate M element with apical denticles and three distinct, often denticulated processes.

The alate Sa element of *A. superbus* is slender with a prominent cusp. The Sb element also has a prominent cusp, two processes with one denticle mid-way on each. Lateral process shorter than posterior process and the latter is denticulate. Denticles vary in size along the posterior process.

The Sb element has a prominent outer lateral process bearing one large denticle. The outer lateral and inner lateral processes bear triangular denticles, which vary in size particularly along the posterior process.

The Sd (Sb_2) element of *A. superbus* is quadriramate. The posterior process is prominent and bears denticles which are not fused at the base. The denticles on the posterior process vary in size and become larger towards the tip. The outer lateral process is also denticulated. The inner lateral processes are long and slender and point downwards from the cusp. The cusp is highly curved and often broken at the tip.

Remarks

In examples from this study *Amorphognathus superbus* elements are rare, often fragmented.

Occurrence

Because M elements of *A. superbus* are extremely rare, only one definite identification has been made in the Dent Group, Greenscoe. Other elements are assigned to this species on the basis of their stratigraphical position and species association. *Amorphognathus superbus* is widely known from upper Ordovician sections in both Europe and North America.

Amorphognathus aff. A. superbus Rhodes, 1953

Plate 2, figs 9-11

Description

Pa element is pastinischaphate with a prominent anterior process and two bifid lobes. All processes bear node-like denticles. The cusp is not conspicuous and the basal cavity extends the length of all processes although it is deeper under the cusp region. Towards the ends of processes the basal cavity becomes a narrow groove.

Pb elements are triangulate, strongly arched and robust. Elements have a tapered anterior processes and a posterior process that is rounded at the tip. The anterior process is denticulate and has at least five discrete triangular denticles. There is often a break in denticles towards the end of the anterior process. Although the outer lateral process is often not denticulated, in some cases it bears a small number (between 2 and 4) discrete small triangular denticles. The outer lateral process is often broken particularly at the junction where the processes meet below the cusp. The basal cavity is deeply excavated and extends into both the anterior and posterior processes. The basal margin of the Pb element of *Amorphognathus aff. A. superbus* is folded inwards making it slightly sinuous in appearance.

The M element of *Amorphognathus aff. A. superbus* is tertiopedate with well developed processes. The M element has three (possibly 4) apical denticles. The outer and inner lateral processes both bear one large denticle.

Sa elements are alate with a denticulated posterior process. Denticles vary in size along the process with the largest, single denticle approximately halfway along the length.

Remarks

Description of the S elements of *Amorphognathus aff. A. superbus* is hindered by the poor reservation of the material. S elements are the most delicate in the *Amorphognathus* apparatus and processes are often broken.

Occurrence

Amorphognathus aff. A. superbus was only recovered from the Nod Gas Formation (Onnian) in Facies 1.

Amorphognathus ordovicicus Branson & Mehl, 1933c

Plate 1, figs 10 & 11

*1933c *Amorphognathus orovicica* Branson & Mehl p. 127, pl. 10 fig. 38

1933c *Ambalodus triangularis* n.sp. Branson & Mehl, p. 128, pl. 10 figs 35-37

1953 *Roundya diminuta* Rhodes, p. 137, pl. 8, 9, 12 ; pl. 9 fig. 6

*1959 *Goniodontus superbus* Ethington, p. 278, pl. 7 figs 1-14

1959 *Trichonodella inclinata* Rhodes, Ethington, p.290, pl. 41 fig. 6

1959 *Tetraprioniodus parvus* n. sp. Ethington, p. 288, pl. 40 fig. 8

1959 *Eoligonodina elongata* Rhodes, p. 277, pl. 40 fig.5

1959 *Keisliognathus simplex* n. sp. Ethington, p. 280, pl. 40 figs 9&10

1978 *Amorphognathus ordovicicus* Branson & Mehl; Bergström, pl. 80 figs. 1-11

1980 *Amorphognathus ordovicicus* Branson & Mehl; Orchard, p. 16, pl. 1-13, 17&18

1985 *Amorphognathus ordovicicus* Branson & Mehl; Savage & Bassettt, p.691, pl. 84 figs 1-21 pl. 85 figs 1-26, pl. 86 figs 1-13

1996 *Amorphognathus ordovicicus* Branson & Mehl; Armstrong *et al.*, p. 14, pl. 8, figs 6, 1-12 and Figure 7).

1997 *Amorphognathus ordovicicus* Branson & Mehl; Ferretti & Barnes, p. 24, pl. 1 figs 1-15

Holotype

Amorphognathus ordovicica Branson & Mehl, 1933c p.127, pl. 10 fig. 38.

Type horizon and locality

Thebes Sandstone, Ozora, Missouri

Diagnosis

Refer to Dzik (1994, p. 94)

Description

The pastinischaphate Pa element has a robust posterior process. The posterior process gives rise to two pairs of lateral processes. The outer lateral process is shorter than the inner. Fused denticles are present on all processes but are more pronounced on the anterior and posterior processes where they are node-like and decrease in size away from the cusp. The basal cavity is pronounced and extends as a deep groove into all processes.

The Pb element is triangulate and strongly arched. The lateral processes vary in length. Six fused denticles apparent on the anterior process which is longer than the posterior process. Denticles are not easily seen on the latter.

The Pc element is bipennate and robust with a denticulated posterior process. The denticles are triangular but fused at the base. The denticles decrease in size away from the cusp which is not inclined. The posterior and anterior processes are not arched in respect to the cusp and the aboral margin is straight. The basal cavity is not deeply excavated and cannot be clearly seen along the processes. The anterior process is commonly broken at its junction with the cusp.

The M element of *A. ordovicicus* has a single cusp like denticle and two processes. The single apical denticle, often has a small triangular-shaped denticle on its inner lateral edge. These elements are rare within all samples containing *Amorphognathus*.

The Sa element is an alate element with a straight cusp. The posterior process is denticulated. Denticles are unfused at the base and triangular in form.

The Sb element is tertiopedate with a prominent cusp, an outer and inner lateral and posterior process. The outer lateral process and posterior process have one denticle mid-way on each. The lateral process is shorter than the posterior process.

Occurrence

Only conclusively identified from the Venstøp Formation, Oslo Graben (Section 7881-1 06). Other samples did not yield diagnostic M elements that could be conclusively assigned to this species.

Amorphognathus aff. A. ordovicicus Branson & Mehl, 1933c

Plate 2, figs 1-8

Description

The Pa element of *Amorphognathus aff. A. ordovicicus* is pastiniscaphate with a posterior, anterior, two outer and inner lateral processes. The element is robust and bears node shaped denticles on all processes.

The Pb element of *Amorphognathus aff. A. ordovicicus* is triangulate but not strongly arched. The anterior process is more tapered towards the tip than the posterior process. Both the anterior and posterior processes are denticulated. The anterior process has between 5 and 6 triangular denticles. These are not evenly spaced but converge nearest the cusp and are fused at the base. The outer lateral process is also denticulated. It bears between 3 and 4 triangular denticles although is often broken at the tip. The basal margin is slightly indented on its inner side and the basal cavity is deeply excavated and extends to the ends of both the anterior and posterior processes.

A single M element of *Amorphognathus aff. A. ordovicicus* has been recovered from this study. This element has a single prominent denticle on the outer lateral process and incipient denticles on the inner edge of the cusp.

Occurrence

This species occurs in the lower Nod Gas Formation (Facies 1A), Gwern-y-Brain, Welshpool.

Genus *Birskfeldia* Orchard, 1980

Birksfeldia circumplicata Orchard, 1980

Plate 3, fig 15

*1980 *Birksfeldia circumplicata*, Orchard, p. 18, pl. 6, figs 1,2,4,7, 13-25

? 1990 *Birksfeldia circumplicata* Orchard, Bergström, p. 26, pl. 4, figs 17-21

1996 *Birksfelda circumplicata* Orchard, Armstrong *et al.*, p. 16, fig 6, fig. 8

Holotype

Birksfeldia circumplicata sp. nov, Orchard (1980), p. 18, pl. 6

Diagnosis

Refer to Orchard (1980, p. 18)

Occurrence

A few elements have been recovered from the Oslo Graben (Section 7881-1) and the Dent group, Greenscoe. Descriptions are hampered by the lack of material and its poor preservation

Genus *Rhodesognathus* Bergström & Sweet, 1966

Type specimen

Ambolodus elegans Rhodes 1953, p.278

Rhodesognathus elegans (Rhodes, 1953)

Plate 3, figs 2&3

*1953 *Ambolodus elegans* Rhodes p. 278, pl. 6, figs 22, 24,21, 23, 25

1977 *Rhodesognathus elegans* (Rhodes) Lindström, p. 535

1985 *Rhodesognathus elegans* (Rhodes) Savage & Bassettt, p. 697, pl. 82, figs 34-37, pl. 83, figs 26 & 27, pl. 84, figs 28 & 29, pl. 85, figs 36-39, pl. 86, figs 23 & 24

Holotype

Ambolodus elegans Rhodes, p. 278, pl. 20, fig. 24

Diagnosis

Refer to Savage & Bassettt (1985, p. 696) and the emended diagnosis of Dzik (1994).

Description

Refer to Savage & Bassettt (1985, p. 696).

Occurrence

Rhodesognathus elegans is abundant in the Nod Glas Formation (Facies 1), Gwern-y-Brain, Welshpool.

Family PTEROSPATHODONTIDAE Cooper, 1977

Genus *Complexodus* Dzik, 1976

Type species

Balognathus pugionifer (Drygant, 1974)

Diagnosis

Refer to Dzik (1994, p.106-107)

Remarks

Complexodus can be distinguished from *Amorphognathus* by its undivided anterior process which branches directly from the cusp.

Complexodus pugionifer (Drygant, 1976)

Plate 3, figs 13&14

*1974 *Balognathus pugionifer* sp. n. Drygant, p.56, pl. 1, figs 4-8

1976 *Complexodus pugionifer* Drygant; Dzik, p. 423, pl. 44, fig. 2

1985 *Complexodus pugionifer* Drygant; Bergström & Orchard, p. 59, pl. 2.3, fig. 6

1994 *Complexodus pugionifer* Drygant; Dzik, p. 123, figs 20-26

Holotype

Balognathus pugionifer sp. n. Drygant, p.56, pl. 1, fig. 4. Lower Tatianba Formation, Tangshan Hillls, China.

Diagnosis

Refer to Dzik (1994, p. 106)

Description

The Pa element is pastinischaphate and less robust than those in the *Amorphognathus* apparatus. Denticles are present on all processes and increase in size on the anterior process towards the prominent cusp. The anterior process branches directly from the upright cusp. The posterior process is also denticulate and has a bifurcating accessory lobe. Both processes are usually broken a short distance from the cusp. The basal cavity extends along all processes although is not deeply excavated.

The Pb element is similar in morphology to that of *Amorphognathus*. However, in the *Complexodus* apparatus, these elements are less robust, and have fewer, more slender denticles on both the anterior and posterior processes.

Occurrence

Representative elements of *Complexodus* are extremely rare within samples from this study. Only Pa and Pb elements are identified and the former are commonly fragmented. *Complexodus pugionifer* occurs low in the Nod Glas Formation (Facies 1), Gwern-y-Brain, Welshpool. This is the first reported occurrence of this species within this formation. Rare *Complexodus pugionifer* elements have also been found in the lower Dent Group, Greenscoe (Broughton in Furness).

Family ICRIODELLIDAE Sweet , 1988

Genus *Icriodella* Rhodes, 1953

Icriodella superba Rhodes, 1953

Plate 3, figs 9&10

*1953 *Icriodella superba* n. sp. Rhodes, p. 288, pl. 20, figs 62, 63, 78, 54, 58

1953 *Trichonodella divaricata* n. sp. Rhodes, p. 313, pl. 21, figs 140, 145,& 146

1953 *Icriodella plana* n. sp. Rhodes, p. 287, pl. 20, figs 67, 74 & 76

1980 *Icriodella superba* Rhodes; Orchard pl. 1, figs, 14, 17, 18, 23, 24 & 26

1985 *Icriodella superba* Rhodes, Savage & Bassettt, p. 698, pl. 83, figs 20-25

Holotype

Icriodella superba n. sp. Rhodes, p. 288, pl. 20, fig. 78

Diagnosis

Pa elements have sub-equal processes and the double row of node-like denticles are fused by transform ridges (refer to Orchard, 1980, p. 21)

Description

Refer to Savage & Bassettt (1980, p. 706)

Occurrence

Rare elements (Pa & Pb) of *Icriodella superba* have been recovered from the Nod Glas Formation and the Oslo Graben. Complete apparatuses have not been recovered and Pa elements are incomplete and are commonly broken behind the cusp.

Remarks

It should be noted that Savage & Bassettt (1985, pl. 81-83) have figured representatives of *Icriodella superba* Pa, Pb and M elements. However, the M and Pb elements are incorrectly identified. The M elements figured by Savage & Bassettt (1985) are Pb elements and the Pb elements are more likely Sc elements.

Family PRIONIODONTIDAE Bassler, 1925

Genus *Prioniodus* Pander, 1856?

Prioniodus ? sp. Orchard

? 1964 *Prioniodus* ? *variabilis* Bergström, p. 63, table V.

1980 *Prioniodus* sp. A, Orchard, pg. 24, pl. 6, figs 5, 9, 11, 12

Occurrence

Rare *Prioniodus* elements have been recovered from the Nod Gas Formation.

Order OZARKODINIDA Dzik, 1976

Remarks

The three dimensional apparatus plan for ozarkodinids has been documented by Rhodes (1953), Nicoll (1985, 1987), Aldridge *et al.* (1987) and most recently by Purnell & Donoghue (1998). This has resulted in the view that the ozarkodinid apparatus consists of 15 elements, including paired Pa, Pb and M elements, with a single Sa element and four other pairs of S elements (Sb_1, Sb_2, Sc_1 and Sc_2).

Family SPATHOGNATHODONTIDAE Hass, 1959

Genus *Plectodina* Stauffer, 1935

Type species

Plectodina dilata Stauffer, 1935, p. 152

Diagnosis

Refer to Ziegler (1981)

Plectodina bullhillensis Savage & Bassettt, 1985

Plate 3, figs 7&8

*1985 *Plectodina bullhillensis*, Savage & Bassettt, p. 702, pl. 80, figs 15-22, pl. 81, 17-27, pl. 83, figs 28-35

Holotype

Pa element NMW 81.6G.22, sample 72 (Hoar Edge Grit, Bullhill Gutter, Shropshire) Savage & Bassettt (1985, p. 695, pl. 81, figs 1-3)

Diagnosis

Refer to Savage & Bassettt (1985, p. 702)

Description

Refer to Savage & Bassettt (1985, p. 702)

Occurrence / Remarks

Pa and Pb *Plectodina bullhillensis* elements have been recovered from the Nod Gas Formation (Facies 2, see Part I, Chapter 2). However, only one M element was found. Elements are often broken and fragmented probably due to their delicate nature.

Plectodina bullhillensis was documented by Savage & Bassettt (1985) from the upper Nod Glas Phosphorites. However, the occurrence of *P. bullhillensis* at this stratigraphic level is unusual as in parts of Shropshire it is found in much younger strata.

Plectodina tenuis (Branson & Mehl, 1933)

* 1933 *Ozarkodina tenuis* n. sp. Branson & Mehl, p. 128, fig. 10, figs 19, 20, 21, 23

966 *Plectodina furcata* (Hinde); Bergström & Sweet, p. 377, pl. 32, figs 17-19; pl. 33, figs 1-4, pl. 34, figs 9-12

1985 *Plectodina tenuis* (Branson & Mehl); Savage & Bassettt, p. 693, pl. 80/81 figs 1-5, 19-35

Description

Refer to Savage & Bassettt (1985, p. 704)

Occurrence

Rare *Plectodina tenuis* Pa elements have been recovered from the Dent Group, Greenscoe, Broughton on Furness. These were poorly preserved.

Genus *Aphelognathus* Branson, Mehl & Branson, 1951

Aphelognathus rhodesi (Lindström, 1959)

Plate 3, fig. 4

*1959 *Ozarkodina rhodesi* n. sp. Lindström, p. 441, pl. 1, figs 1&2

1959 *Prioniodus pulcherrima* n. sp. Lindström, p. 442, pl. 3, figs 19 & 20

1959 *Cordylodus* cf. *C. spurius* Branson & Mehl, Lindström, p. 451, pl. 4, figs 19, 20,21

1959 *Trichonodella parabolica* n. sp. Lindström, p. 450, figs 18-22

1980 *Aphelognathus nudus* sp. nov. Orchard, p. 18, pl. 2, figs 1, 2 & 3

1980 Aphelognathus rhodesi (Lindström) Sweet, p. 49, figs 1-6, p. 51, figs 51-52

1985 Aphelognathus rhodesi (Lindström) Savage & Bassettt, p. 701, pl. 34-46

Holotype

Ozarkodina rhodesi. n sp. Lindström, p. 441, pl. 1, figs 1& 2

Diagnosis

Refer to Savage & Bassettt (1985, p. 698)

Description

Refer to Savage & Bassettt (1985, p. 698)

Occurrence

Lower Dent Group at Greenscoe, Broughton in Furness, the Lake District. Pa elements form the majority of the elements of this species with the Dent Group at this locality.

Family Cyrtoniodontidae Hass, (1959)

Genus *Phragmodus* Branson & Mehl, 1933b

Type species *Phragmodus primus*, Branson & Mehl, 1933b

Diagnosis Refer to Sweet (1981a, p. 245-246)

Phragmodus undatus Branson & Mehl, 1933b

Plate 3, figs 5&6

*1933b *Phragmodus undatus* Branson & Mehl, p.115, pl.8, figs 22-26

1966 *Phragmodus undatus* Branson and Mehl; Bergström & Sweet, p.369

1985 *Phragmodus* cf. *P. undatus* Branson & Mehl, Savage & Bassettt, pg. 707, pl. 86

1995 *Phragmodus undatus* Branson & Mehl, Leslie & Bergström p. 970, fig 4, 1-6

Syntypes

Phragmodus undatus Branson & Mehl, 1933, pl. 8, figs. 22-26

Diagnosis

Refer to Sweet (1981a, p.267)

Description

Refer to Leslie & Bergström (1995)

Occurrence

Only a few *Phragmodus undatus* elements have been recovered from the Nod Glas Formation. Nevertheless, these were sufficient to assign this name.

Order PRIONIODINIDA

Family PERIODONTIDAE

Genus *Periodon* Hadding, 1913

Type species *Periodon aculeatus* Hadding, 1913

Periodon grandis (Ethington, 1959)

Plate 3, fig. 1

*1959 *Loxognathus grandis* n. sp. Ethington, p. 281, pl. 40 fig. 6

1966 *Periodon grandis* (Ethington) Bergström & Sweet p. 363-365, pl. 30, figs 1-8.

1979 *Periodon* cf. *aculeatus* Hadding; Kennedy, Barnes & Uyeno, pp. 544-546, pl. 1, fig. 8

1989 *Periodon grandis* (Ethington) McCracken & Nowlan, p. 1889, pl. 3, figs 7-9

1995 *Periodon grandis* (Ethington); Rasmussen, p.61, pl. 1, fig. 19

Holotype

1959 *Loxognathus grandis* n. sp. Ethington, p. 281, pl. 40 fig. 6

Occurrence

A few elements (M and Pa only) have been recovered from samples in the Oslo Graben. No other sections during this study have yielded *Periodon grandis* elements.

Genus *Hamarodus* Viira, 1974

Hamarodus europaeus (Serpagli, 1967)

Plate 3, fig. 12

*1967 *Distomodus europaeus* Serpagli, p. 64, pl. 4, figs 1-6

1976 *Hamarodus europaeus* (Serpagli), Dzik, p. 435, fig. 36

1980 *Hamarodus europaeus* (Serpagli) Orchard, p. 21, pl. 4, figs 22,25,29-31

1996 *Hamarodus europaeus* (Serpagli) Armstrong *et al.*, p. 19, pl. 9, figs 5 & 6

Holotype

Distomodus europaeus Serpagli (1967, p. 64)

Description

Refer to Orchard (1980, p. 21)

Occurrence

Rare *Hamarodus europaeus* elements were recovered from the lower Dent Group at Greenscoe during this study.

Order PROTOPANDERODONTIDA Sweet, 1988

Family DAPSILODONTIDAE Sweet 1988

Genus *Dapsilodus* Cooper, 1976

Type species

Distacodus obliquicostatus Branson & Mehl, 1933

Diagnosis

Refer to Armstrong (1990, p.70)

Dapsilodus mutatus (Branson & Mehl, 1933)?

Plate 4, fig. 1

? 1933c * *Belodus* (?) *mutatus* n. sp. Branson & Mehl, 1933c p. 126, pl. 10, fig 17

1980 *Dapsilodus mutatus* Orchard, pl. 5, figs. 6, 15, 16, 21

Holotype

Belodus (?) *mutatus* n. sp. Branson & Mehl, p. 126, pl. 10, fig 17

Description

Refer to Orchard (1980, p. 20)

Occurrence

Dapsilodus mutatus ? elements are present in low numbers in the Nod Gas Formation, Gwern-y-Brain, Welshpool, the Dent Group at Greenscoe and the Oslo Graben. Full descriptions are hindered by the lack of elements and poor preservation.

Order BELODELLIDA Sweet, 1988

Family BELODELLIDAE Khodalevich & Tschernich, 1973

Genus *Walliserodus* Serpagli, 1967

Type Species *Acodus curvatus* Branson & Branson, 1947 designated by Cooper (1975, p. 995).

Walliserodus curvatus (Branson & Branson, 1947)

Plate 5, figs 6,7, 8, 9, 10

*1947 *Acodus curvatus* Branson & Branson p. 554, pl. 81, fig. 20

1975 *Walliserodus curvatus* Branson & Branson, Cooper, p. 995, pl. 1, figs 10, 11, 16-21

1990 *Walliserodus curvatus* (Branson & Branson) Armstrong, p.124-126, pl. 21, figs 6-15

Holotype

Acodus curvatus Branson & Branson, 1947, p. 554, pl. 81, fig. 20. Specimen C672-4 from the Brassfield Formation, Kentucky, USA

Diagnosis

Refer to Armstrong (1990, p. 121)

Description

Refer to Armstrong (1990, p.125-126)

Occurrence

Walliserodus curvatus has been identified in the Oslo Graben, Dent Group and the Nod Gas Formation where only a few isolated but commonly fragmented elements have been recovered.

Order PANDERODONTIDA Sweet, 1988

Family PANDERODINTIDAE Lindström, 1970

Genus *Panderodus* Ethington, 1959

Type species

Paltodus unicostatus Branson & Mehl, 1933

Diagnosis

Refer to Sweet (1979, p. 62)

Panderodus panderi (Stauffer, 1940)

Plate 5, fig. 12

*1940 *Paltodus panderi* Stauffer p.427, pl. 23, figs 219-220

1959 *Panderodus panderi* (Stauffer); Stone & Furnish, pg. 229, pl. 31, fig. 4

1990 *Panderodus recurvatus* (Rhodes) Armstrong; p. 104-7, pl. 16, figs 1-11

1995 *Panderodus panderi* (Stauffer); Sansom *et al.*, Text-figure 7

Holotype

Paltodus panderi Stauffer, 1940, pl. 60, fig. 8.

Diagnosis

Refer to the diagnosis of *Panderodus recurvatus* (Rhodes) in Armstrong (1990, p. 106).

Description

Refer to Armstrong (1990, p. 106)

Occurrence

Panderodus panderi has only been identified herein from the Venstøp Formation in the Oslo Graben where only a few isolated elements have been identified.

Panderodus unicostatus (Branson & Mehl 1933)

Plate 4, figs 3,4,5 & 6, Plate 5, figs 1-3

*1933 *Paltodus unicostatus* Branson & Mehl, 1933, p.42, pl. 3, fig.3

1977 *Panderodus unicostatus* (Branson & Mehl); Barrick, p.56-57, pl. 3, figs 1, 2, 5 & 6

1995 *Panderodus unicostatus* (Branson & Mehl); Sansom *et al.*, Text-figure 7

Syntypes

Paltodus unicostatus Branson & Mehl, 1933, pl. 3, fig. 3

Diagnosis

Refer to Barrick (1977, p. 56)

Occurrence

Panderodus unicostatus is common in samples from the Nod Gas Formation, Dent Group and all sections discussed from the Oslo Graben.

Order PROTOPANDERODONTIDA Sweet, 1988

Family DREPANOISTODONTIDAE Fåhraeus & Nowlan, 1978

Genus *Drepanoistodus* Lindström, 1971

Type species

Oistodus forseps Lindström 1955, p. 574

Diagnosis

Refer to Lindström (1971, p. 42)

Drepanoistodus suberectus (Branson & Mehl, 1933)

Plate 4, figs 8, 9, 10, Plate 5, figs 1-3

*1933c *Oistodus suberectus* Branson & Mehl, p. 111, pl. 9, fig. 7

1966 *Drepanoistodus suberectus* (Branson & Mehl); Bergström & Sweet, p. 330, pl. 35, figs 22-27

1990 *Drepanoistodus suberectus* (Branson & Mehl); Armstrong *et al.*, p. 130, pl. 22, figs 7-10

1996 *Drepanoistodus suberectus* (Branson & Mehl); Armstrong *et al.*, p17-18, pl. 9, figs 2&3

Holotype

Oistodus suberectus Branson & Mehl, 1933c, p. 111, pl. 9, fig. 7. From the middle Ordovician, Plattin Formation, Jefferson County, Missouri.

Diagnosis

Refer to Armstrong (1990, p. 130)

Description

Refer to Armstrong (1990, p. 130)

Occurrence

Drepanoistodus suberectus elements have been recovered from the Oslo Graben (all sections), the Nod Gas Formation, Gwern-y-Brain, Welshpool and the Dent Group at Greenscoe, Broughton in Furness.

Family PROTOPANDERODONTIDAE Lindström, 1970

Genus *Protopanderodus* Lindström, 1971

Protopanderodus liripipus Kennedy *et al.*, 1979

Plate 4, figs 11, 12 & 13

*1979 *Protopanderodus liripipus* Kennedy *et al.* p. 546, pl. 1, figs 9-19

1989 *Protopanderodus liripipus* Kennedy *et al.*; McCracken, p. 18, pl. 3, figs 15, 16, 18, 20-25

1995 *Protopanderodus liripipus* Kennedy *et al.*; Armstrong, p. 18, pl. 9, figs 13-14

1995 *Protopanderodus liripipus* Kennedy *et al.*; Rasmussen, pl. 1, fig. 18

Holotype

Protopanderodus liripipus Kennedy *et al.* (1979) p. 546, pl. 1, figs 9-19

Diagnosis

Refer to Orchard (1980, p. 24)

Occurrence

Protopanderodus liripipus elements have been recovered from the Nod Gas Formation and from all sections in the Oslo Graben.

Family STRACHANOGNATHIDAE Bergström, 1981

Genus *Strachanognathus* Rhodes, 1955

Strachanognathus parvus Rhodes, 1955

Plate 5, fig.11

*1955 *Strachanognathus parvus* Rhodes, p. 132, pl. 7, fig. 16, pl. 8, figs 1-4

1991 *Strachanognathus parvus* Rhodes, McCracken, p. 52, pl. 2, fig. 36

1996 *Strachanognathus parvus* Rhodes, Armstrong *et al.*, p. 18, pl. 9, figs 15-16

Holotype

Strachanognathus parvus Rhodes, p. 132, pl. 7, fig. 16

Description

Refer to Armstrong *et al.* (1996, p. 17)

Occurrence

Strachanognathus parvus is extremely rare and only occurs in the lower Dent Group at Greenscoe in the samples analysed herein. *Strachanognathus parvus* is however, reported to be common in the Ordovician rocks of Baltoscandia and Britain where it ranges from the lower Llanvirn to the upper Ashgill (Armstrong *et al.*, 1996).

? **Order** PROTOPANDERODONTIDA Sweet, 1988

? **Family** PROTOPANDERODONTIDAE Lindström, 1970

Genus *Scabbardella* Orchard, 1980

Scabbardella altipes (Henningsmoen, 1948)

Plate 5, figs 4&5

* 1948 *Drepanodus altipes* Henningsmoen, p. 420, pl. 25, fig. 14

1980 *Scabbardella altipes* (Henningsmoen), Orchard p. 25, 5 figs 2-5, 7, 8, 12, 14, 18, 20, 23, 24, 28, 30, 33, 25

1991 *Scabbardella altipes* (Henningsmoen), Bergström & Massa, p. 1339, pl. 1, figs 1, 3, 4.

1996 *Scabbardella altipes* (Henningsmoen), Armstrong *et al.*, p. 13, pl. 5, figs 1-6

Holotype

Drepanodus altipes Henningsmoen (1948 p. 420, pl. 25, fig. 14)

Description

Refer to Orchard (1980, p. 25)

Occurrence

Scabbardella altipes is common in the Nod Gas Formation and has also been recovered (although in very low numbers) from the Oslo Graben.

Order UNKNOWN

Family Nov. 5

Genus *Pseudooneotodus* Drygant, 1974

Type species

Oneotodus? beckmanni (Bischoff & Sannemann, 1958)

Diagnosis

Refer to Barrick (1977, p.57)

Pseudooneotodus beckmanni (Bischoff & Sannemann, 1958)

Plate 4, fig. 2

*1958 *Oneotodus* ? *beckmanni* Bischoff & Sannemann, p. 98, pl.15, figs 22-25

Holotype

Oneotodus ? *beckmanni* Bischoff & Sannemann, 1958, pl. 15, fig. 25. Specimen Bi Sa 1958 / 85 from the lower Devonian of Frankenwald, south central Germany.

Description

Refer to Orchard (1980, p. 24-25)

Occurrence

One *Pseudooneotodus beckmanni* element has been recovered from the Nod Glas Formation. It also occurs in the Oslo Graben throughout all the three sections from North Raudskjer, Frognøya and Hadeland, although consistently in very low numbers (usually fewer than 3 elements per sample).

Family Nov. 6 (Aldridge & Smith, 1993)

Genus *Eocarniodus* Orchard, 1980

Eocarniodus gracilis (Rhodes, 1955)

Plate 3, fig. 11

*1955 *Prioniodus gracilis* sp. nov Rhodes, p. 136, pl. 8, figs 5&6

1964 *Prioniodus aflexa* sp. nov. Hamar, p. 277, pl. 3, figs 15, 18 & 19

1980 *Eocarniodus gracilis* Orchard, 1980p 20, pl. 2, figs 14, 18-21, 24-26, 28, 30, 31, 33, 34, 36, 38

Holotype

Prioniodus gracilis Rhodes (1953, p. 136, pl. 8 fig. 5)

Description

Refer to Orchard (1980, p. 20)

Occurrence

Eocarniodus gracilis occurs in the Oslo Graben (Sections 16881-1 & 7881-1) in the Nod Glas Formation and in the Dent Group. It has been recovered in low numbers at all localities and is found associated with genera of the *Amorphognathus* Biofacies (as defined by Sweet & Bergström, 1984).

Appendix 1B - Plates

PLATE 1

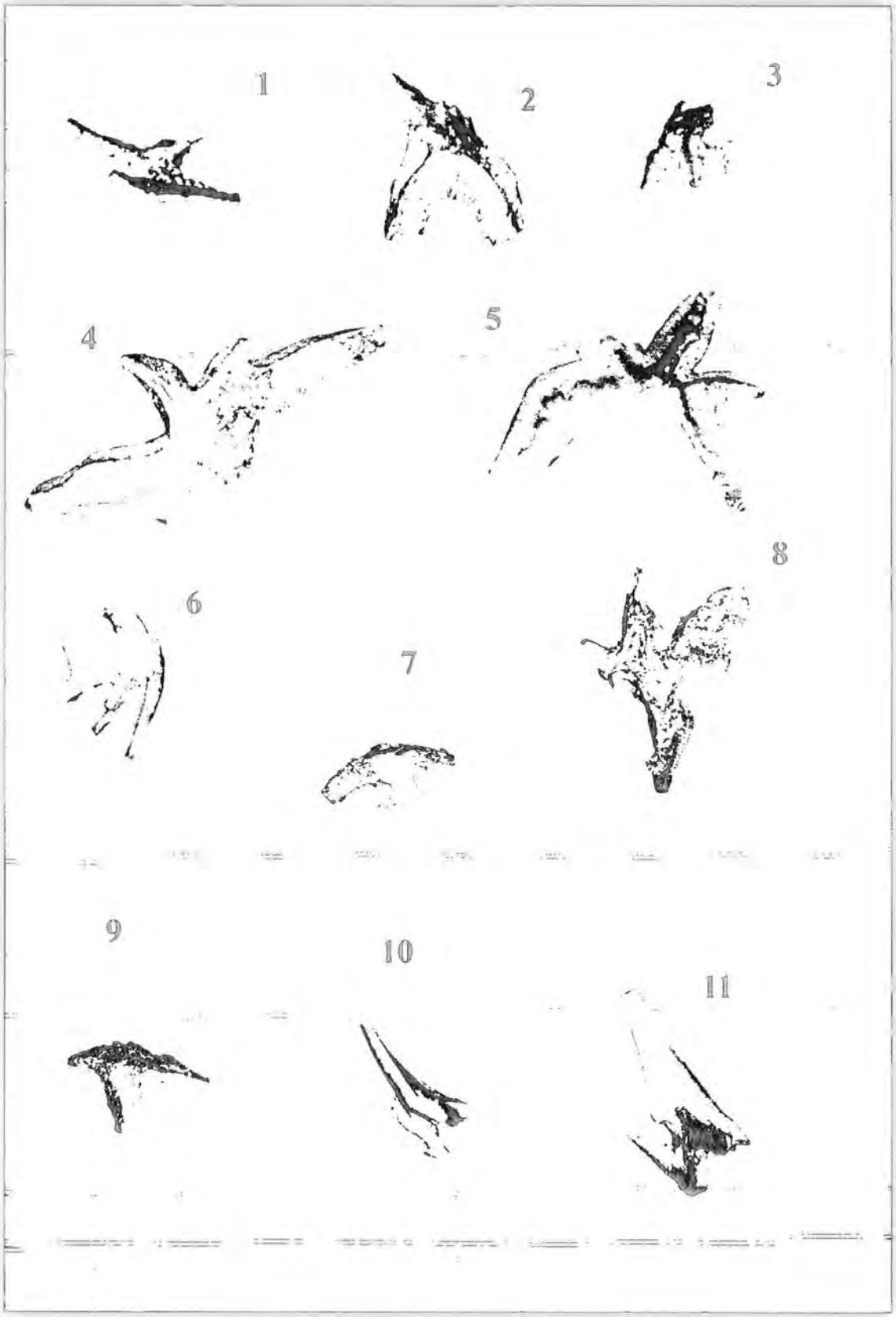

PLATE 2

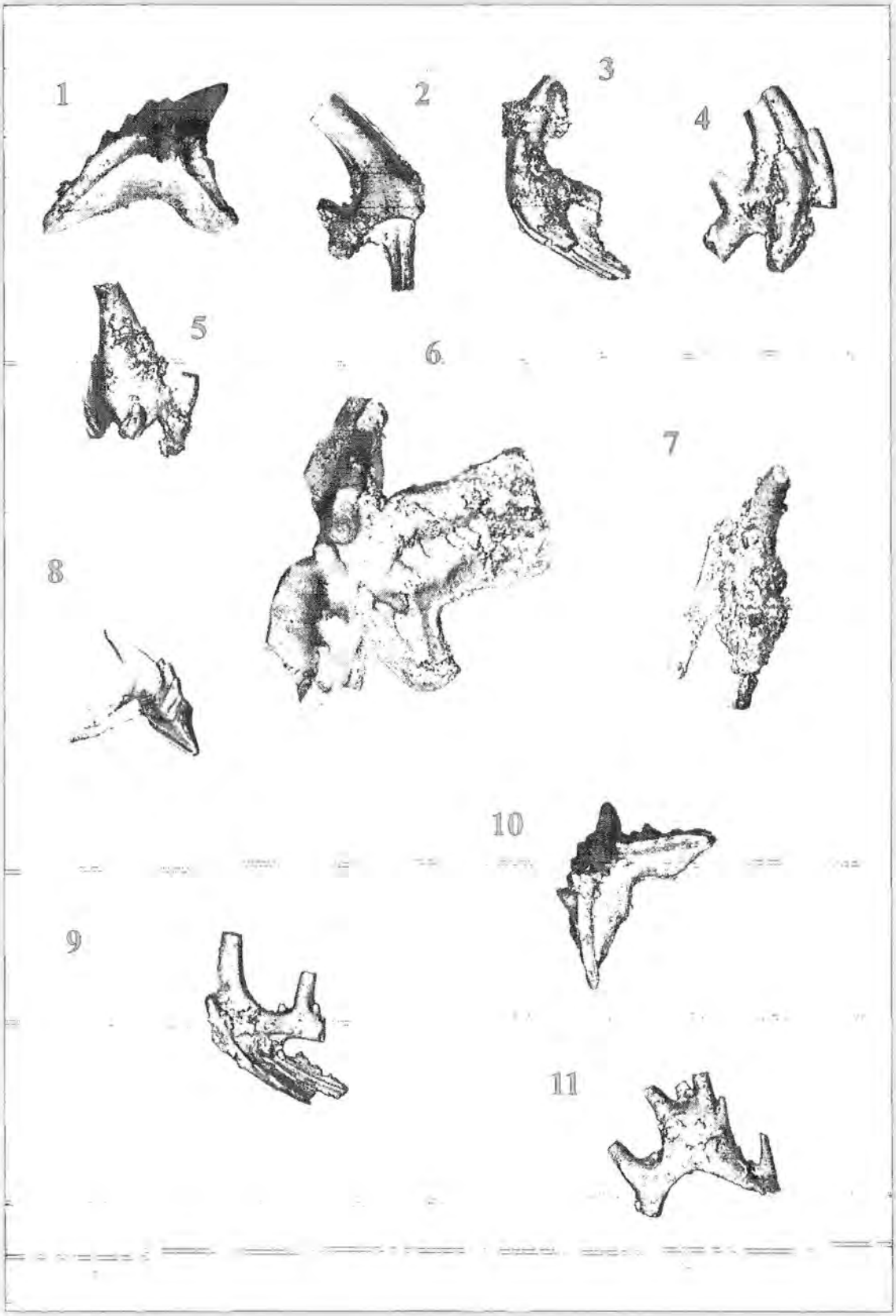

PLATE 3

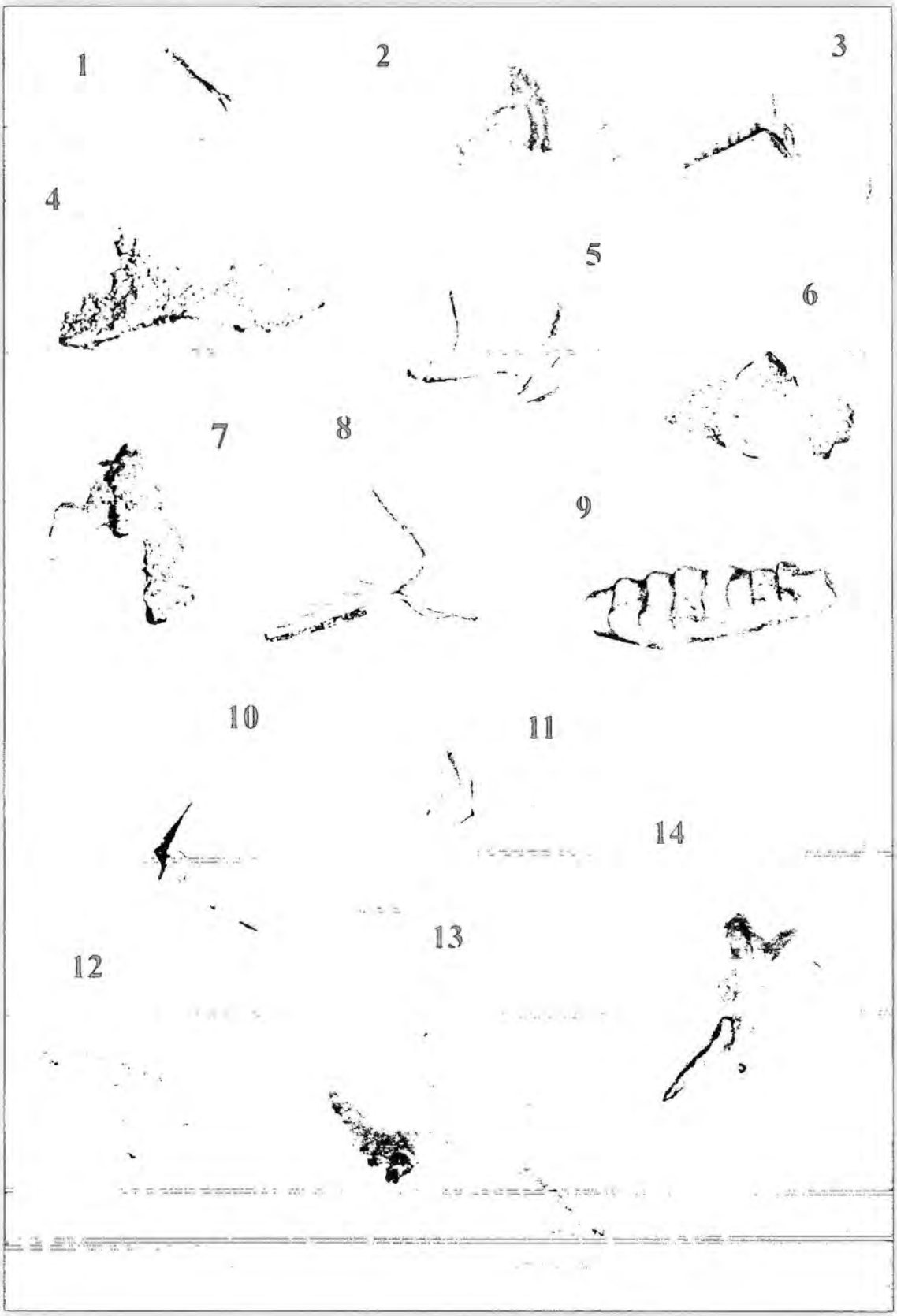

PLATE 4

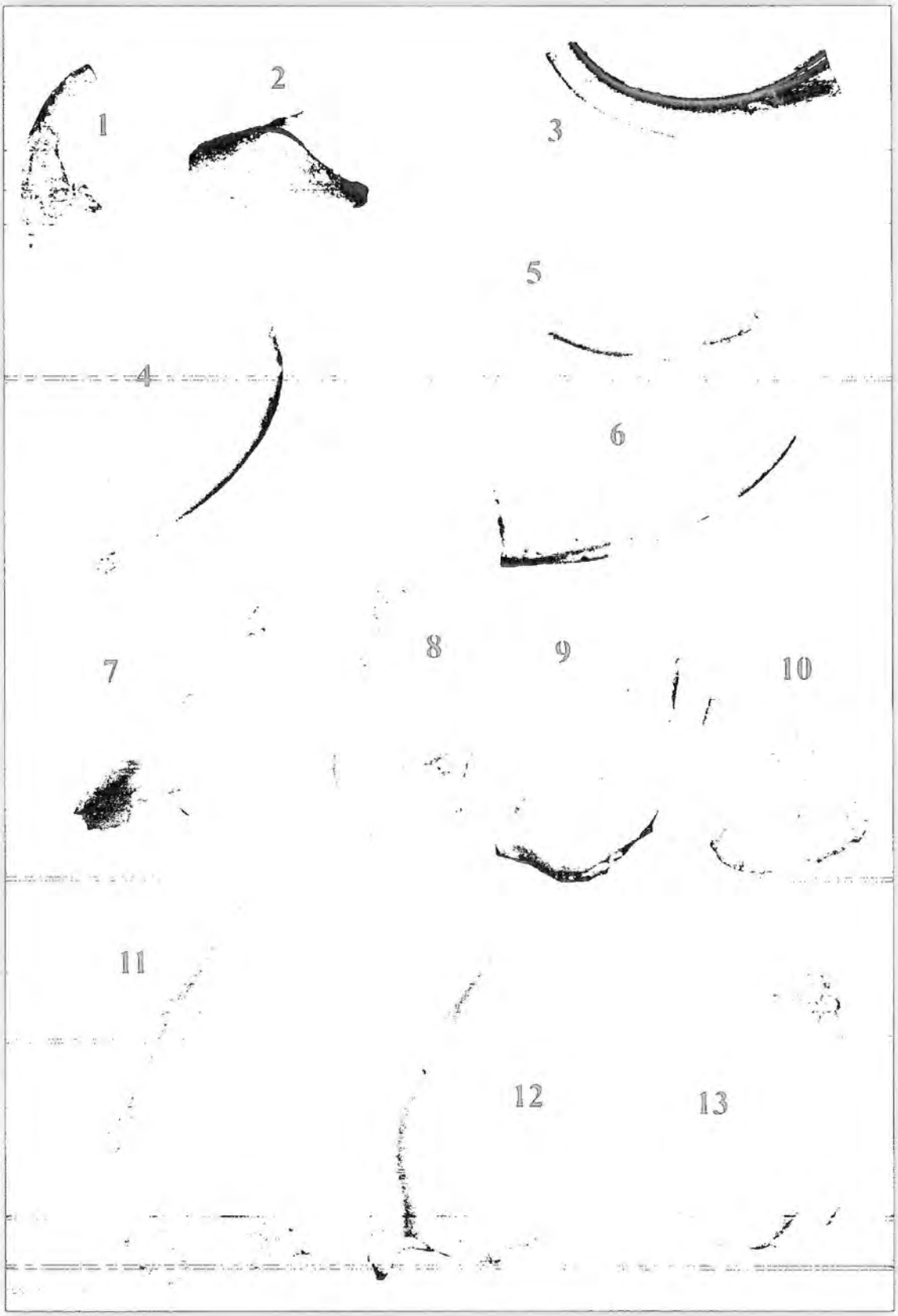

PLATE 5

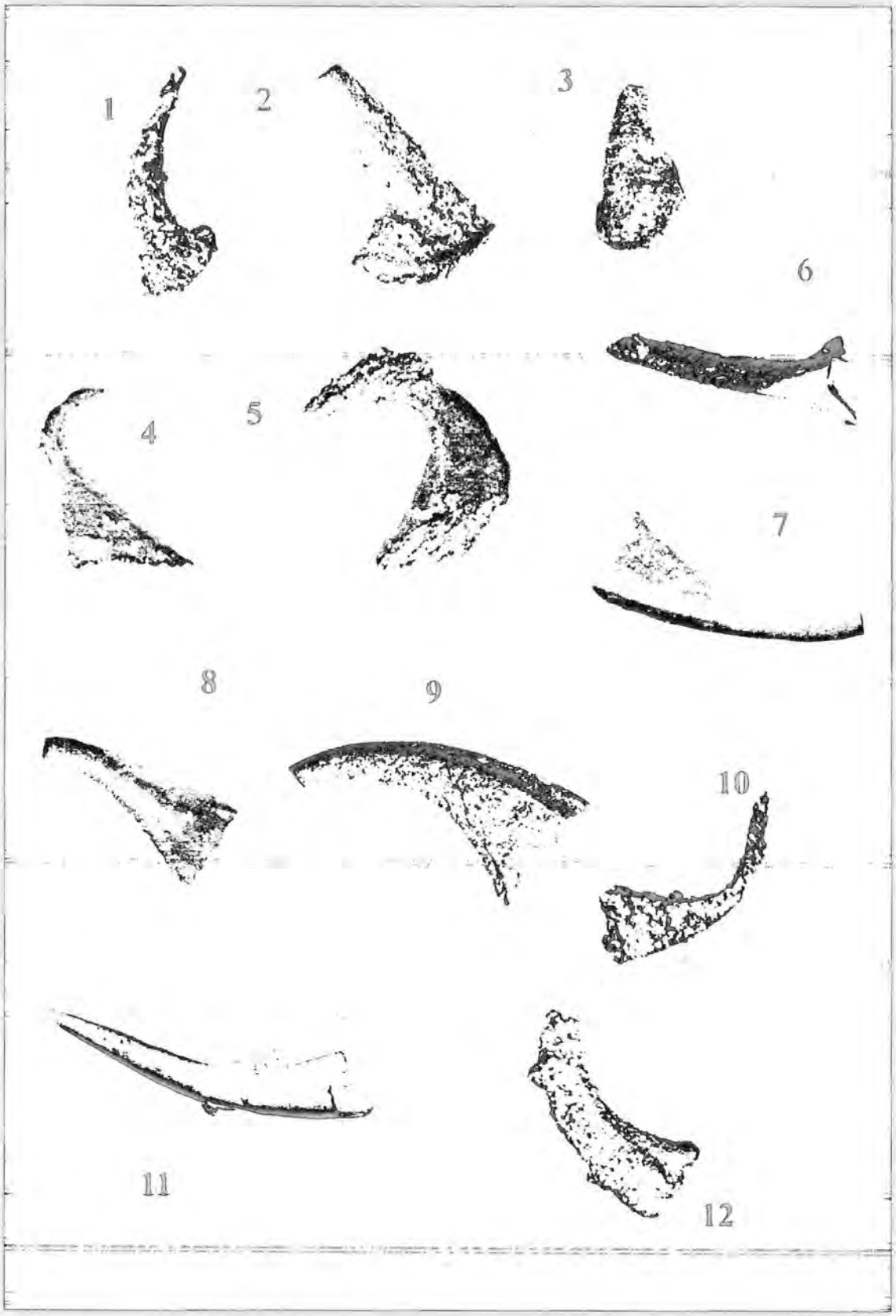

Appendix 1C – Abundance tables

PLATE 1

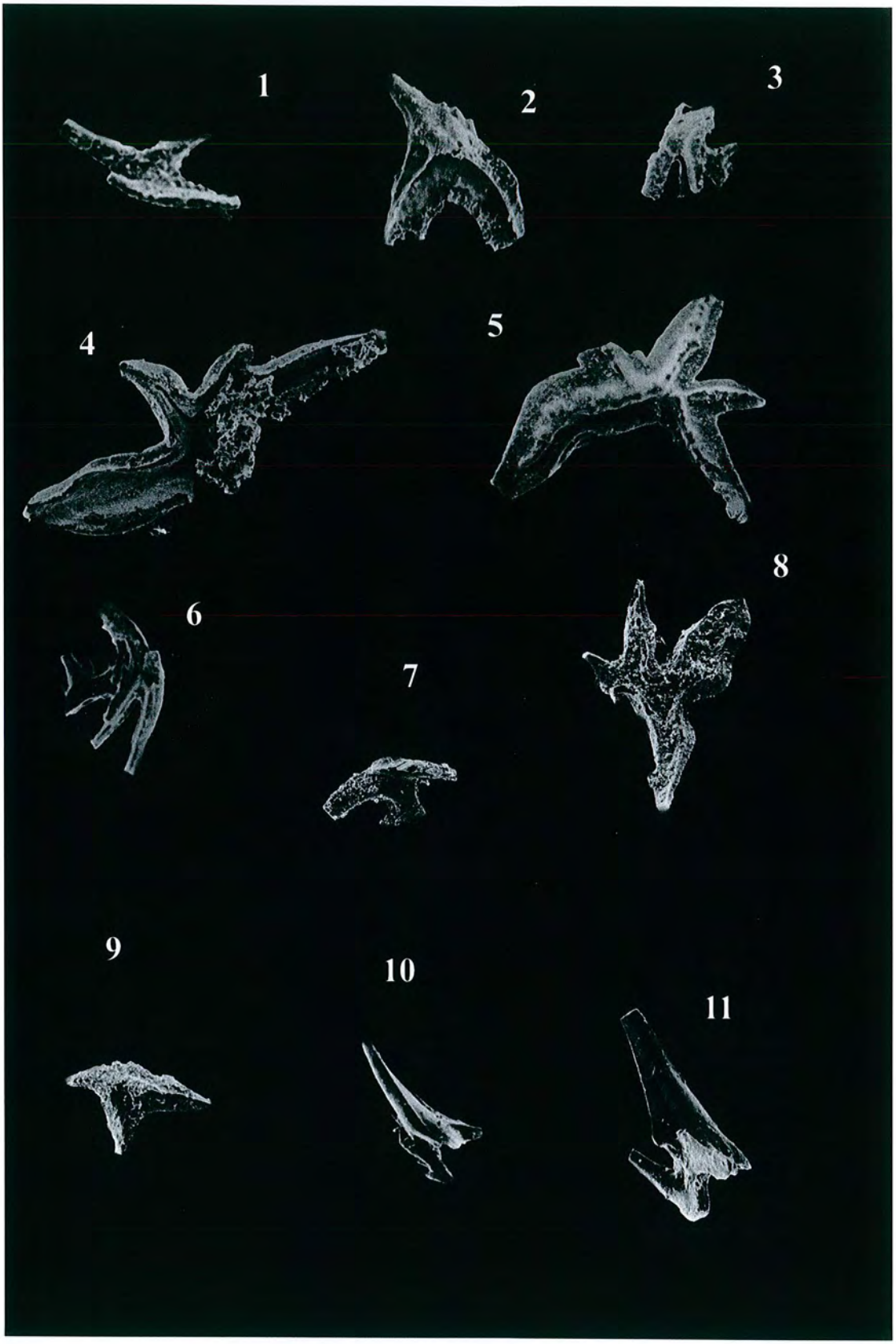

PLATE 1

Figures 1-6 from the Dent Group, Greenscoe, Lake District

Figures 7-11 from the Oslo Graben

1. Lateral view of *Amorphognathus superbus* (RHODES, 1953) Sb element. Specimen number 1847 00 (Sample number: D730) x60
2. Lateral view of *Amorphognathus superbus* (RHODES, 1953) Pb element. Specimen number 1847 01 (Sample number: D730) x60
3. Lateral view of *Amorphognathus superbus* (RHODES, 1953) Sb_2 (Sd) element. Specimen number 1847 03 (Sample number: D730) x60
4. Aboral view of *Amorphognathus superbus* (RHODES, 1953) Pa element. Specimen number 1847 38(Sample number: D730) x60
5. Oral view of *Amorphognathus superbus* (RHODES, 1953) Pa element. Specimen number 1847 39 (Sample number: D730) x60
6. Lateral view of *Amorphognathus superbus* (RHODES, 1953) Sb_2 (Sd) element. Specimen number 1847 04(Sample number: D730) x150
7. Lateral view of *Amorphognathus superbus* (RHODES, 1953) Sc element. Specimen number 1881 35 (Sample number: 13881-1 03) x65
8. Aboral view of *Amorphognathus superbus* (RHODES, 1953) Pa element. Specimen number 1881 37 (Sample number: 13881- 03) x65
9. Outer lateral view of *Amorphognathus superbus* (RHODES, 1953) Pb element. Specimen number 1883 02 (Sample number: 7881-1 02)
10. Outer lateral view of *Amorphognathus ordovicicus* (BRANSON & MEHL, 1933) Sb element. Specimen number 1883 10 (Sample number: 7881-1 06) x70
11. Posterior view of *Amorphognathus ordovicicus* (BRANSON & MEHL, 1933) M element. Specimen number 1883 12/13 (Sample number: 7881-1 06) x70

PLATE 2

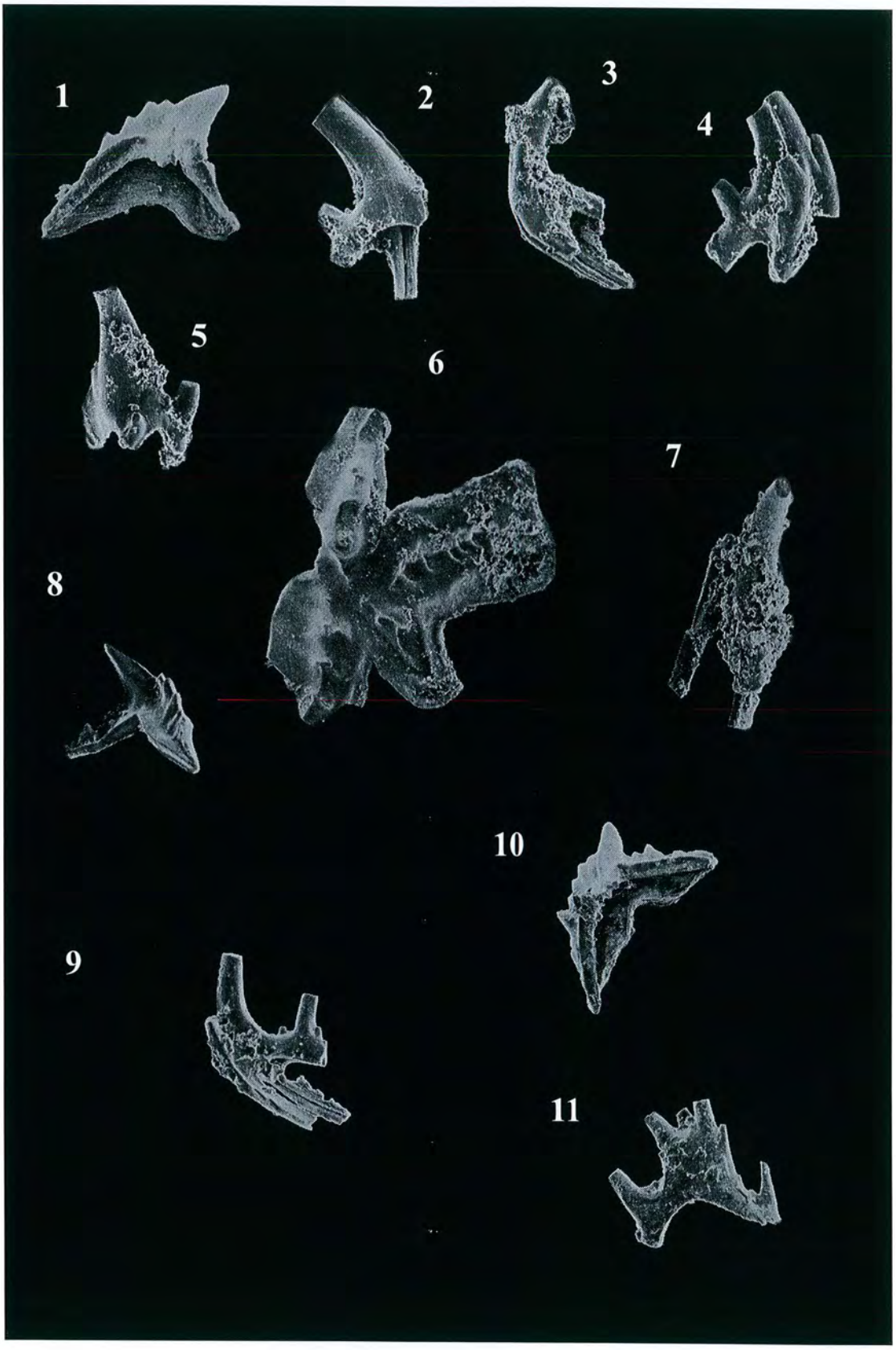

PLATE 2

Figures 1-12 from the Nod Glas Formation, Gwern-y-Brain, Welshpool

1. Outer lateral view of *Amorphognathus* cf. *A. ordovicicus* (BRANSON & MEHL, 1933) Pb element. Specimen number 1831 20 (Sample number: D584) x150
2. Oblique view of *Amorphognathus* cf. *A. ordovicicus* (BRANSON & MEHL, 1933) Sb element. Specimen number 1831 18 (Sample number: D584) x200
3. Lateral view of *Amorphognathus* cf. *A. ordovicicus* (BRANSON & MEHL, 1933) Sc element. Specimen number (Sample number: D584) x200
4. Lateral view of *Amorphognathus* cf. *A. ordovicicus* (BRANSON & MEHL, 1933) Sd element. Specimen number 1832 06 (Sample number: D584) x180
5. Posterior view of *Amorphognathus* cf. *A. ordovicicus* (BRANSON & MEHL, 1933) M element. Specimen number 1846 39 (Sample number: D584) x150
6. Oral view of *Amorphognathus* cf. *A. ordovicicus* (BRANSON & MEHL, 1933) Pa element. Specimen number 1832 323 (Sample number: D584) x70
7. Posterior view of *Amorphognathus* cf. *A. ordovicicus* (BRANSON & MEHL, 1933) Sa (?) element. Specimen number 1832 42 (Sample number: D584) x250
8. Inner lateral view of *Amorphognathus* cf. *A. ordovicicus* (BRANSON & MEHL, 1933) Pb element. Specimen number 1846 10 (Sample number: D584) x 60
9. Lateral view of *Amorphognathus* cf. *A. superbus* (RHODES, 1953) Sb_2 (Sd) element. Specimen number 1847 01 (Sample number: D593) x200
10. Outer lateral view of *Amorphognathus* cf. *A. superbus* (RHODES, 1953) Pb element. Specimen number 1846 25 (Sample number: D593) x70
11. Anterior view of *Amorphognathus* cf. *A. superbus* (RHODES, 1953) M element. Specimen number 1846 39 (Sample number: D583) x150

PLATE 3

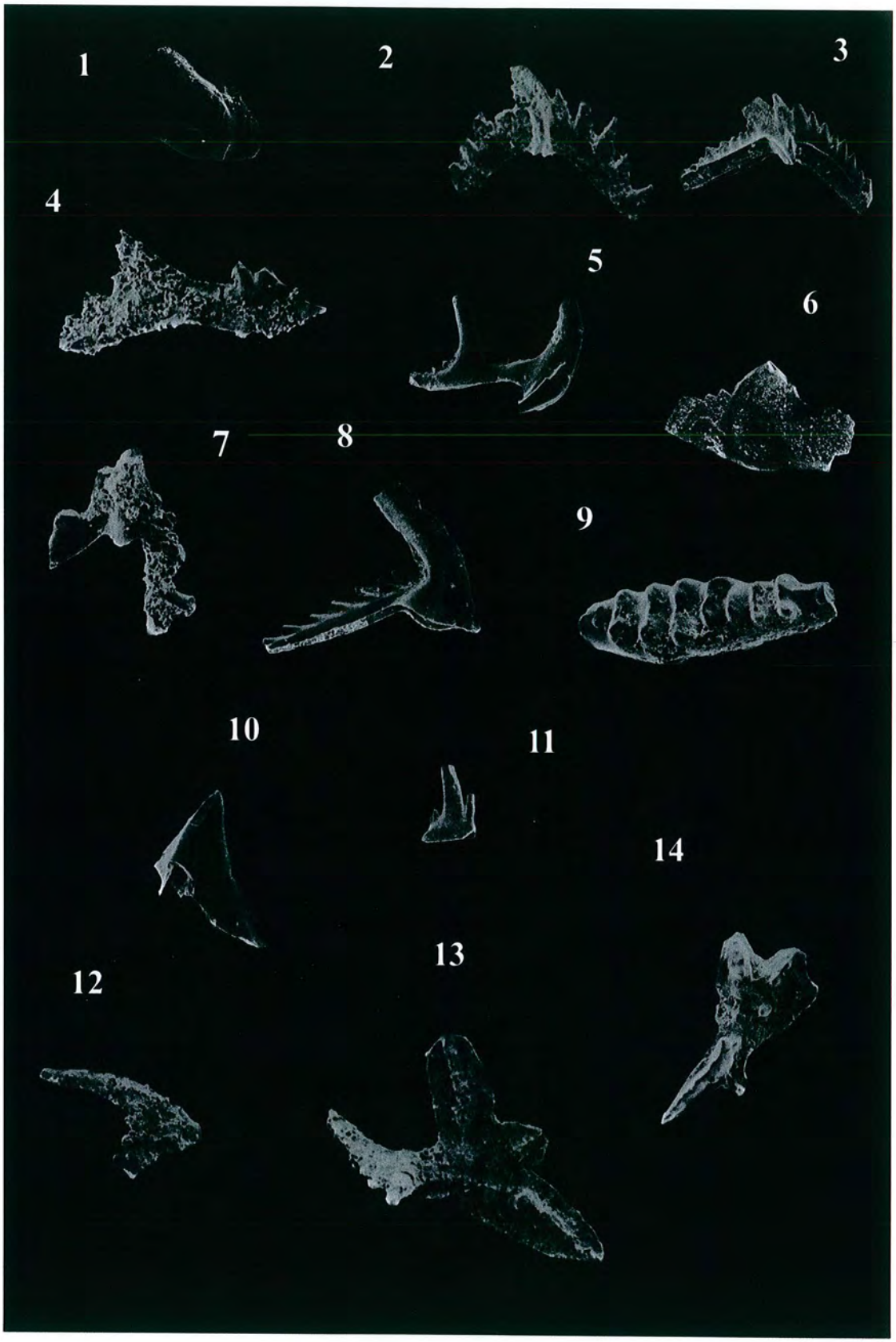

PLATE 3

1. Lateral view of *Periodon grandis* M element. Specimen number 1883-43 (Sample number: 7881-1 07) x100
2. Posterior view of *Rhodesognathus elegans* (RHODES, 1953) Sb element. Specimen number 1837-10 (Sample number: D730) x60
3. Outer lateral view of *Rhodesognathus elegans* (RHODES, 1953) Pb element. Specimen number 1846-38 (Sample number: D593) x70
4. Lateral view of *Aphelognathus rhodesi* (LINDSTRÖM, 1959) Pa element. Specimen number 1837-13 (Sample number: D729) x60
5. Lateral view of *Phragmodus undatus* (BRANSON & MEHL, 1933)Sc element. Specimen number 1832-0 (Sample number 16881-1) x150
6. Anterior view of *Phragmodus undatus* (BRANSON & MEHL, 1933) Pa element Specimen number 1883-18 (Sample number: 16881-1 07) x150
7. Posterior view of *Plectodina bullhillensis* (SAVAGE & BASSETT, 1985) Sb element. Specimen number 1883-6 (Sample number: D586) x 70
8. Lateral view of *Plectodina bullhillensis* (SAVAGE & BASSETT, 1985) M element Specimen number 1846-18 (Sample number: D586) x70
9. Oral view of *Icriodella superba* (RHODES, 1953) Pa element. Specimen number 1846-24 (Sample number: D593) x80
10. Lateral view of *Icriodella superba* (RHODES, 1953) Pb element. Specimen number 1846-3 (Sample number: D593) x70
11. Lateral view of *Eocarniodus gracilis* (RHODES, 1955). Specimen number 1846-36 (Sample number: D593) x70
12. Lateral view of *Hamarodus europaeus* (SERPAGLI, 1967) Sc element. Specimen number 1837-9 (Sample number D730) x60
13. Oral view of *Complexodus pugionifer* (DRYGANT, 1976) Pa element. Specimen number 1837-17 (Sample number: D730) x60
14. Oral view of *Complexodus pugionifer* (DRYGANT, 1976) Pa element. Specimen number 1846-31 (Sample number: D593) x60

PLATE 4

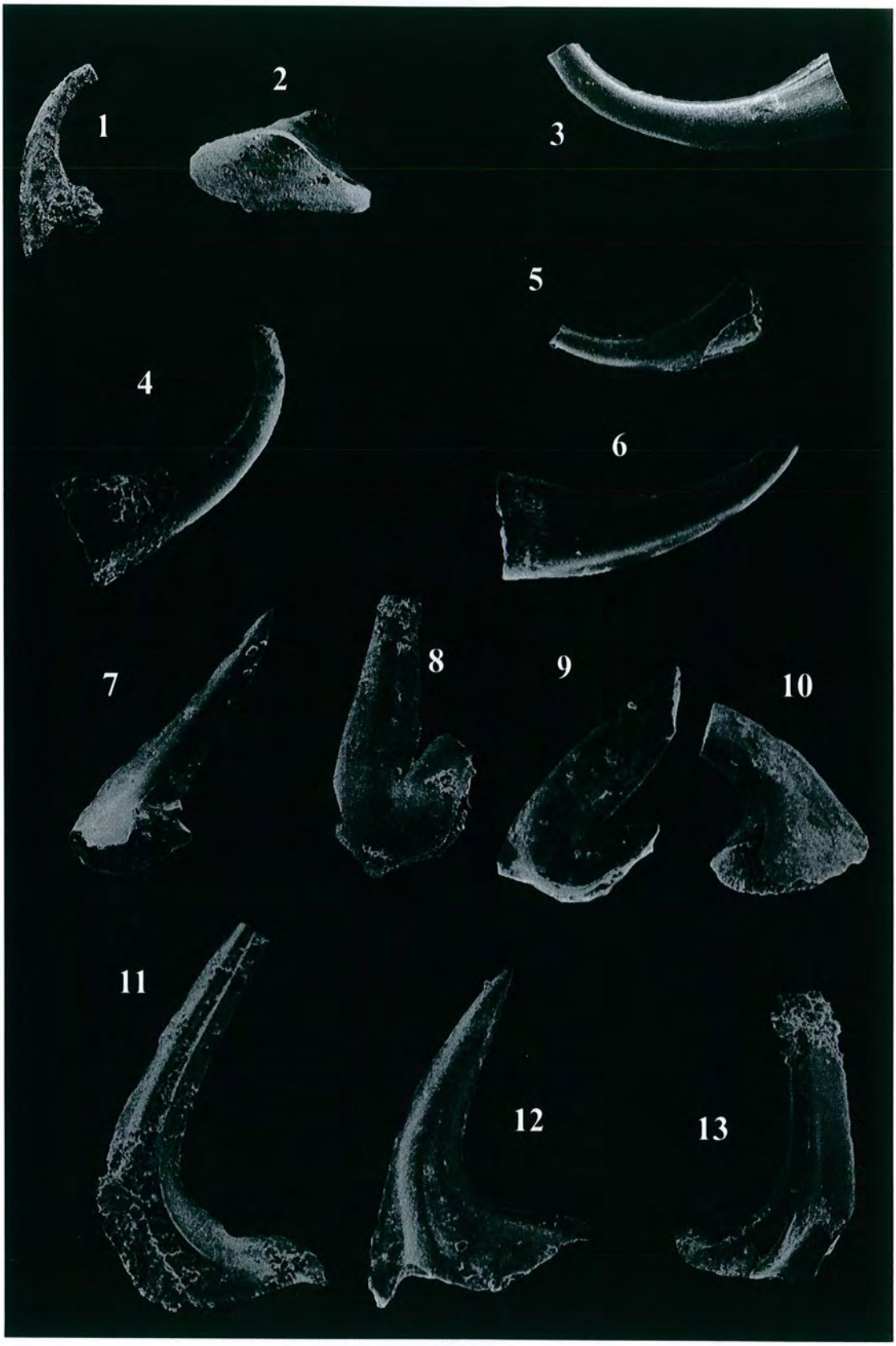

PLATE 4

Figures 1-13 from the Nod Gas Formation, Gwern-y-Brain Stream, Welshpool

1. Lateral view of *Dapsilodus mutatus* (BRANSON & MEHL, 1933). Specimen number 1831-33 (Sample number: D584) x 70
2. Lateral view of *Pseudooneotodus beckmanni* (BISCHOFF & SANNEMANN, 1958). Specimen number 1832-01 (Sample number: D584) x 150
3. Lateral view of graciliform element of *Panderodus unicostatus* (BRANSON & MEHL, 1933). Specimen number 1832-322 (Sample number: D584) x 150
4. Lateral view of graciliform element of *Panderodus unicostatus* (BRANSON & MEHL, 1933). Specimen number 1846-33 (Sample number: D593) x 70
5. Lateral view of graciliform element of *Panderodus unicostatus* (BRANSON & MEHL, 1933). Specimen number 1846-00 (Sample number: D584) x 70
6. Lateral view of falciform element of *Panderodus unicostatus* (BRANSON & MEHL, 1933). Specimen number 1846-16 (Sample number: D586) x70
7. Lateral view of *Drepanoistodus suberectus* (BRANSON & MEHL, 1933). Specimen number 1832-41 (Sample number: D584) x100
8. Lateral view of *Drepanoistodus suberectus* (BRANSON & MEHL, 1933). Specimen number 1846-26 (Sample number: D593) x 60
9. Lateral view of *Drepanoistodus suberectus* (BRANSON & MEHL, 1933). Specimen number 1846-41 (Sample number: 593) x70
10. Lateral view of *Drepanoistodus suberectus* (BRANSON & MEHL, 1933). Specimen number 1846-42 (Sample number: D593) x70
11. Lateral view of *Protopanderodus liripius* (KENNEDY *ET AL.*, 1979). Specimen number 1832-39 (Sample number: D584) x70
12. Lateral view of *Protopanderodus liripius* (KENNEDY *ET AL.*, 1979). Specimen number 1846-42 (Sample number: D593) x70
13. Lateral view of *Protopanderodus liripius* (KENNEDY *ET AL.*, 1979). Specimen number 1846-06 (Sample number: D584) x70

PLATE 5

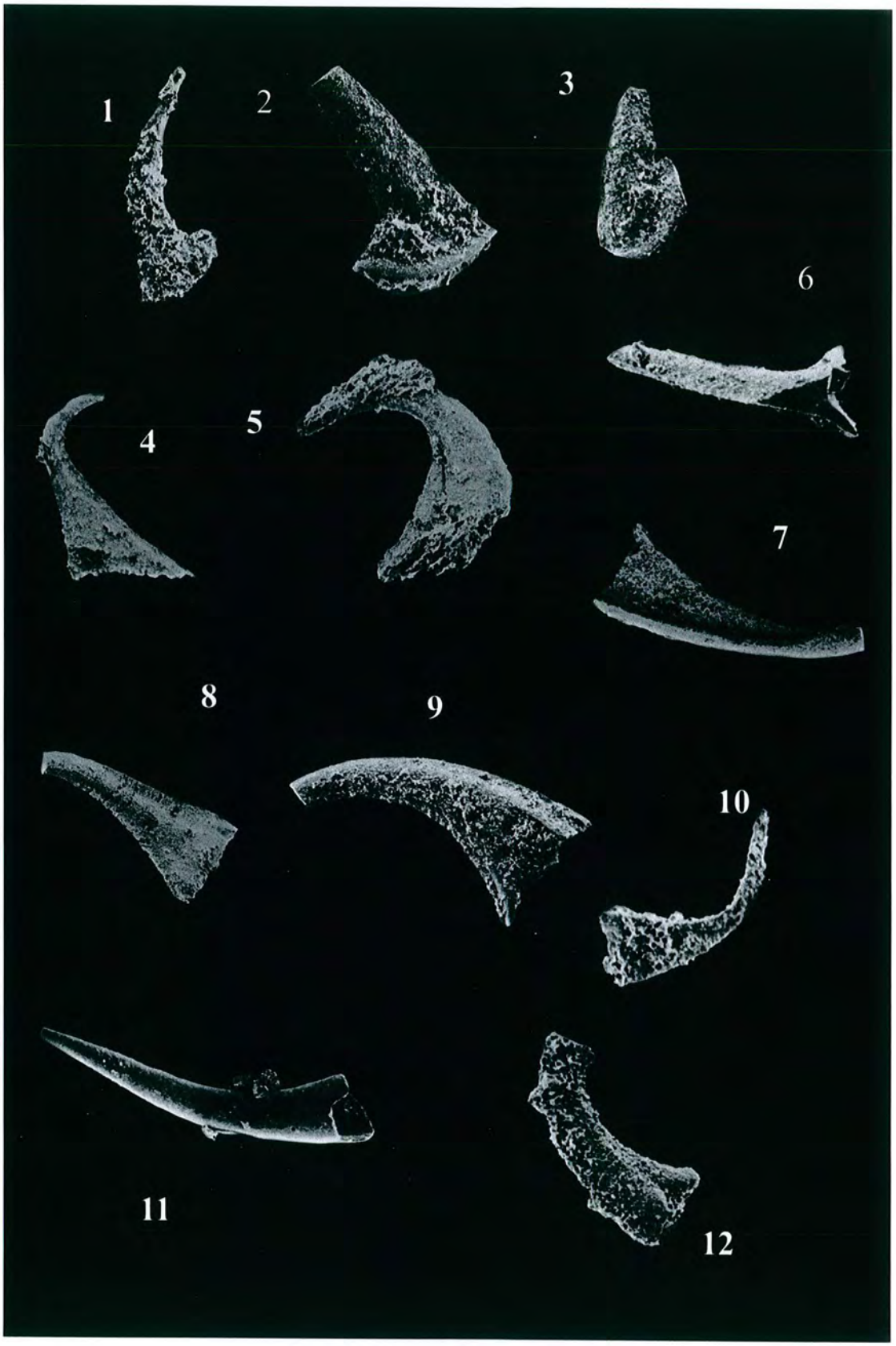

PLATE 5

Figures 1- 7 from the Nod Gas Formation, Gwern-y-Brain, Welshpool

1. Lateral view of *Drepanoistodus suberectus* (BRANSON & MEHL, 1933). Specimen number 1837-16 (Sample number: D593) x60
2. Lateral view of *Drepanoistodus suberectus* (BRANSON & MEHL, 1933). Specimen number 1837-00 (Sample number: D593) x60
3. Lateral view of *Drepanoistodus suberectus* (BRANSON & MEHL, 1933 Specimen number 1837-01 (Sample number: D593) x60
4. Lateral view of *Scabbardella altipes* (HENNINGSMOEN, 1948). Specimen number 1848-14 (Sample number: D593) x 60
5. Lateral view of *Scabbardella altipes* (HENNINGSMOEN, 1948). Specimen number 1848-15 (Sample number: D585) x60
6. Lateral view of *Walliserodus curvatus* (BRANSON & BRANSON, 1947). Specimen number 1884-20 (Sample number: D586) x70
7. Lateral view of *Walliserodus curvatus* (BRANSON & BRANSON, 1947). Specimen number 1848-10 (Sample number: D586) x60

Figures 8-12 from the Oslo Graben

8. Lateral view of *Walliserodus curvatus* (BRANSON & BRANSON, 1947). Specimen number 1883-20 (Sample number: 16881 03) x60
9. Lateral view of *Walliserodus curvatus* (BRANSON & BRANSON, 1947). Specimen number 1884-20 (Sample number: 13881 03) x70
10. Lateral view of *Walliserodus curvatus* (BRANSON & BRANSON, 1947). Specimen number 1883-39 (Sample number: 13881 03) x70
11. Lateral view of *Strachanognathus parvus* (RHODES, 1953). Specimen number 1883-11 (Sample number: 7881-1 06) x70
12. Lateral view of *Panderodus panderi* (STAUFFER, 1940) graciliform element. Specimen number 1884-14 (Sample number: 13881-02) x70

Weight processed (g)	172	1742	1468	502	918	1485
Formation	Gaer	Gaer	Nod	Nod	Nod	Nod
Sample number	D587	D592	D593	D586	D585	D584
Amorphognathus aff. *A. superbus*						
Pa	2		3	frags	1+frags	
Pb		1			7	
M			1			
Sa			1			
Sb			1		2	
Sc			1			
Sd		1	3		3	
Amorphognathus aff. *A. ordovicicus*						
Pa						4+frags
Pb						20
M						1
Rhodesognathus elegans						
Pa	1	5	14			
Pb						
M						
Sa		2?	6?			
Complexodus pugionifer						
Pa			2			1
Icriodella superba						
Pa	2	1	5			
Pb		1				
M		1				
Prioniodus sp.						
Pa			4			1?
Plectodina bullhillensis						
Pa	1	2	5	11		
Pb						
M						
Sa	1	1				
Sb						
Sc	1					
Phragmodus undatus						
Pa			1			1

Weight processed (g)	172	1742	1468	502	918	1485
Formation	Gaer	Gaer	Nod	Nod	Nod	Nod
Sample number	D587	D592	D593	D586	D585	D584
Dapsilodus mutatus						
	1	3	10			3
Walliserodus curvatus						
	1	1		1?	1	2
Panderodus unicostatus						
	2	8	28	5	1	2
Drepanoistodus suberectus						
			2			
Protopanderodus liripipius						
			6	1?	2	6
Scabbardella altipes						
		4	13		1?	2
Pseudooneotodus beckmanni						
						1
Eocarniodus gracilis						
			2			
Subtotal	12	31	108	18	18	44
Fragments	2	12	43	24	62	40
Total	**14**	**43**	**151**	**42**	**80**	**84**

Locality/section	Greenscoe Road Cutting (SD 221 756)				
Sample number	728	729	730	731	732
Weight processed (g)	1154.8	1343	1068	996.5	1359.7
Species present					
Amorphognathus superbus					
Pa	7		1	2 frags?	
Pb	1	3	1		
Pc					
M		2			
Sa			1		
Sb	1				
Sd		3	1		
Complexodus pugionifer					
Pa		2	1		
Rhodesognathus elegans					
Pa		3	1		?
Pb					?
Aphelognathus rhodesi					
Pa		22			
Plectodina tenius					
Pa		4			3
Pb					1
M		1			
? Birksfeldia					
Pa	2	1	2frags?		
Hamerodus europaeus					
		1			2
Eocarniodus					
		3	6	1	
Dapsilodus sp.					
	5	4		1?	9
Drepanoisodus suberectus					
	1	7	7	4	2
Panderodus unicostatus					
	9	62	60	4	15
Subtotal	**26**	**118**	**79**	**9**	**32**
Fragments	11	12	40	5	12
Total	**37**	**130**	**119**	**14**	**44**

Locality/section	13881-1	Tonnerudtangen						
Sample number	1	2	3	5	7	8	9	10
Weight processed	2125g	2419g	2472	2272	2679	2302	2177	2420
Species present								
Amorphognathus sp.		9	9	2	1	5	1	2
Pseudooneotodus beckmanni		1						
Dapsilodus mutatus			1					
Panderodus unicostatus			3		1			4
Drepanoistodus suberectus			1					
Protopanderodus liripipius			1					
Walliserodus curvatus				2			1	
Total	**0**	**10**	**15**	**4**	**2**	**5**	**2**	**6**

Locality/section	7881-1	Frognoya							
Sample number	1	2	3	4	6	7	8	9	11
Weight processed	1893	2139	1474	2370	2071	1837	2703	2456	2183
Species present									
Amorphognathus sp.	2	15	1		62	11		17	
Pseudooneotodus beckmanni		1				1			
Dapsilodus mutatus	1	8		4		1			1
Panderodus panderi					2				
Panderodus unicostatus	3	14	4	5	10	19			
Drepanoistodus suberectus	1								
Protopanderodus liripipius	2	8	3	1					
Walliserodus curvatus			1	1		1	1		
Periodon grandis									
Eocarniodus gracilis					4				
Sp. A		3							
Icriodella superba				1					
Birksfeldia							27		
Total	**9**	**49**	**9**	**12**	**78**	**34**	**4**	**1**	**1**

Locality/section	16881-1	Raudskjer						
Sample number	1	2	5	6	9	10	11	12
Weight processed (g)	2244	2305	2671	2466	2610	1885	2096	1589
Species present			4					
Amorphognathus sp.					2	17		2
Pseudooneotodus beckmanni								
Dapsilodus mutatus		1	1		2	1	2	4
Panderodus unicostatus		2	1			3	4	
Drepanoistodus suberectus	1			2				
Protopanderodus liripipius			15	4	2	4		3
Walliserodus curvatus		1			2			
Periodon grandis								
Eocarniodus gracilis						1		2
Total	**1**	**4**	**22**	**6**	**8**	**26**	**6**	**11**